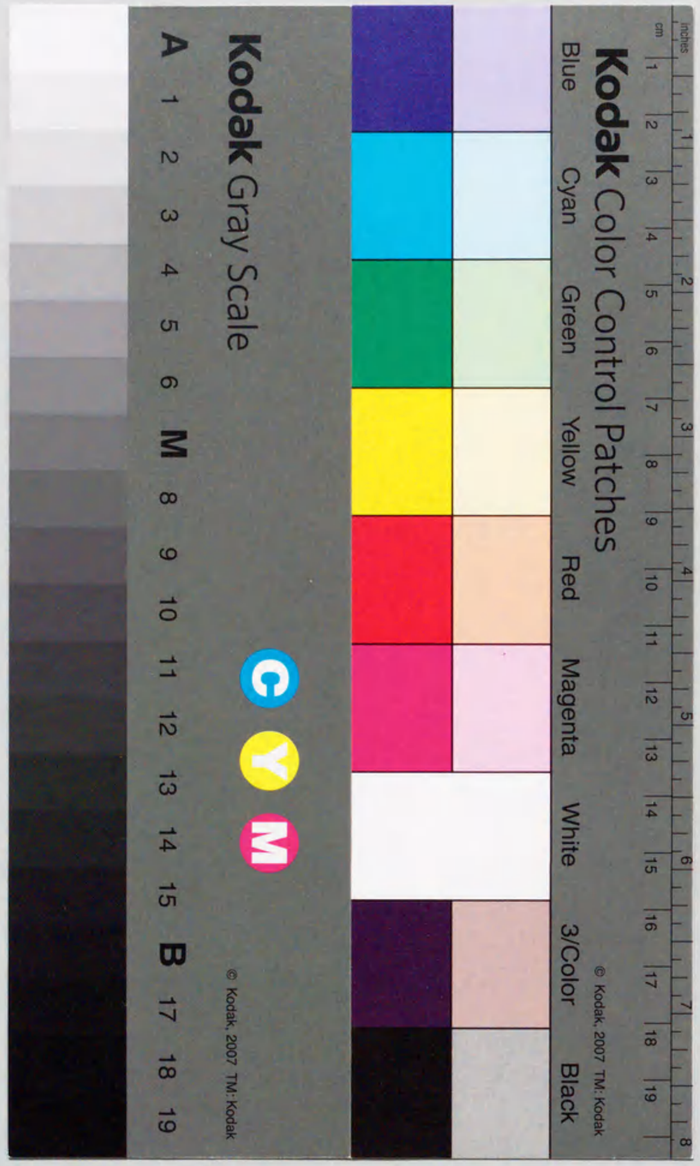

Theory for Multidimensional Tunneling and its Application to Chemical Reactions

Graduate School of Human Informatics,
Nagoya University, Nagoya 464-01, Japan

Hiroshi Ushiyama

1997

Theory for Multidimensional Tunneling and its Application to Chemical Reactions

Graduate School of Human Informatics,
Nagoya University, Nagoya 464-01, Japan

Hiroshi Ushiyama

1997

Preface

A potential barrier is impenetrable to a particle whose energy is lower than the height of the barrier in classical mechanics. However, in quantum mechanics, the probability that the particle passes through the barrier is not zero. This phenomenon is called the tunneling effect. The tunneling effect is the most remarkable and important quantum phenomenon and has been studied in many fields of science such as the scanning tunneling microscope, the mesoscopic device in solid state physics and proton transfer in physical chemistry. The energy splitting caused by proton transfer in malonaldehyde, the rate constants of tunneling reactions in solid hydrogen and the synthesis of formaldehyde through tunneling at low temperature range are additional examples in physical chemistry. In spite of the importance of tunneling, only one-dimensional tunneling has been clearly understood. The tunneling effect in the chemical reaction systems has been usually studied as a one-dimensional problem along a certain tunneling coordinate. However, a chemical reaction itself is essentially a multidimensional problem. Therefore to understand the tunneling chemical reaction, a theory for multidimensional tunneling is required.

There are two purposes in the present thesis. One is the construction of a semiclassical theory for multidimensional tunneling. And the other is the semiclassical study on chemical reactions through tunneling in order to answer the following questions: What is an essential difference between one-dimensional tunneling and multidimensional tunneling? In other words, can we study multidimensional tunneling along a certain tunneling coordinate?

The present thesis consists of two parts. Part I is devoted to the construction of a semiclassical tunneling theory for multidimensional systems. By introducing a quantity of 'parity of motion' which can take only positive or negative unity into each coordinate of the Hamilton-Jacobi equation, a semiclassical theory which provides complex-valued action integrals in real-valued configuration space is constructed. The complex-valued action integral

is propagated as a tunneling solution of the Hamilton-Jacobi equation along a real-valued tunneling path. The 'parity of motion' modifies the ordinary classical Hamiltonian. The tunneling paths are generated by solving a set of the modified canonical equations of motion in real-valued phase space with negative parities. Therefore the complex-valued action integrals can be constructed in as large systems as classical mechanics can study. These complex-valued action integrals have a layer structure which consists of many sheets and every sheet is characterized in terms of its own set of parities. Among them, two special sheets exist. One is Newtonian sheet which consists of only positive parities and is filled with classical trajectories. The other is the instanton one which has no positive parities and generates the so-called instanton paths. The sheets except for the Newtonian sheet represent tunneling motion. The complex-valued action integrals can be included in any semiclassical formalism. In Chapter II, these complex-valued action integrals along real-valued tunneling paths are incorporated into the time-dependent semiclassical kernel. As the number of negative parities gets larger, the imaginary part of the action integral becomes large and hence the norm of the semiclassical kernel decreases.

In Part II, on the basis of the semiclassical theory constructed in Part I, chemical reactions through tunneling are studied. In Chapter I, the behavior of dynamical tunneling paths (which correspond to tunneling paths among two or more different vibrational modes in a molecule) is examined on the Hénon-Heiles potential and the effect of chaos on the dynamical tunneling is discussed. In Chapter II, the 'quasi-semiclassical method' in which a system is basically treated by the quasi-classical method and the real-valued tunneling paths are applied only to tunneling motion is proposed. To study the multidimensional effects on tunneling reaction, the 'quasi-semiclassical method' is applied to some typical tunneling reactions in the collinear three atomic collision systems on the so-called LEPS potential. To examine which mode, vibrational or translational mode, should be excited to enhance the tunneling reaction, the effect of initial energy distribution on tunneling probabilities is studied with changing the mass balance and the anisotropy of the potential surface. The effect of the initial translational energy on tunneling is also examined to see which type of tunneling paths

dominates with changing the mass balance. The final energy distribution in the product molecules is also discussed. From the studies in Chapter II, a 'tunneling tube' which is a bunch of tunneling paths with large tunneling probabilities has been found. This is a distinguished feature of multidimensional tunneling from one-dimensional tunneling and the most remarkable feature peculiar to multidimensional tunneling.

Finally, the general conclusions of the present thesis are given at the end of this thesis.

List of publications

[1] K. Takatsuka and H. Ushiyama, "Tunneling Solutions of the Hamilton - Jacobi Equation for Multidimensional Semiclassical Theory", Physical Review **A51**, 4353 (1995)

[2] H. Ushiyama and K. Takatsuka, "Statistical Redistribution of Trajectories from a Torus to Tori by Chaotic Dynamical Tunneling", Physical Review **E53,** 115 (1996)

[3] H. Ushiyama and K. Takatsuka, "Semiclassical Study on Multidimensional Effects in Tunneling Chemical Reactions. Tunneling Paths and Tunneling Tubes." accepted for publication in The Journal of Chemical Physics.

[4] H. Ushiyama and K. Takatsuka, "Dynamical Tunneling in a Weakly Chaotic Systems", in The proceedings of the International Conference on *Dynamical Systems and Chaos*. (World Scientific Singapore, 1995)

Acknowledgment

The present thesis is the summary of the author's studies from 1992 to 1997 at Graduate School of Human Informatics, Nagoya university.

The author cordially thanks Professor Kazuo Takatsuka for his kind guidance, valuable suggestions, stimulating discussions and continuous encouragement. He also thanks Professor Kenichi Yoshikawa, Professor Masaki Sasai and Professor Nobuaki Koga for their kind guidances and continuous encouragements. Acknowledgment is also made to Naoyuki Hashimoto, Chihiro Seko, Atsuko Inoue, Yuri Tomonaga, and Yasuki Arasaki for valuable discussions.

Finally it is also his pleasure to thank his family for sympathy and continuous encouragement.

Contents

General Introduction

The tunneling effect has been one of the most remarkable and important quantum phenomena in many fields of science from atomic physics to astrophysics [1]. In physical chemistry [2], the tunneling effect cannot be neglected in proton transfer reaction because of the small mass of a proton. Many experimental investigations of tunneling reactions have been reported. For example, the energy splitting caused by the proton transfer in malonaldehyde [3], the rate constants of tunneling reactions in solid hydrogen [4], the synthesis of formaldehyde through tunneling at low temperature range [5] and so on have been studied vigorously. The rate constants of tunneling reaction in solid hydrogen are temperature independent at very low temperature [4]. It is one of the most remarkable features peculiar to tunneling reactions.

In spite of various experimental studies of tunneling reactions in chemical systems, tunneling has never been clearly understood except for a one-dimensional problem [1, 2]. Tunneling in a one-dimensional or a separable system has been studied in detail by the WKB theory. Therefore the tunneling effect in chemical systems has been usually studied as a one-dimensional problem along a certain tunneling coordinate [2]. Many definitions of the tunneling coordinates (tunneling paths) in prototypical bimolecular exchange reactions such as $H+H_2 \rightarrow H_2+H$ have been proposed [6-8]. Among them, two types of paths are well-known. One is the Marcus-Coltrin path [6] which emanates from the so-called turning points of the vibrational modes transversal to the intrinsic reaction coordinate and has been used in practical calculations. Takayanagi et al. have applied the variational transition-state theory to the rate constants of $H+H_2$ reaction and its isotopic analogs along the Marcus-Coltrin path at very low temperature [9]. The other is the Miller-George path [7] which is the real parts of a complex trajectory taken into account of the classical S-matrix theory [10].

To study tunneling in a large dimensional chemical system, two approximate approaches

are often used [2]. One is the so-called 'adiabatic' or 'slow-flip' approximation and the other is the so-called 'sudden' or 'frozen bath' approximation. The adiabatic approximation is applied to the case in which a tunneling particle moves much slower than the other particles and the motion of the other particles adjusts adiabatically. Therefore multidimensional tunneling can be studied along the minimum energy path. On the other hand, the sudden approximation is applied to the case in which the tunneling particle moves much faster than the other particles and the motion of the other particles can be fixed during tunneling. Hence the straight line which connects the reactant and product valleys is selected as a tunneling path and multidimensional tunneling can be studied along this path.

Recently, Thompson et al. have applied the 'quasi-classical treatment with tunneling paths' to multidimensional tunneling in various chemical systems [11]. This method has been first proposed by Waite and Miller [12] and applied practically by Makri and Miller [13]. In the 'quasi-classical treatment with tunneling paths', a system is basically studied by quasi-classical treatment and each time a turning point occures, tunneling is treated as a one-dimensional problems along the minimum energy or the straight line path. In this method, only the multidimensional effects of the system before tunneling are taken into account.

However, the one-dimensional treatment of the tunneling effect generally leads to incorrect estimates of the tunneling splitting [14], rate constants, and the tunneling factor κ in the transition state theory at low temperature range [15] because multidimensional effects of chemical systems are not well considered in these one-dimensional treatments. The one-dimensional treatment of the tunneling effect is based on the assumption of the separability of a certain tunneling coordinate and the other coordinates during tunneling. However, chemical reaction itself is essentially a multidimensional problem and we cannot expect the separability of the tunneling coordinate and the other coordinates. What is an essential difference between one-dimensional tunneling and multidimensional tunneling? In other words, can we study multidimensional tunneling along a certain tunneling coordinate? To answer these questions, a semiclassical theory for multidimensional tunneling and its applications to chemical systems are required.

Many scientists have tried to understand multidimensional tunneling, but few semiclassical theories have been proposed [16-22]. The instanton theory which generates a classical path (an instanton path) on the inverted potential is quite well-known and has been applied to various problems [16]. Banks, Bender and Wu have introduced 'the most probable escape path' which is a classical path that has the minimum action on the inverted potential and is perpendicular to the boundary of classical forbidden region [17]. In this theory and the instanton theory, multidimensional tunneling can be studied along the particular path. Because the classical path on the inverted potential has pure imaginary momenta, these theories can construct only a pure imaginary action integral and turn out to underestimate the tunneling effect.

Recently, Huang, Feuchtwang, Culter and Kaze [18] have proposed the method on the basis of the Huygens principle that complex solutions of Hamilton-Jacobi equation can be propagated globally in real-valued configuration space. Takada and Nakamura [19] have constructed not only pure imaginary but also complex solutions of Hamilton-Jacobi equation in two dimensional systems. They solved numerically the Huygens principle of Huang et al.[18] in a tunneling region. A non-pure-imaginary complex solution is important because it gives a new kind of tunneling that had not been considered before. However, the procedure based on the Huygens principle requires terrible tasks for numerical calculation and can be applied to only two-dimensional systems.

One of the greatest virtues of Hamilton-Jacobi equation is that it gives local solutions such as classical trajectories through the canonical equations of motion [23]. A really multi-dimensional problem, of more than two degrees of freedom, can be solved because a solution is propagated along a trajectory. This idea always lies behind any semiclassical theory, even for a tunneling problem.

With these situations in mind, we develop, in Part I, a new semiclassical theory which can propagate a complex solution of Hamilton-Jacobi equation along a real-valued tunneling path in real-valued configuration space. In Part II, on the basis of the semiclassical theory for multidimensional tunneling constructed in Part I, some basic chemical reactions through

tunneling are investigated.

References

[1] L. D. Landau and E. M. Lifshitz, *Quantum mechanics*, (Pergamon, New York, 1958); L. I. Schiff, *Quantum mechanics*, (McGraw-Hill, New York, 1968).

[2] W. H. Miller, Chem. Rev. **87**, 19, (1987); G. C. Schatz, Chem. Rev. **87**, 19, (1987); A special issue on "Tunneling in Chemical Reactions," edited by V. A. Benderskii, V. I. Goldanskii and J. Jortner, Chem. Phys. **170** (1993); V. A. Benerskii, D. Makarov and C. A. Wight, the hole volume of Adv. Chem. Phys. Vol. LXXXVIII (1994); G. C. Schatz, Ann. Rev. Phys. Chem. **39**, 317 (1988).

[3] S. L. Baughcum, Z. Smith, E. B. Wilson and R. W. Duerst, J. Am. Chem. Soc. 106, 2260 (1984); P. Turner, S. L. Baughcum, S. L. Coy and Z. Smith, ibid. 106, 2265 (1984).

[4] T. Miyazaki, T. Hiraku, K. Fueki and Y. Tsuchihashi, J. Phys. Chem. **95**, 26 (1991); T. Miyazaki, S. Kitamura, H. Morikita and K. Fueki, J. Phys. Chem. **96**, 10331 (1992).

[5] K. Hiraoka, in *Proceedings of the 2nd meeting on tunneling reaction and low temperature chemistry*, edited by T. Miyazaki and Y. Aratono (Japan Atomic Energy Research Institute 1996), p. 1.

[6] R. A. Marcus and M. E. Coltrin, J. Chem. Phys. **67**, 2609 (1977)

[7] T. F. George and W. H. Miller, J. Chem. Phys. **56**, 5772 (1972) ; ibid. **57**, 2458 (1972); W. H. Miller, N. C. Handy and J. E. Adams, J. Chem. Phys. **72**, 99 (1980)

[8] R. T. Skodji, D. G. Truhlar and B. C. Garrett, J. Chem. Phys. **75**, 3019 (1981); B. C. Garrett and D. G. Truhlar, A. F. Wagner and T. H. Dunning, Jr., J. Chem. Phys. **78**, 4400 (1983); B. C. Garrett and D. G. Truhlar, J. Chem. Phys. **79**, 4931 (1983); B. C. Garrett and D. G. Truhlar, J. Chem. Phys. **81**, 309 (1984).

[9] T. Takayanagi, N. Masaki, K. Nakamura, M. Okamoto, S. Sato and G. C. Schatz, J. Chem. Phys. **86**, 6133 (1987); T. Takayanagi, K. Nakamura and S. Sato, ibid. **90**, 1641 (1989).

[10] W. H. Miller, Advan. Chem. Phys. **25**, 69 (1974).

[11] T. D. Swell and D. J. Thompson, Chem. Phys. Lett. **193**, 347 (1992); Y. Guo, T. D. Swell and D. L. Thompson, Chem. Phys. Lett. **224**, 470 (1994); Y. Qin and D. L. Thompson, J. Chem. Phys. **100**, 6445 (1994); T. D. Swell, Y. Guo and D. J. Thompson, J. Chem. Phys. **103**, 8557 (1995); Y. Guo, Y. Qin, D. C. Sorescu and D. J. Thompson, J. Chem. Phys. **104**, 4041 (1996); Y. Guo and D. J. Thompson, J. Chem. Phys. **105**, 1070 (1996); Y. Guo and D. J. Thompson, J. Chem. Phys. **105**, 7480 (1996).

[12] B. A. Waite and W. H. Miller, J. Chem. Phys. **73**, 3713 (1980).

[13] N. Makri and W. H. Miller, J. Chem. Phys. **91**, 4026 (1989).

[14] N. Shida, P. F. Barbara and J. E. Almlöf, J. Chem. Phys. **91**, 4061 (1989).

[15] D. G. Truhlar, B. C. Garrett and S. J. Klippenstein, J. Phys. Chem. **100**, 12771 (1996) and references therein.

[16] L. S. Schulman, *Techniques and Applications of Path Integration*, (Wiley, New York, 1981); A. Auerbach, S. Kivelson and D. Nicole, Phys. Rev. Lett. **53**, 411(1984); A. Auerbach and S. Kivelson, Nucl. Phys. **B257** [FS14], 799(1985).

[17] T. Banks, C. M. Bender and T. T. Wu, Phys. Rev. D. **8**, 3346; T. Banks and C. M. Bender, ibid. **8**, 3366 (1973).

[18] Z. E. Huang, T. E. Feuchtwang, P. H. Culter and E. Kaze, Phys. Rev. **A41**, 32 (1990).

[19] S. Takada and H. Nakamura, J. Chem. Phys. **100**, 98 (1994) ; ibid. **102**, 3977 (1995).

[20] A. M. Ozorio de Almeida, J. Phys. Chem. **88**, 6139 (1984).

[21] M. Wilkinson, Physica **21D**, 341 (1986).

[22] Stephen C Creagh, J. Phys. A: Math. Gen. **27**, 4969 (1994).

[23] H. Goldstein, *Classical Mechanics*. (Addison-Wesley, Reading, 1980); V.I. Arnold, *Mathematical Methods of Classical Mechanics*, (Springer, Berlin, 1978); R. Abraham and J.E. Marsden, *Foundation of Mechanics*, 2nd. ed. (Addison-Wesley, Reading 1985).

Part I.

Semiclassical Theory for Multidimensional Tunneling

Chapter I.

Tunneling Solutions of the Hamilton-Jacobi Equation for Multidimensional Semiclassical Theory

Abstracts

A new class of complex solutions to the time-independent Hamilton-Jacobi equation in the real-valued configuration space that represent multidimensional non-classical motions such as dynamical tunneling, namely energetically allowed but dynamically forbidden transition, as well as the ordinary tunneling are shown. We introduce a quantity called "parity of motion" into each coordinate in configuration space for the Hamilton-Jacobi equation, and thereby construct the new solutions. Positive parity induces merely ordinary classical motion, while the negative one allows non-classical motion like tunneling. These solutions are classified by a given set of the parities, each class of which forms a sheet in the entire solution space. New canonical equations of motion are derived, with which non-classical paths are generated in each sheet. Furthermore, it is shown that each sheet is associated with two kind of action integrals: One, which is real-valued, satisfies the principle of least action, thereby generates both ordinary and tunneling trajectories, but is not a solution to the Hamilton-Jacobi equation, while the other action is a solution to the time-independent Hamilton-Jacobi equation, and is complex-valued in a tunneling region. Only in Newtonian mechanics, which forms an extreme sheet having all the parities positive, these two actions happen to coincide with each other. Numerical examples for dynamical tunneling among tori in Hénon-Heiles system and ordinary potential tunneling in a three dimensional system are presented.

I. Introduction

The tunneling effect is one of the most fundamental concepts that only quantum mechanics has revealed [1,2]. Many phenomena related with tunneling are widely observed and applied in many areas of microscopic science and technology. Nevertheless, the understanding to this phenomenon to date does not seem complete yet. This is mostly because the tunneling effect is usually discerned based on classical concepts such as the energy of a classical path. This fact suggests, on the other hand, that new insight in classical mechanics, such as Hamilton chaos [3], can renew the current interest in the tunneling effect. In return, the definition of tunneling can become more and more vague depending on how classical mechanics is extended. Here, in the present chapter, the word tunneling is used almost as a synonym of "non-classical motion". In particular, we are not confined to the usual tunneling (called potential tunneling) in which the total energy of a path is lower than a potential. Rather, our attention is paid more to tunneling (dynamical tunneling) that connects energetically accessible but dynamically separated classical-paths.

The study of classical chaos has made great progress during these couple of decades [3], although the importance of non-integrability has long been recognized since the age of Poincaré. The stability of the orbits of the planets and classical ergodicity as a theoretical foundation of statistical mechanics are among subjects under strong focus [4]. Semiclassical studies on the mechanism of quantization of classical chaos is also one of the most exciting problems in fundamental science [5,6], since the Einstein-Brillouin-Keller (EBK) conditions [7], or the torus quantization, is not relevant to nonintegrable (chaotic) systems. The role of tunneling in chaos is another very interesting subject, since the infinite valuedness of a chaotic solution of the Hamilton-Jacobi equation can give birth to infinitely many caustics almost everywhere [8], from each of which tunneling could take place.

We address, in the present chapter and succeeding papers, to the problem of tunneling and geometry of caustics in a weakly chaotic system. By weak chaos, we mean a situation in

which relatively *thin* quasiseparatrices [3a], or chaotic zone, coexist with tori that are surrounded by the separatrices in phase space. In molecular vibration as an example, different tori separated geometrically by a quasiseparatrix give rise to qualitatively different vibrational modes. On the other hand, trajectories in the quasiseparatrix undergo these possible modes alternately with unpredictable sequence of transitions [9]. This very curious behavior extends the concept of the so-called large amplitude motion in molecular vibration. The quantum version of this weak chaos has also been studied in our laboratory [10].

Here, we concentrate on tunneling from one torus to another. In order to treat this problem and the usual potential tunneling as well, an appropriate multidimensional semiclassical theory [11] is necessary. For one-dimensional case, in which dynamical tunneling has no way to appear, semiclassical theory for tunneling has been well established [12]. In a multidimensional case, it is quite well known that the so-called instanton path is considered naturally in the framework of path integrals. [11b,13] In particular, the method of path decomposition expansion [13] has led to a deep understanding to multidimensional tunneling, although no dynamical tunneling has been treated. Generating the instanton paths is particularly simple, because they are required to run "classically" on a reversed potential. Recently, Huang, Feuchtwang, Culter, and Kaze [1] have devised an innovative method based on the Huygens principle to propagate "global" solutions of the time-independent Hamilton-Jacobi equation in the tunneling region. Both tunneling paths and the action integral are calculated simultaneously in a kind of iterative manner. Takada and Nakamura [2] have made a major progress in this line: They have settled the connection problem among the solutions in different branches, and actually carried out numerical calculations of the method of Huang et al. in two dimensional systems and thereby found out a new class of global solution. Since their works are relevant to our study, they will be referred to later.

In the present chapter, we will show that the time-independent Hamilton-Jacobi equation [14] has a new class of complex-valued "local" solutions in the real configuration space, namely a complex action integral along a new kind of real-valued trajectory. This is accomplished by introducing "parity of motion" that takes direct advantage of the property

inherent to the Hamilton-Jacobi equation. A parity, which can be either 1 or –1, is assigned to each coordinate. It is shown that a given set of the parities gives rise to its own canonical equations of motion. The entire set of trajectories thus generated by all the possible combinations of the parities form a layer structure composed of many sheets, each of which sheet is characterized in terms of a parity set. [The sheet here means essentially a new branch of solutions. However, the word branch is reserved for the usual sense in the Hamilton-Jacobi theory and the WKB approximation [11]. A single sheet therefore can have many branches.] For the parity of 1, motion in this coordinate is essentially the same as that of Newtonian mechanics. On the other hand, motion in a direction to which the parity of –1 is assigned tends to climb a potential slope against the force applied. In this way, classical mechanics can be extended beyond the ordinary Newton mechanics. However, the "non-classical" solutions are of physical relevance only when considered in the context of quantum (or semiclassical) mechanics. For instance, tunneling is regarded as a sequence of paths that starts in the ordinary space (sheet) with all the positive parities, and jumps into one of non-classical sheets at a some caustic point and stay there for a short "time", then comes back to the original space. Furthermore, it is shown that two different action integrals are associated with each sheet. One is real-valued, and satisfies the principle of least action and thereby generates non-classical (tunneling) paths, but is not a solution to the Hamilton-Jacobi equation. The other is a complex-valued solution to the time-independent Hamilton-Jacobi equation. Both these action-integrals and geometry of paths should be connected smoothly with those of the neighboring sheets, respectively. We thus find local but non-classical solutions to the Hamilton-Jacobi equation. One of the greatest advantages of constructing the local solutions is, of course, its applicability to many dimensional system. The solution space includes two extreme sheets. One is that for the Newtonian mechanics as stated above, and the other is that for the so-called instanton paths [11b,13] for which all the parities are negative. Our theory claims with explicit construction that in-between these extremes there exist many independent solutions.

The structure of the present chapter is as follows. In Section II, we extend classical

mechanics so that non-classical paths can be generated. The action integral which is a solution of the time-independent Hamilton-Jacobi equation is constructed in Sec.III. Some numerical examples for various tunnelings, including dynamical tunneling among different tori, are presented in Sec.IV. The present chapter concludes in Sec.V with some remarks.

II. Parity of Motion

A. The stationary state Hamilton-Jacobi equation

Our goal in the present chapter is to find local and non-classical solutions in the time independent Hamilton-Jacobi (HJ) equation [14] for a given energy E,

$$\frac{1}{2}\sum_k \left(\frac{\partial W}{\partial q_k}\right)^2 + V(\vec{q}) = E, \tag{2-1}$$

where V is a potential energy in configuration space $\{q_i,\ i=1,\cdots,N\}$. We use the so-called mass-weighted coordinates so that all the masses that otherwise should have been included in Eq.(2-1) can be taken to be unity. HJ equation corresponds to the standard classical Hamiltonian

$$H = \sum_k \frac{1}{2} p_k^2 + V(\vec{q}). \tag{2-2}$$

The solutions of HJ equation are vital to quantum mechanics as well, since as is well known, HJ equation can be found as the lowest order approximation to the WKB expansion of the Schrödinger equation [11,12]. However, it has been suggested by Schrödinger himself that HJ equation is more than equivalent to Newtonian (or Hamiltonian) mechanics. This can be seen clearly by a transformation [15]

$$W = K \log\psi \tag{2-3}$$

that leads to

$$\frac{K^2}{2}\sum_k\left(\frac{\partial\psi}{\partial q_k}\right)^2 + (V(\vec{q}) - E)\psi^2 = 0. \tag{2-4}$$

Then, the following variational functional

$$I(\psi, \psi') = \int f(\psi(\vec{q}), \psi'(\vec{q}))\, d\vec{q} \tag{2-5}$$

with

$$f(\psi, \psi') = \frac{K^2}{2}\sum_k\left(\frac{\partial\psi}{\partial q_k}\right)^2 + (V(\vec{q}) - E)\psi^2, \tag{2-6}$$

is made stationary, where ψ' is a collective representation of the first derivatives of ψ with respect to all q_k's. The Euler-Lagrange variational procedure under appropriate boundary conditions gives the stationary state Schrödinger equation

$$-\frac{K^2}{2}\sum_k\frac{\partial^2\psi}{\partial q_k^2} + V(\vec{q})\psi = E\psi \tag{2-7}$$

with a replacement $K = \hbar$. This derivation suggests that solutions to the Schrödinger equation could be constructed in terms of the general solutions, including non-classical ones, of HJ equation. (We are not claiming that HJ equation is equivalent to the Schrödinger equation.)

In the pure classical (Newtonian) mechanics, it is sufficient to consider only the real-valued solutions in a real configuration space. However, the most important point in the above quantum-classical correspondence is the relation of Eq.(2-3), where a wavefunction can be either positive or negative, or even complex in this space. Accordingly, the function W in this situation should be generally complex in the real space. In fact, Takada and

Nakamura [2] are probably the first who actually constructed not only pure imaginary but also complex global-solutions to HJ equation in two dimensional systems. They solved numerically the Huygens principle of Huang et al.[1] in a tunneling region. A non-pure-imaginary complex solution is important because it gives a new kind of tunneling that had not been considered before (see ref.[2] and our later discussion). We thus remain in the real-valued configuration space rather than making analytical continuation into a multidimensional complex space, which is a standard, but never simple, idea in the sophisticated versions of semiclassical theory [11a,12,16,17,18].

On the other hand, one of the greatest virtues of HJ equation is that it gives local solutions such as classical trajectories through the canonical equations of motion [14]. A really multidimensional problem, of more than 2 degrees of freedom, can be solved because a solution is propagated along a trajectory. This idea always lies behind any semiclassical theory, even for a tunneling problem. We therefore attempt to propagate a local complex solution of HJ equation along a path that is newly constructed in real-valued configuration space.

B. Parity of Motion

Upon looking at HJ equation, Eq.(2-1), we immediately notice that it is invariant to multiplying the following constant σ_k for each coordinate k such that

$$\frac{1}{2}\sum_k\left(\frac{1}{\sigma_k}\frac{\partial W}{\partial q_k}\right)^2 + V(\vec{q}) = \frac{1}{2}\sum_k\left(\frac{\partial W}{\partial q_k}\right)^2 + V(\vec{q}) = E, \tag{2-8}$$

provided that $\sigma_k^2 = 1$. We call this constant "parity of motion", since it is simply 1 or –1. The effect of the parities is not as trivial as it seems at first sight. Rewrite HJ equation as

$$\frac{1}{2}\sum_k(\dot{q}_k)^2 + V(\vec{q}) = \frac{1}{2}\sum_k\left(\frac{\partial L_{cl}}{\partial\dot{q}_k}\right)^2 + V(\vec{q}) = E, \tag{2-9}$$

with use of the standard relation between the classical Lagrangian L_{cl} and W [14]

$$\frac{\partial L_{cl}}{\partial \dot{q}_k} = \frac{\partial W}{\partial q_k} = \dot{q}_k. \tag{2-10}$$

Here again, one can introduce the parities into Eq.(2-9) as

$$\frac{1}{2}\sum_k \left(\frac{1}{\sigma_k}\frac{\partial L}{\partial \dot{q}_k}\right)^2 + V(\vec{q}) = \frac{1}{2}\sum_k \left(\frac{\partial L}{\partial \dot{q}_k}\right)^2 + V(\vec{q}) = E, \tag{2-11}$$

where we have distinguished L from L_{cl}, since we may be already out of bounds of Newtonian mechanics. Comparison of Eqs.(2-9) and (2-11) suggests a dynamical relation

$$\dot{q}_k = \frac{1}{\sigma_k}\frac{\partial L}{\partial \dot{q}_k}. \tag{2-12}$$

If $\sigma_k = 1$ for all k, this is nothing but Newtonian mechanics. However, we show below that a consistent theory of mechanics can be constructed also for general sets of $\{\sigma\} = \{\sigma_1, \sigma_2, \cdots\}$. First of all, define a real-valued parameter θ that mimics the role of time. (Note again that we are thinking of the time-independent HJ equation, and thus no physical time is involved here.) The dynamics is evolved along θ. Each coordinate has its own chronological parameter such that

$$\tau_k = \frac{\theta}{\sqrt{\sigma_k}}. \tag{2-13}$$

Next we regard the relation given in Eq.(2-12) as the re-definition of a Lagrangian $L(q,\dot{q},\theta)$ for non-classical motion,

$$\dot{q}_k = \frac{dq_k(\theta)}{d\theta} = \frac{1}{\sigma_k}\frac{\partial L(q,\dot{q},\theta)}{\partial \dot{q}_k}, \tag{2-14}$$

the explicit form of which will be constructed later. The corresponding momentum is defined,

on the other hand, by

$$p_k = \frac{dq_k(\theta)}{d\tau_k} = \sqrt{\sigma_k}\,\dot{q}_k, \tag{2-15}$$

which is pure imaginary for the anti-Newtonian motion. The reason for this definition will become clear later. A real-valued quasi-momentum is defined by

$$\bar{p}_k = \frac{1}{\sqrt{\sigma_k}} p_k = \frac{1}{\sigma_k}\frac{\partial L(q,\dot{q},\theta)}{\partial \dot{q}_k}, \tag{2-16}$$

which is essentially equivalent to $\dot{q}_k$. $\bar{p}_k$ will be utilized in practical calculation, whereas p_k has only theoretical significance to facilitate investigation of, for example, symmetry property in differential forms (see Sec.IID).

The equation of motion can be derived as usual in terms of the Euler-Lagrange variational principle,

$$\delta \int_{\theta_1}^{\theta_2} L(q,\dot{q},\theta)\,d\theta = 0, \tag{2-17}$$

which is immediately followed by

$$\frac{d}{d\theta}\left(\frac{\partial L}{\partial \dot{q}_k}\right) - \frac{\partial L}{\partial q_k} = 0, \tag{2-18}$$

that is

$$\sigma_k \dot{\bar{p}}_k = \sigma_k \frac{d\bar{p}_k}{d\theta} = \frac{\partial L}{\partial q_k}. \tag{2-19}$$

On the other hand, since we have the total derivative of the Lagrangian as

$$d\left(L - \sum_k \sigma_k \bar{p}_k \dot{q}_k\right) = \sum_k \sigma_k \left(\dot{\bar{p}}_k dq_k - \dot{q}_k d\bar{p}_k\right), \tag{2-20}$$

a Hamiltonian $H(\{\sigma\})$ can be introduced as usual by putting

$$d\,H(\{\sigma\}) = -\sum_k \sigma_k \left(\bar{p}_k d q_k - \dot{q}_k d\,\bar{p}_k\right) \tag{2-21}$$

and hence

$$H(\{\sigma\}) + L = \sum_k \sigma_k \bar{p}_k \dot{q}_k . \tag{2-22}$$

Equation (2-21) leads to a new set of canonical equations of motion for a non-classical motion as

$$\begin{cases} \sigma_k \dot{\bar{p}}_k = -\dfrac{\partial H(\{\sigma\})}{\partial q_k} \\ \sigma_k \dot{q}_k = \dfrac{\partial H(\{\sigma\})}{\partial \bar{p}_k}, \end{cases} \tag{2-23}$$

from which the explicit form of the Hamiltonian can be obtained as

$$H(\{\sigma\}) = \sum_k \frac{\sigma_k}{2} \bar{p}_k{}^2 + V(\vec{q}). \tag{2-24}$$

The corresponding Lagrangian is also written down explicitly with use of the relation of Eq.(2-22). In these equations up to Eq.(2-24), the Hamiltonian has been denoted by $H(\{\sigma\})$ in order to remind that it is not the same as the standard Hamiltonian of Eq.(2-2). In what follows, we shall simply write it as H, unless otherwise confusion is expected.

Judging from the equations of Eq.(2-23), it would be almost appropriate to regard the role of the parities as

$$\sigma_k = \begin{cases} 1 & \text{for classical (Newtonian) motion} \\ -1 & \text{for non - classical (anti - Newtonian) motion .} \end{cases}$$

However, it should be noted that these motions are generally coupled among different coordinates in a non-separable system. Also, it is clear from the foregoing derivation that any local separability has not been applied.

The above equations of motion hold for an individual set of parities $\{\sigma_1, \sigma_2, \cdots\}$, and thus all the trajectories generated in each set constitute a sheet, which in turn leads to a layer structure in the entire solution space, which is depicted in Fig.1. We have two extreme sheets here, one being located at the top with all the parity positive, while the other at the bottom having all the negative parities. The former is trivially for the ordinary Newton mechanics. The latter is also obvious that the paths there are the so-called instanton paths [11b,13].

Further, it is quite easy to show

$$\frac{d\,H}{d\,\theta} = 0. \tag{2-25}$$

So, the Hamiltonian still bears the physical meaning as energy, and the energy is conserved along a path.

C. The principle of least action

The mechanics thus generalized leads us to a natural definition of an action integral such that

$$W_{\rm cl} = \sum_k \int \sigma_k \bar{p}_k dq_k . \tag{2-26}$$

This real-valued integral is to be taken along a path generated by Eq.(2-23) within a given

sheet. Since we will introduce another action integral in the next section, we shall call W_{cl} the path-action.

As is checked easily, W_{cl} is not a solution of HJ equation, unless all the parities happen to be positive unity. Nonetheless, the path-action is theoretically important, since it satisfies the principle of least action just as in Newtonian mechanics, and is thus responsible for generating both classical and non-classical paths. The proof for the principle of least action proceeds with almost complete parallelism with that for the standard analytic mechanics [14]. We take a variation of

$$W_{cl} = \sum_k \int_{\theta_1}^{\theta_2} \sigma_k \, \bar{p}_k \, \dot{q}_k \, d\theta = \int_{\theta_1}^{\theta_2} (L + H) \, d\theta \tag{2-27}$$

such that

$$\Delta W_{cl} = \Delta \int_{\theta_1}^{\theta_2} L \, d\theta + E(\Delta\theta_2 - \Delta\theta_1) , \tag{2-28}$$

where Δ requires the variation to be taken as a problem of free boundary, which should be compared to the variation δ in Eq.(2-17) under the fixed boundary conditions [14a]. After some lengthy manipulations, we reach

$$\Delta W_{cl} = \left[\left(-\sum_k \sigma_k \, \bar{p}_k \, \dot{q}_k + L + H \right) \Delta\theta \right]_{\theta_1}^{\theta_2} = 0 \tag{2-29}$$

that completes the proof. In the proof, the fundamental relations, namely, the energy conservation, Eq.(2-25), the Lagrange's variational principle, Eq.(2-17), and Hamiltonian-Lagrangian relation, Eq.(2-22), are all made use of.

D. Transformation property

The transformation property of the present mechanics has not yet been fully investigated.

In order to see the invariance property inherent to the Hamilton system, the following coordinates are convenient,

$$\begin{cases} Q_k = \sqrt{\sigma_k} \, q_k \\ P_k = \sqrt{\sigma_k} \, \bar{p}_k = p_k , \end{cases} \tag{2-30}$$

where both Q_k and P_k are pure imaginary, if $\sigma_k = -1$. Then Eq.(2-23) is transformed to

$$\begin{cases} \dot{P}_k = -\dfrac{\partial H(\{\sigma\})}{\partial Q_k} \\ \dot{Q}_k = \dfrac{\partial H(\{\sigma\})}{\partial P_k} \end{cases} \tag{2-31}$$

which looks much similar to the Hamilton canonical equations, and thereby rationalizes the definition of the momentum in Eq.(2-15). The proof for the theorem of absolute invariance due to Poincaré-Cartan [14c] can be applied to our case, which claims that a flow in phase space induced by the Hamiltonian $H(\{\sigma\})$ should conserve a two-form

$$\omega^2 = \sum_{k=1}^{N} dP_k \wedge dQ_k \tag{2-32}$$

and the higher order differential forms analogous to this. The Stokes theorem [14] brings Eq.(2-32) back to the expression of the path-action, Eq.(2-26). The integrability of non-classical trajectories can be studied on the basis of Eqs.(2-26) and (2-32).

An important consequence from Eq.(2-32) is the Liouville theorem. The conservation of phase-space volume is thus assured in each sheet. Note again that the two-form in Eq.(2-32) is real-valued irrespective of the parities. However, the volume-conservation should not be confused with rapid (exponential) diminishing of the amplitude of a tunneling wavefunction, which is relevant to tunnel probability. This is our subject in the next section.

III. Two Kind of Action Integrals

A. An action integral as a solution to HJ equation

As noted above, the path-action, Eq.(2-26), is not a solution of the time-independent HJ equation, once any one of the parities is set negative. This situation is markedly different from the basic idea due to Jacobi that an action integral satisfying HJ equation should give birth to a trajectory as its characteristic line [14]. This idea does not hold here. To be more precise, an action integral that satisfies HJ equation can be different from the path-action W_{cl} in non-classical domain.

In fact, once a path is obtained, a solution to HJ equation (W_{HJ}), which is called HJ-action, can be readily constructed in such a way that

$$W_{HJ} = \sum_k \int \sqrt{\sigma_k}\, \bar{p}_k\, dq_k . \tag{3-1}$$

Again this integral is to be taken along the path. With the help of the usual relation (cf. Eq.(2-16))

$$\frac{\partial W_{HJ}}{\partial q_k} = \sqrt{\sigma_k}\, \bar{p}_k = p_k \tag{3-2}$$

and the Hamiltonian of Eq.(2-24), the proof for W_{HJ} to satisfy HJ equation is straightforward. Note also that not only W_{HJ} of Eq.(3-1) but also other functions such as

$$W = \sum_k \int \sigma_k \sqrt{\sigma_k}\, \bar{p}_k\, dq_k \tag{3-3}$$

can be a solution as well, since the latter is simply the complex conjugate of Eq.(3-1). It is quite straightforward to see that only in Newtonian mechanics W_{HJ} coincides with W_{cl}.

Unlike W_{cl}, W_{HJ} can become complex, the imaginary part of which comes from the coordinates of negative parities. By writing

$$W_{HJ} = W_R + i\, W_I \tag{3-4}$$

HJ equation is split into

$$\frac{1}{2}\sum_k \left\{ \left(\frac{\partial W_R}{\partial q_k} \right)^2 - \left(\frac{\partial W_I}{\partial q_k} \right)^2 \right\} + V(\vec{q}) = E \tag{3-5}$$

and

$$\vec{\nabla} W_R \bullet \vec{\nabla} W_I = 0. \tag{3-6}$$

These two relations have to be satisfied by any solution of HJ equation, and they are in fact satisfied by W_{HJ}. The second equation is fulfilled because the coordinates with positive and negative parities are chosen to be orthogonal to each other.

B. Tunneling probability

A semiclassical wavefunction can be generally written as [11]

$$\psi = A \exp\left(\frac{i}{\hbar} W_{HJ} \right). \tag{3-7}$$

The pre-exponential factor A need not be explicit here [11]. Inserting Eq.(3-4) into Eq.(3-7), one gets

$$\psi = A \exp(-\frac{1}{\hbar} W_I)\ \exp(\frac{i}{\hbar} W_R), \tag{3-8}$$

where the phase convention to W_{HJ} is taken so that W_I becomes positive. The first exponential term represents the decrease of the norm of the wavefunction in a non-classical region.

In the classical limit, that is $\hbar \to 0$, a wavefunction in Eq.(3-8) becomes obviously zero for any non-zero value of W_I, and thus we observe no tunneling practically. Accordingly, in macroscopic situation one can by no means realize the sheets other than the Newtonian one. However, as soon as one enters into microscopic physics, the non-Newtonian parts must be considered.

C. Connection problem

The Hamilton-Jacobi equation has in general multi-valued solutions. As long as a set of the parities is fixed, any path generated by Eq.(2-23) remains in the same sheet, and each sheet defines an independent branch of solutions. Tunneling solutions are hence obtained by connecting a non-classical sheet with the classical one smoothly. In other words, tunneling begins when a classical path of $\{\sigma\} = \{1, 1, 1, \cdots\}$ is connected at a point by changing one or more parities. After residing in tunneling sheet(s) for a while it comes back to a classical path at another point by returning to $\{\sigma\} = \{1, 1, 1, \cdots\}$, and tunneling is over. From the view point of the Hamilton-Jacobi theory alone, any complicated transition among sheets is equally accepted as far as the connections can take place smoothly. However, as a path stays in a tunneling region for a longer time, more precisely larger θ, the survival probability of a tunneling wavefunction becomes exponentially smaller, as is suggested in Eq.(3-8). This is more likely so, when the number of the negative parities is larger.

At a point on a path where some of the parities are changed, the HJ-actions have to be connected smoothly as well as the geometry of the path. In addition, HJ equation (2-1) and the energy conservation law Eq.(2-25) require energy to be conserved globally through the connected paths. All these arguments suggest that a path should have zero momentum in a direction in which a parity is changed. Generally speaking, a coordinate normal to a caustic

surface in configuration (q-) space, is accepted as such a direction [1]. Suppose that a trajectory encounters a caustic point with no degeneracy. An orthogonal transformation of the coordinate system is performed so that the coordinate normal to the caustic surface is given a negative parity. For all the other (orthogonal) directions, the momenta and parities remain unchanged. Hence, the trajectory enters a sheet to which a single negative parity is assigned. We therefore note that a different direction normal to a caustic surface gives rise to a different way of assignment of the parity set, even though the number of the negative parities are same.

Caustics are generally defined in a classical region with a Jacobian determinant in such a way that [11]

$$\det \left| \frac{\partial \vec{q}_f}{\partial \vec{p}_i} \right| = 0, \tag{3-9}$$

where $\vec{p}_i = \{p_1, p_2, p_3, \cdots\}$ and $\vec{q}_f$ are a momentum vector at the initial point and a position vector at the final end of a trajectory, respectively. The inverse of the Jacobian determinant is known to represent the density of paths in configuration space [11]. Caustics are important not only from the geometrical requirements, but because the amplitude of a wavefunction, the factor A in Eq.(3-7), becomes large (in fact, infinite in the primitive WKB function) at caustics, since A is essentially proportional to the square inverse of the Jacobian determinant [11]. The calculation of caustics and coordinate transformation for any set of the parities are defined in an analogous manner. The initial vector $\vec{p}_i$ in Eq.(3-9) should be replaced with a quasi-momentum $\bar{\vec{p}}_i = \{\bar{p}_1, \bar{p}_2, \bar{p}_3, \cdots\}$. The computation of the Jacobian determinant can be carried out with a straightforward extension.

A trajectory can bifurcate occasionally by switching its parities. In Fig.2 is shown a schematic diagram of the proliferation of many bifurcations from a trajectory in a 3D system. Suppose first that we have a classical trajectory with a parity set {1,1,1} for $\{x, y, z\}$ coordinates, respectively. At a caustic point, this path can bifurcate into two trajectories; one continues to be classical. A non-classical path is also generated by setting a new set, for

instance $\{-1,1,1\}$, after an orthogonal transformation of the coordinates according to the geometry of the caustic surface. Hence it should be understood that the sets of parities in Fig.2 are not necessarily assigned to the same coordinates $\{x, y, z\}$. The path thus having entered into a tunneling region can change its parities at another point and it either gets out the tunneling region, enters different tunneling regions, or remains in the same tunneling region. In this way, infinitely many series of bifurcation can continue. Incidentally, the number of the zero-eigenvalues in Eq.(3-9) is not necessarily one at a caustic point, although this degeneracy is a minor case in general. Should it happen, some of the corresponding parities can be changed simultaneously. However, note that the number of parities to be changed can be smaller than the order of degeneracy. Therefore a path at this point can bifurcate into the number of paths. This aspect will be discussed in a great detail in our forthcoming paper [19].

Mathematically one can enjoy many variety of bifurcations of non-classical trajectories. But, most of them are of little physical relevance because their quantum mechanical amplitudes can be very small due to Eq.(3-8). In particular, a trajectory bearing more negative parities tends to have a smaller contribution. So does a trajectory staying longer in a non-classical region. Thus trajectory that are physically significant are to be selected in this principle. More will be described in the presentation of the following numerical examples.

IV. Numerical Examples of Tunneling Paths

In order to see which kind of tunneling paths are generated, we present three numerical examples in this section. Basically, all the numerical calculations shown below have been done on a common basis: For a given potential function in an N ($N \geq 2$) dimensional system, a classical trajectory is started with positive parities only. Along a path, caustics are found through the direct calculation of Eq.(3-9). The geometry of each caustic surface determines an orthogonal transformation of the coordinates, which in turn is used to assign a

new set of parities. A new trajectory resumes running after some of the parities are turned to be negative with the same momenta as before. In particular, zero component of the momentum should be assigned to the direction of the negative parity. Hence the trajectory is smoothly bifurcated. Then the newly born tunneling path runs for a while in the new coordinates until it hits another conjugate point. There, the similar procedure is repeated to let the path return into the classical region.

Tunneling probability depends dramatically on the magnitude of the Planck constant in semiclassical situation. However, since we have no reason to choose a particular magnitude of $\hbar$ in our adopted models, no result of tunneling probability will be reported, although we have carried out the computations.

2D double-well potential

The first example is a rather simple Hamiltonian system having a widely known potential called the squeezed double well [13b], that is

$$H = \frac{p_x^{\,2}}{2m_x} + \frac{p_y^{\,2}}{2m_y} + \frac{1}{8}(x-1)^2(x+1)^2 + \frac{1}{2}\left[2.25 + 5\left(x^2-1\right)^2\right]y^2, \tag{4-1}$$

where $m_x = m_y = 1.0$ [20]. The potential surface is drawn in Fig.3. The squeezed double well is one of the potential functions for which Auerbach and Kivelson extensively studied two-dimensional potential-tunneling in terms of the instanton paths with their path decomposition expansion [13]. This pioneering work has also treated the amplitude factor in their adiabatic fluctuation approximation [13b]. Our main aim in the present chapter, on the other hand, is to show new tunneling trajectories that are not instanton paths.

A trivial example of a turning point can be found on the straight line $y = 0$, namely the x -axis. Changing the two parities into negative unity, an instanton path is generated [13b]. But, our interest here is not in such a case. A trajectory in the right valley of Fig.3(a) has the energy $E = 0.12$, which is to be compared with the energy at the saddle point

$E = 0.125$. Thus this is simply a potential tunneling. The trajectory encounters a caustic point at the left-most part, as is visibly confirmed. There, only the parity of the x-direction is changed to be negative, and the trajectory enters into a tunneling region. No coordinate transformation is required in the present case. The trajectory in Fig.3(b) represents the tunneling. In order to emphasize how the tunneling path looks like, we intentionally let it proceed without changing the parity at the first caustic point, which is seen in the left-most point in the figure. This is, of course, an extremely unfavorable procedure that should result in a very small tunneling probability. At an instance when the tunneling trajectory comes to the third caustic point, which is again seen at the left-most part, the negative parity has been brought back to be positive, and a trajectory comes out in the left side valley as a purely classical path. This is seen as the trajectory in the left-hand-side valley of Fig.3(a).

3D double-well potential

The next system is a straightforward extension of the above example to a three dimensional system as

$$H = \frac{p_x^{\,2}}{2m_x} + \frac{p_y^{\,2}}{2m_y} + \frac{p_z^{\,2}}{2m_z} + \frac{1}{8}(x-1)^2(x+1)^2 + \frac{1}{2}\left[2.25 + 5\left(x^2-1\right)^2\right]y^2 + \frac{1}{2}\left[2.25 + 5\left(x^2-1\right)^2\right]z^2 \tag{4-2}$$

with $m_x = m_x = 1.0$, and $m_z = 1.0087$. The masses are chosen so as to break the symmetry for the reason of graphic presentation. The energy of a trajectory under study is $E = 0.108$, and again the saddle point is as high as $E = 0.125$. Two purely classical trajectories in Fig.4(a) sit in two symmetrical valleys which are separated by a saddle, the right one being the starting trajectory. At a caustic point along this trajectory, a tunneling path is born as shown in Fig.4(b). As in the 2D case above, the tunneling trajectory has only one negative parity in the x-direction, and again the three way trip has been enforced for presentation. At the caustic point in this tunneling path, all the parities are brought back to positive values,

and a classical trajectory in the left valley of Fig.4(a) comes about. This example verifies that the theory can be easily applied to as large a system as the ordinary classical trajectory method can produce. Nonetheless, to our best knowledge, we are aware of no other calculation for 3D tunneling of non-instanton type by means of the other methods.

Dynamical tunneling in Hénon-Heiles system

We consider dynamical tunneling in the well-known Hamiltonian system due to Hénon and Heiles [21], that is

$$H = \frac{p_x^{\,2}}{2m_x} + \frac{p_y^{\,2}}{2m_y} + \frac{1}{2}\left(x^2+y^2\right) + x^2 y - \frac{1}{3}y^3. \tag{4-3}$$

To make the dynamics a little simpler by breaking symmetry, we take the masses as $m_x = 1.0087$ and $m_y = 1.0$. The potential has a basin around the origin which can bound trajectories of the energy less that 1/6. The contour plot and the perspective view mainly of the basin area is drawn in Fig.5. On the other, no trajectory is trapped outside the basin. The most significant feature of the potential is that the basin area does not have potential barrier in the angular direction around the origin. Nevertheless, the system bears several distinctive modes. A clear example is given in Fig.6, in which all the trajectories share the same energy $E = 0.09$, but have different initial conditions [9]. All the trajectories start from $x = y = 0$ at the initial time with the positive momenta $p_x, p_y \geq 0$. The trajectories are labeled with f_x that means the initial ratio of the energy assigned to x-coordinate to the total one. Two different type of librations, and rotations (left-ward and right-ward) are confirmed in Fig.6. They are all supposed to wind around different tori.

Since the initial condition can be changed continuously with f_x, one can ask himself what happens in between these clear-cut modes. For example, what is the mode of a trajectory of a parameter f_x in a very small interval [0.522, 0.533]. (See Fig.6.) This is actually a motion in a thin quasiseparatrix and is quite interesting. The motion first shows either

libration (as in $f_x = 0.533$) or left or right rotation (as in $f_x = 0.522$) depending on f_x chosen. This mode is very clear at least macroscopically and can be identified numerically with a clear-cut quantity [9]. Then, all of sudden a transition from the mode to one of the other possible modes occurs. The transitions among the clear modes continue with no definite frequency [9]. This weakly chaotic mode defines a new kind of large amplitude motion. We have studied the spectroscopic characterization of its quantum analog [10].

When a quantum state is localized mainly in a torus area rather than the thin quasiseparatrix, one can consider a possibility of tunneling among the available tori such as those described above, namely, dynamical tunneling. A classical trajectory of $f_x = 0.533$ having a libration mode is considered here just as an example. (See Fig.6.) It has many caustic points widely distributed in the configuration space, as is seen in Fig.7(a). The outer caustics enveloping the trajectory in the region of large values of $x^2 + y^2$, where the potential energy becomes very close to the total energy, form systematic caustic lines. It has turned out that all the tunneling paths starting from this type of caustics go outside the basin without encountering a caustic point inside it. They eventually run away infinitely far from the origin, and hence does not give rise to dynamical tunneling. On the other hand, the caustics depicted in Fig.7(b), which are extracted from those of Fig.7(a), are actually associated with dynamical tunneling. A little more than 10 % of the caustics examined are thus responsible for dynamical tunneling. This results suggests that *chance* of tunneling would not be small. In our quantum mechanical calculations, on the other hand, we have often observed that mixing of rotation and libration modes are so strong that they are not well separated [10], which should reflect frequent occurrence of the tunneling.

Among the caustics in Fig.7(b), we pick up a point located at $(x, y) = (-0.33, -0.10)$ [see Fig.8(a) for the scale], and follow a tunneling path emanating there. Since the caustic line has an angle about 13.8 degrees measured counter-clockwise from the positive x -axis, the coordinates are rotated by the same angle clockwise to form, say, (x', y')-coordinates, so that the zero-momentum component directs towards the y'-axis. The parity in this direction is changed to be negative unity and the tunneling path runs until the first caustic is encountered

along this path (Fig.8(b)). At this point, namely $(x', y') = (0.32, 0.09)$ [corresponding to $(x, y) = (0.29, 0.16)$], the (x', y')-coordinate system is rotated 30.4 degrees anti-clockwise to the (x'', y'')-coordinates. Then the parities are brought back to {1, 1}. A new classical path thus resumed happens to be bound with the mode of left-rotation in the basin (Fig.8(c)).

We have also examined the instability of the tunneling path, since our system is weakly chaotic and the individual modes such as the libration and rotation modes are separated classically by the chaotic zones. Chaos can be detected by looking at the eigenvalues of the following Jacobian matrix [3-5]

$$\frac{\partial(\bar{q}_f, \bar{p}_f)}{\partial(\bar{q}_i, \bar{p}_i)}, \tag{4-4}$$

the minor of which has already appeared in Eq.(3-9). Since our system is a two dimensional Hamilton system, its eigenvalues should be obtained as a set $\{e^{ia}, e^{-ia}, e^{ib}, e^{-ib}\}$ [14]. A complex value a or b indicates (local) chaos, while if both are real, the system is stable. Figure 9 displays the largest absolute magnitude among the eigenvalues as a function of the chronological parameter θ. As seen directly, this particular tunneling-path is considerably unstable. In fact, the Liapunov exponent evaluated from this curve is 0.888. Although the role of chaos in tunnel probability is not yet clear, it would be conceived that a stable tunneling path should have a stable family of tunneling paths around it (with some finite measure) and hence contribute positively to the tunneling probability. In any case, the interplay between tunneling and chaos requires much study [19].

The second example is a path of dynamical tunneling from the same classical path as the first example of $f_x = 0.533$ but starting from a different caustic point (Fig.10). The tunneling path is rather more complicated here. It starts at a point (0.09, –0.09), which is marked by "A" in Fig.10(b). Only a slight rotation of the coordinates is required in this case. It proceeds rightward first, and happens to encounter a turning point at the point "B". This particular point is not detected by the condition of Eq.(3-9), but by [11b]

$$\frac{\partial E(q_f, q_i, \theta)}{\partial \theta} = 0, \tag{4-5}$$

where $E(q_f, q_i, \theta)$ is an energy for a path to require to travel from q_i to q_f during a given "time" θ. At this turning point, one can change two parities at the same time or one of the two parities, which can give rise to three new paths. This phenomenon is quite interesting and will be reported elsewhere. In this occasion, we do not consider this possibility. The path is simply bounced back without changing the parities there, and thus retraces the same path to another caustic point C of $(-0.37, -0.16)$. There the tunneling is over and a new classical path is generated as shown in Fig.10(c). Again, the tunneling path is chaotic, as shown in Fig.11, and the Liapunov exponent has been in fact 1.064.

V. Concluding Remarks

We have shown that complex solutions for the time-independent Hamilton-Jacobi equation can be propagated along newly constructed paths in the real-valued configuration space. The paths are generated with introducing the parity set, and the entire space of the all possible solutions forms a layer structure composed of independent sheets, each of which defines a branch of solutions to be characterized by a parity set. Two extremes of the sheets are assigned to the ordinary Newton mechanics for which all the parities are positive unity, and to the space of instanton paths having all the parities negative. It has been also shown that equations of motion are associated with each sheet to evolve trajectories, and that two kind of action integrals are integrated along a path. One is the path-action, which is real and satisfies the principle of least action, but is not a solution of HJ equation. The other, called H-J action, can take a complex value and satisfies the Hamilton-Jacobi equation. These two actions happen to coincide with each other only in Newton mechanics.

These local solutions in the non-Newtonian sheets, for which at least one of the parities is negative, are of physical significance to represent tunneling only when they are

considered in the semiclassical or quantum context. In particular, it is the HJ-action that should be taken in the WKB wavefunction, the imaginary part of which represents the decay of a wavefunction in a tunneling region.

Some numerical examples have been presented. In particular, we have clearly shown dynamical tunneling between the distinctive modes in the Hénon-Heiles Hamiltonian. Since the chaotic nature of the tunneling trajectories leads to an interesting phenomenon, we will report more on this in our forthcoming paper [19]. We also have calculated a tunneling path of non-instanton type in three dimensional space for which only one direction bears a negative parity. This numerical calculation has demonstrated that the present theory can be applied to large systems in a straightforward manner. In a large system, only the instanton-type theory has been a practical method so far [13]. However, it is quite natural to expect that an instanton-type path, in which all the parities are set negative, would results in only an extremely small tunneling probability as the degrees of freedom increase. We will report the effect of high dimensionality to dynamical tunneling as well as tunneling in a curved space in our future article [19].

We have not described very precisely the connection problem of solutions in neighboring sheets. Takada and Nakamura gave an excellent theory for the multidimensional connection problem of global solutions of the time independent HJ equation [1]. The connection problem is quite important to our scheme, too. However, since we have treated the local solutions in the present chapter, and since our theory can be readily extended to the time dependent Hamilton-Jacobi equation, this aspect will be reported with more examples of three or higher dimensional systems as well as tunneling in scattering problems [19].

References

[1] Z.H. Huang, T.E. Feuchtwang, P.H. Culter, and E. Kaze, Phys. Rev. **A41**, 32 (1990).

[2] S. Takada and H. Nakamura, J. Chem. Phys. **100**, 98 (1994), and references cited therein.

[3] (a) A.J. Lichtenberg and M.A. Lieberman, *Regular and Stochastic Motion* (Springer, Berlin, 1983).

(b) V.I. Arnold and A. Avez, *Ergodic Problems of Classical Mechanics* (Benjamin, Reading, Massachusetts, 1968).

[4] (a) R.Z. Sagdeev, D.A. Usikov, and G.M. Zaslavsky, *Nonlinear Physics* (Harwood Academic Publishers, 1988).

(b) M. Tabor, *Chaos and Integrability in Nonlinear Dynamics* (Wiley, New York, 1989).

(c) D.K. Campbell Ed. *Chaos* (American Institute of Physics, New York, 1990).

[5] (a) A.M. Ozorio de Almeida, Hamiltonian Systems: *Chaos and Quantization* (Cambridge Univ. Press, Cambridge, 1988).

(b) M.C. Gutzwiller, *Chaos in Classical and Quantum Mechanics* (Springer, New York, 1990).

(c) H.A. Cerdeira, R. Ramaswamy, M.C. Gutzwiller, and G. Casati, *Quantum Chaos* (World Scientific, Singapore, 1991).

[6] (a)M.C. Gutzwiller, J. Math. Phys. **11** (1970), 1791 ; **12** (1971), 343.

(b)R.B. Balian and C.Bloch, Ann. Phys. **60** (1970) 401; *ibid.* **85** (1974) 514.

(c) K. Takatsuka, Phys. Rev. **A45**, 4326 (1992);

K. Takatsuka, Prog. Theoret. Phys. **91**, 421 (1994), and references cited therein.

[7] I.C. Percival *Adv. Chem. Phys.* **36** 1 (1977)

[8] S. Tomsovic and E.J. Heller, Phys. Rev. Lett. **67** (1991), 664 ;

P.W. O'Connor, S. Tomsovic, and E.J. Heller, Physica **D55** (1991), 340 ;

M.A. Sepúlveda, S. Tomsovic, and E.J. Heller, Phys. Rev. Lett. **69** (1992), 402;

S. Tomsovic and E.J. Heller, Phys. Rev. Lett. **70** (1993), 1405.

[9] K. Takatsuka, Chem. Phys. Lett. **204**, 491 (1993); K. Takatsuka, Bull. Chem. Soc. **66**, 3189 (1993).

[10] N. Hashimoto and K. Takatsuka, J. Chem. Phys. 103, 6914 (1995).

[11] As reviews of semiclassical theory, see

(a) M.V. Berry and K.E. Mount, Rep. Prog. Phys. **35** (1972), 315;

(b) L.S. Schulman, *Techniques and Applications of Path Integration* (Wiley, New York, 1981);

(c) V.P. Maslov and M.V. Fedoriuk, *Semiclassical Approximation in Quantum Mechanics* (Reidel, Dordrecht, 1981).

[12] L.D. Landau and E.M. Lifshitz, *Quantum Mechanics* (Pergamon, New York, 1958).

[13] (a) A. Auerbach, S.Kivelson, and D. Nicole, Phys. Rev. Lett. **53**, 411 (1984).

(b) A. Auerbach and S.Kivelson, Nucl. Phys. **B257** [FS14] 799 (1985).

[14] (a) H. Goldstein, *Classical Mechanics*. 1980 (Addison-Wesley, Reading).

(b) E.T. Whittaker, *A Treatise on the Analytical Dynamics of Particles and Rigid Bodies, 4th Ed.* (Cambridge Univ. Press, Cambridge, 1959).

(c) V.I. Arnold, "Mathematical Methods of Classical Mechanics," Springer, Berlin (1978),

(d) R. Abraham and J.E. Marsden, "Foundation of Mechanics," 2nd. ed. Addison-Wesley, Reading (1985).

[15] See, for instance,

W. Yourgrau and S. Mandelstam, *Variational Principles in Dynamics and Quantum Theory* (Dover, New York, 1979)

[16] J. Knoll and R. Schaeffer, Ann. Phys. **97**, 307 (1976).

[17] M. Wilkinson, Physica **21D**, 341 (1986).

[18] T. Banks, C. Bender, T.T. Wu, Phys. Rev. **D8**, 3346 (1973); T. Banks and C.M. Bender, Phys. Rev. **D8**, 3366 (1973).

[19] H. Ushiyama and K. Takatsuka, to be published.

[20] The parameters used in Eq.(4-1) have been taken from ref.[2].

[21] M. Hénon and C. Heiles, Astron. J., **69**, 73 (1964).

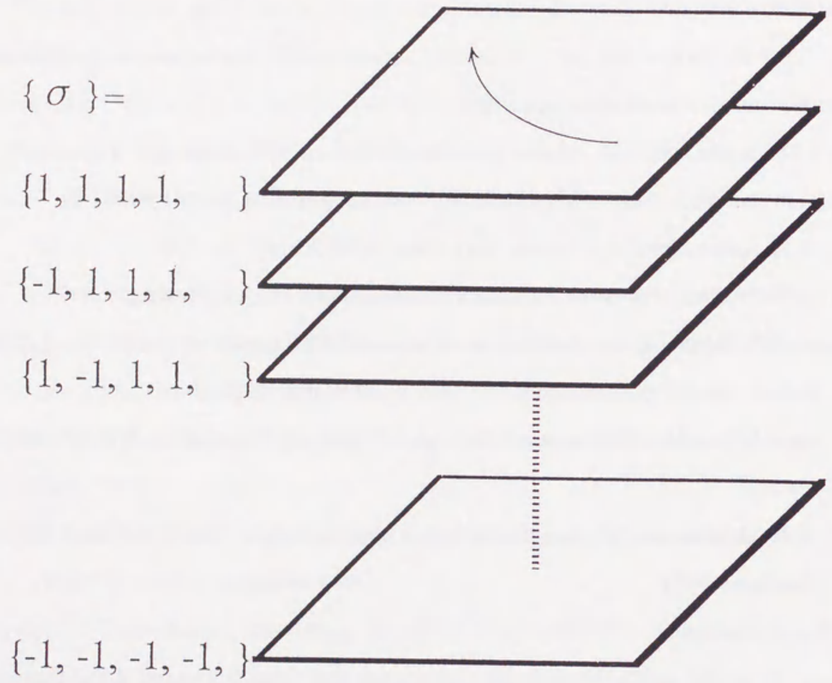

Figure 1. The layer structure of the solution space of the Hamilton-Jacobi equation classified by the parity sets. The top and bottom sheets are, respectively, for Newtonian mechanics and the instanton paths.

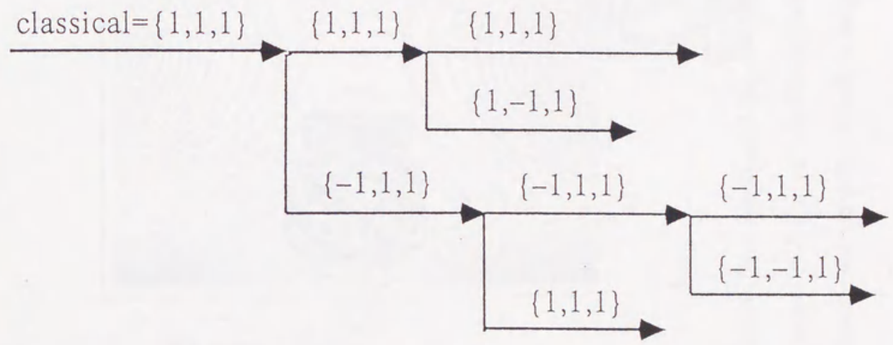

Figure 2. Bifurcation of paths by changing the parities of motion.

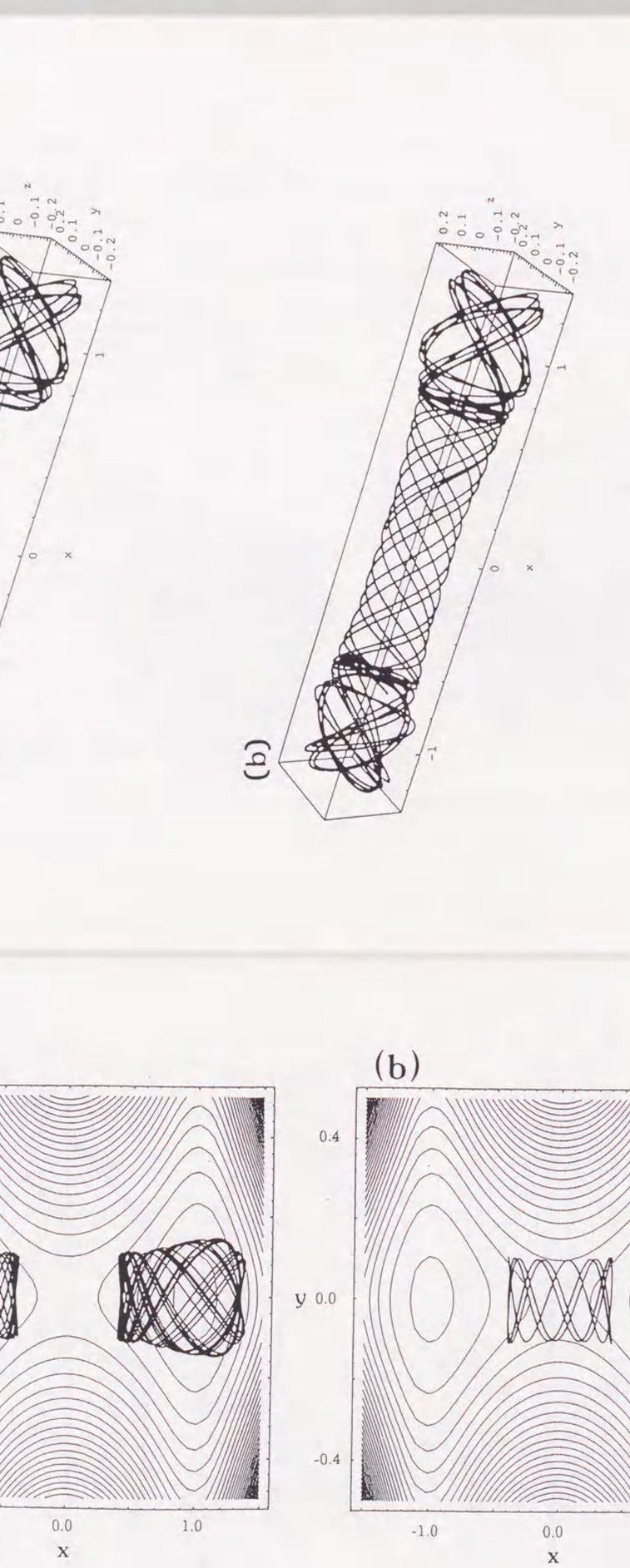

Figure 3. (a) Two-dimensional double well potential and two classical trajectories running on its classically allowed valleys. The trajectory begins from the bottom of the right valley, and ends up by popping out to the left valley one after tunneling. (b) A tunneling path connecting the two trajectories.

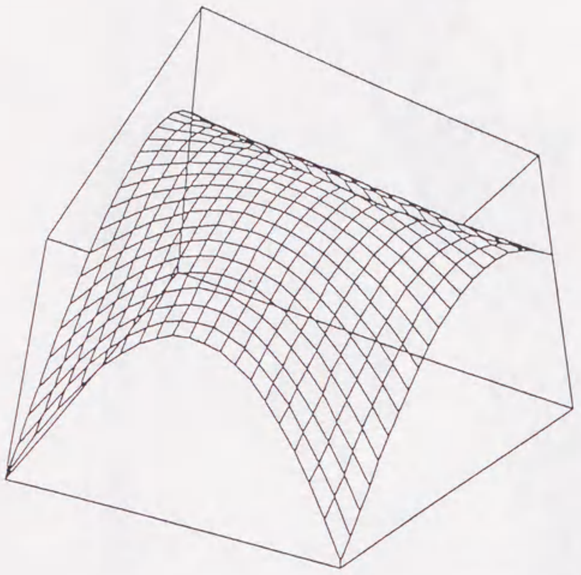

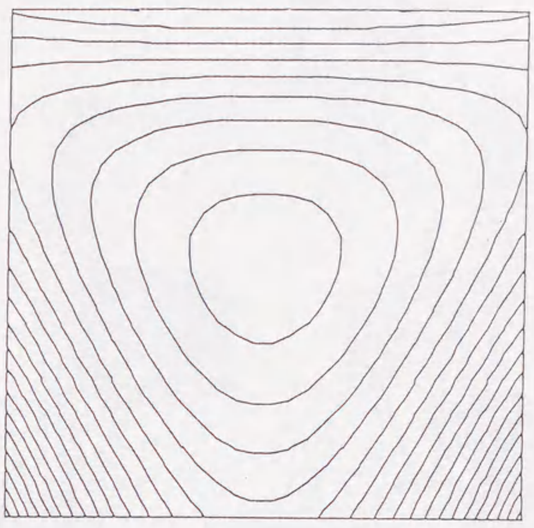

Figure 5. The basin area of the Hénon-Heiles potential. There is no potential barrier in the angular direction.

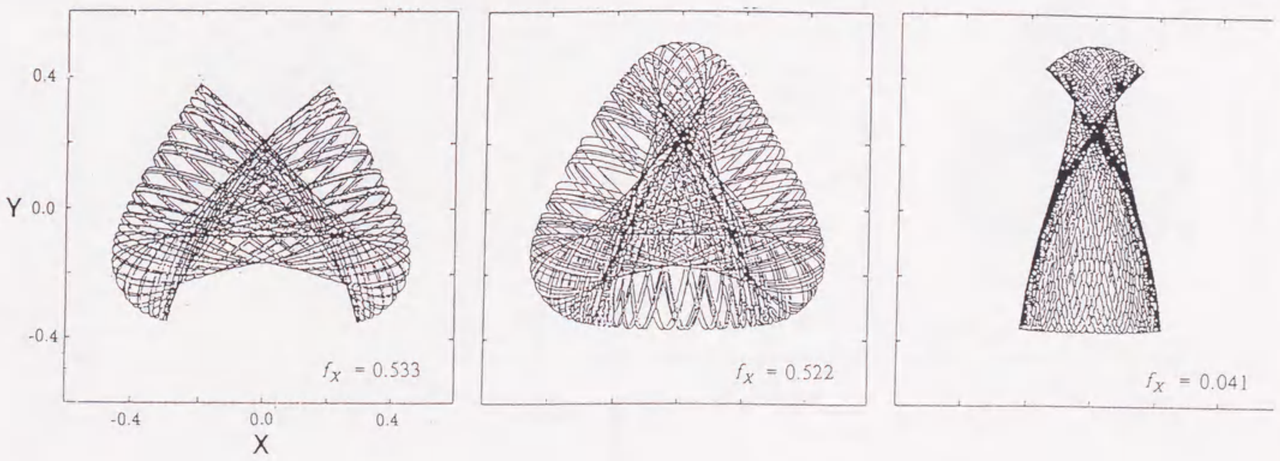

Figure 6. Some of the typical modes in the Hénon-Heiles system. All theses have the same energy E=0.09 and different initial conditions labeled with f_x.

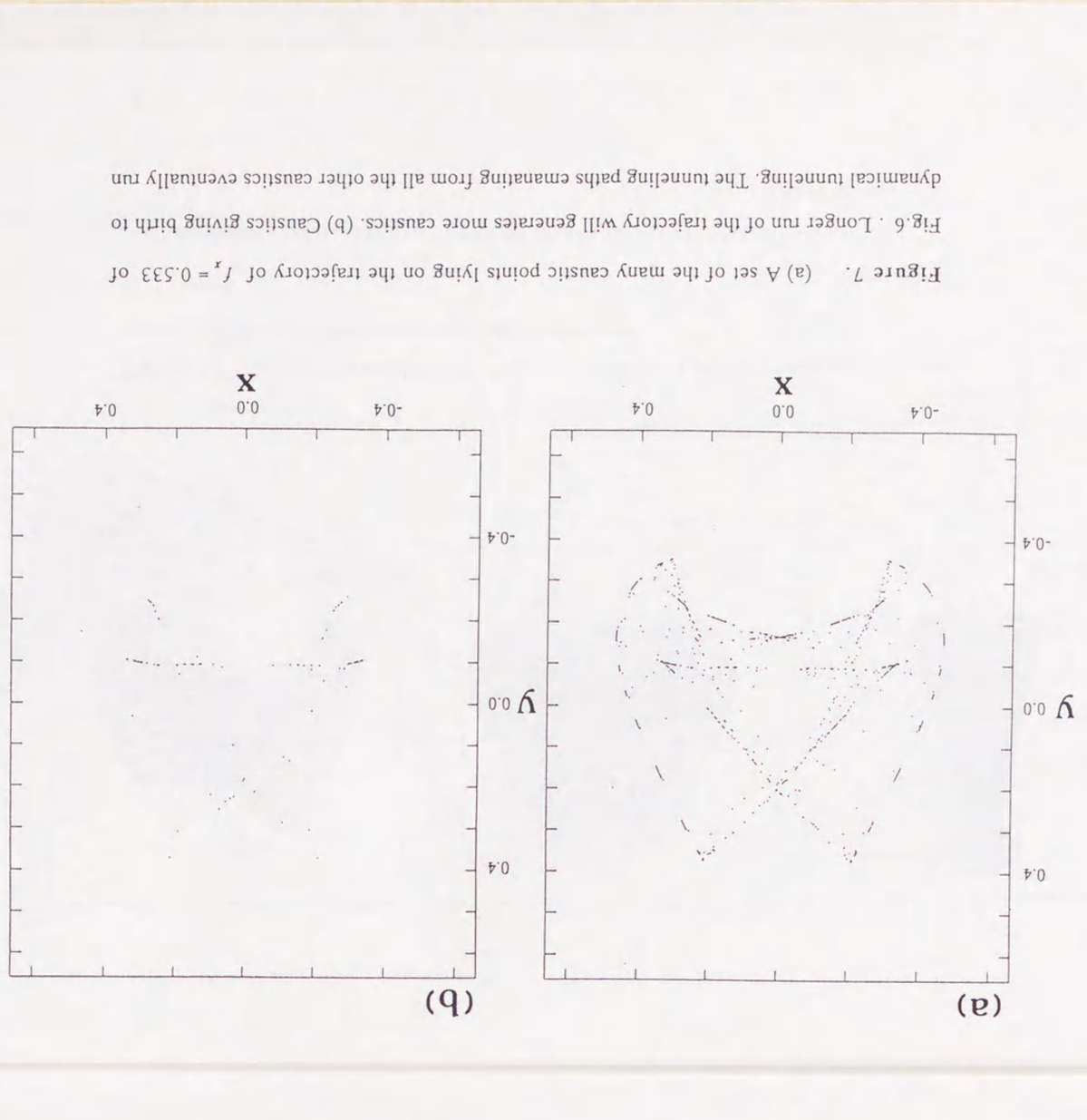

Figure 7. (a) A set of the many caustic points lying on the trajectory of $f_x = 0.533$ of Fig.6 . Longer run of the trajectory will generates more caustics. (b) Caustics giving birth to dynamical tunneling. The tunneling paths emanating from all the other caustics eventually run

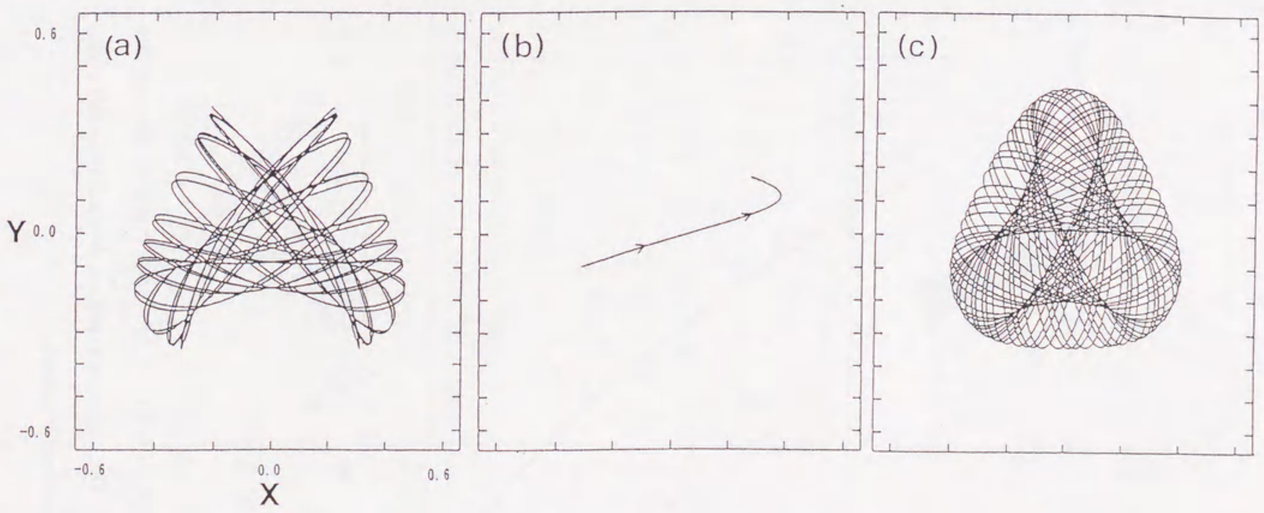

Figure 8. An example of dynamical tunneling. (a) An initial classical path corresponding to Fig.6 encounters a caustic at $(x, y) = (-0.33, -0.10)$. (b) A tunneling path starting there and has its first caustic at $(x, y) = (0.29, 0.16)$. (c) From this point are born the final classical path of left-rotation.

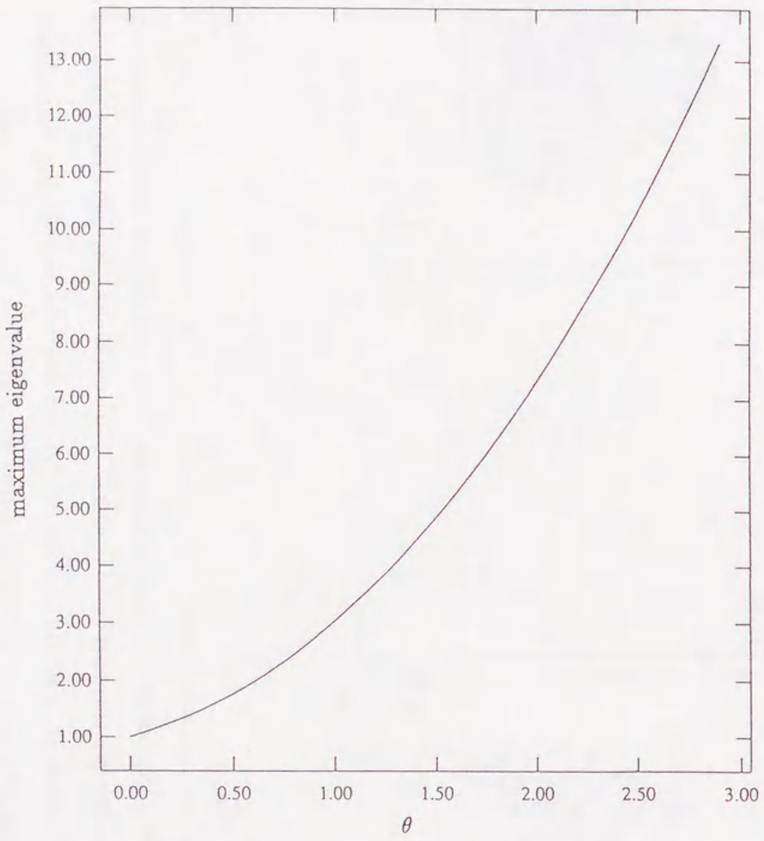

igure 9. The stability of the tunneling path of Fig.8. The largest among the absolute alues of the eigenvalues is plotted versus θ. The Liapunov exponent obtained from this curve 0.888, and hence this tunneling path is considerably unstable.

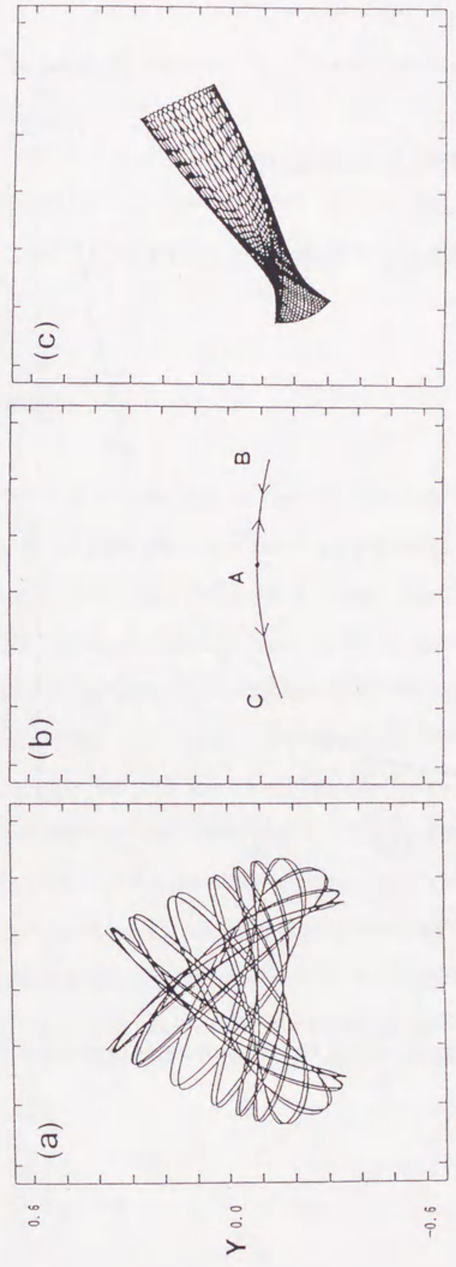

Figure 10. The second example of dynamical tunneling from the same trajectory as that in Fig.8. (a) Another caustic is found at point A (0.09, −0.09). (b) A tunnel path is generated at that point and proceeds to point B which is a turning point. It is forced to bounce back there without returning to the classical domain and reaches point C, which is a caustic point. There it comes back to the Newtonian sheet. (c) A new librational mode shows up there.

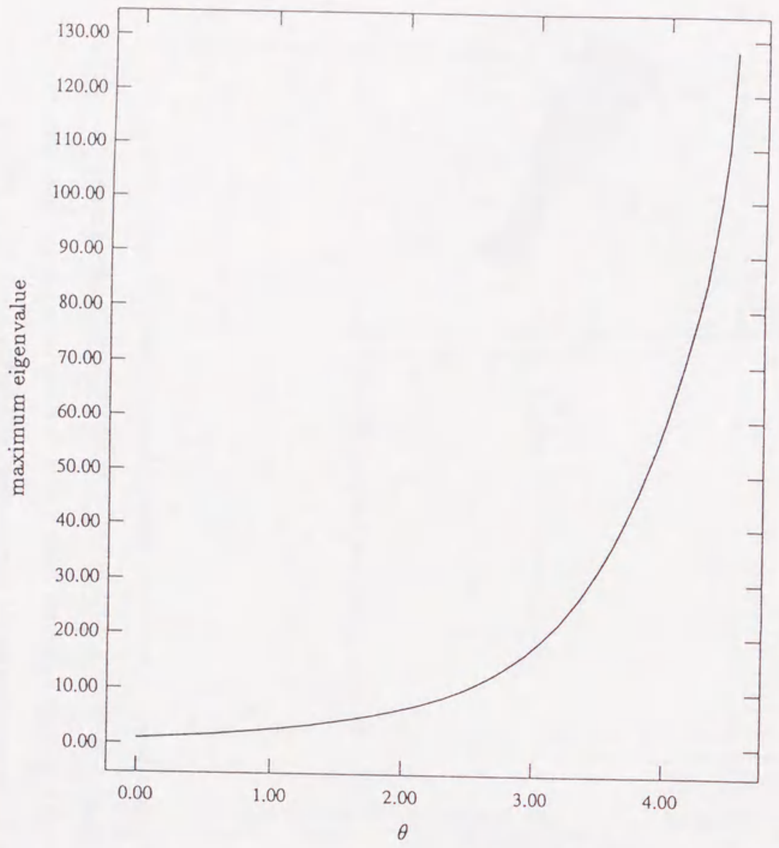

Figure 11. The stability of the tunneling path of Fig.10 The Liapunov exponent is 1.064. This is also unstable.

Chapter II.

Semiclassical Tunneling Theory for Multidimensional Tunneling Chemical Reaction

abstracts

A new semiclassical theory to describe the tunneling by incorporating non-classical solutions of the time-dependent Hamilton-Jacobi equation to the Feynman kernel is constructed. A systematic class of complex-valued (non-classical) solutions for the time-independent Hamilton Jacobi equation has been found that are generated along non-Newtonian paths in real-valued configuration space [K. Takatsuka and H. Ushiyama, Phys. Rev. **A51**, 4353(1995) which corresponds to the last chapter]. The straightforward extension applies in the present chapter to the time-dependent Hamilton-Jacobi equation, the solutions of which describe the tunneling in chemical reactions. It is shown that no damping factor due to the tunneling does not arise from the pre-exponential factor in thus obtained non-classical kernel, since it is still real-valued, aside from the complex phase due to the Maslov index, and moreover its functional form is essentially the same as in the non-tunneling case. Thus only the imaginary part of the action integral is responsible for the damping.

I. Introduction

The study of the quantum mechanical tunneling has its long standing history. Nevertheless, tunneling is getting more prominent as its universality in various branches of science and technology is recognized. Among others, our concern in the present thesis is about the tunneling in chemical reactions [1]. In particular, we study the effects of multidimensionality and/or many-body effects on tunneling in chemical reactions. A gap lying between one- and two-dimensional tunneling theories is quite deep and wide, just as in other general subjects in science. One dimensional tunneling has been clearly understood and nothing much is left for further study [2,3]. Two dimensional tunneling can generally undergo energy transfer between the available modes. Cooperative or resonant tunneling in which two or more protons transfer simultaneously can happen only in systems with even higher dimensions as in water clusters, DNA chains, and so on. Recently, Clary et al. [4] have developed an extensive study of tunneling splitting in water dimer and trimer by means of the quantum Monte Carlo method. However, theoretical study on high-dimensional tunneling in *reaction dynamics* is still a very tough problem. Our aim in the present chapter is the construction of a new semiclassical theory for the study on multidimensional tunneling in *reaction dynamics*.

Our semiclassical theory rests on our earlier finding that the Hamilton-Jacobi equation [5] has a systematic class of non-classical (local) solutions that are complex-valued but generated along non-Newtonian trajectories [6,7]. Both the Newtonian (purely classical) paths and the instanton paths are extreme cases of our general solutions. The non-classical solutions are incorporated to the Feynman kernel [8, 9], which in turn is converted to a time dependent semiclassical theory of tunneling. The Hamilton-Jacobi equation has an invariance in the square term of the momenta, to which one can introduce the quantity of parity of motion that can take only positive or negative unity [6]. Once the negative parity is assigned to a coordinate, the corresponding motion in this direction looks anti-Newtonian, that is, the particle can climbs against a potential field, while the other coordinates with the positive

parities undergo the ordinary Newtonian motions. It is not unnatural to regard the anti-Newtonian motion as a "classical version" of tunneling. The anti-Newtonian and Newtonian coordinates can exchange the energy, and thereby bears the multidimensional effect of tunneling. The set of parities classifies the type of tunneling, whereby the entire phase space forms a sheet structure [6]. For instance, the instanton paths form a sheet in which all the assigned parities are negative. All the paths thus generated are real-valued in the ordinary configuration space (the time-coordinate is also kept real), while the associated solution to the Hamilton-Jacobi equation can be complex, the imaginary part of which arises from the anti-Newtonian coordinates. Although we here incorporate these non-classical solutions into the path integral formalism, it is also possible to apply them in the Bohm-Maslov type semiclassical theory [10]. It is readily guessed in any semiclassical formalism that as the number of the negative parities is larger, the norm of a tunneling wavefunction dumps more significantly. Moreover, we will show that the damping factor due to the tunneling originates only from the complex action integral, but does not from the pre-exponential (amplitude) factors.

II. Time-Dependent Semiclassical Kernel for Tunneling

A. Tunneling solutions in the time-dependent Hamilton-Jacobi equation

We begin with the non-classical solutions to the time-dependent Hamilton-Jacobi (HJ) equation [6], which are to be incorporated into the semiclassical kernel [9,11]. Among the nonclassical solutions, we particularly attempt to seek the complex solutions in real-valued configuration space and time. One of the reasons for this has been described in our previous paper [6] in conjunction with the relationship between the Schrödinger and HJ equations. Yet more concrete reason is that Huang et al. [12] have proposed the so-called Huygens principle to obtain the *global* complex (non-classical) solutions in real-valued configuration space from the time-independent HJ equation, which has actually been realized numerically by Takada

and Nakamura [13]. Our approach in ref.[6] and here is to generate complex solutions along real-valued but non-Newtonian paths. This attitude is exactly the same as the ordinary classical trajectory calculations in place of resorting to the global (wave-like) solutions of the HJ equation.

First of all, we remark that the HJ equation is invariant to the following constant σ_k, which should satisfy $\sigma_k^{\,2}=1$, in each coordinate k such that

$$\frac{\partial S}{\partial t}=H=\frac{1}{2}\sum_k\left|\frac{\partial S}{\partial q_k}\right|^2+V(q)=\frac{1}{2}\sum_k\left|\frac{1}{\sigma_k}\frac{\partial S}{\partial q_k}\right|^2+V(q), \tag{2-1}$$

where S is the Hamilton principal function [5] and $V(q)$ is a potential function in the real-valued configuration space $q=(q_1,q_2,\cdots,q_M)$. Throughout the present chapter, we use the so-called mass-weighted coordinates so that all the masses are scaled to unity. We call the constants σ_k "parity of motion". Although the Hamiltonian is invariant to the parities, dynamics different from that of Newton is generated as shown below. As will be summarized later, the signs of the parity indicate [6]

$$\begin{cases}\sigma_k=+1 & \text{classically allowed in the direction } k\\ \sigma_k=-1 & \text{classically forbidden in the direction } k.\end{cases}$$

In the standard classical mechanical, the dynamics follows from

$$\dot{q}_k=\frac{\partial S}{\partial q_k}=\frac{\partial L_{cl}}{\partial \dot{q}_k} \tag{2-2}$$

that defines the classical Lagrangian in the HJ equation. However, as suggested in Eq.(2-1), the following dynamics can be deduced

$$\dot{q}_k=\frac{dq_k}{dt}=\frac{1}{\sigma_k}\frac{\partial L}{\partial \dot{q}_k}, \tag{2-3}$$

which in turn defines a non-classical Lagrangian, which is different from L_{cl}. In order to

materialize this dynamics, we next define momentum p_k and its associated quasi-momentum $\overline{p}_k$ as

$$p_k=\sqrt{\sigma_k}\,\overline{p}_k \quad (=\sqrt{\sigma_k}\,\dot{q}_k). \tag{2-4}$$

When $\sigma_k=-1$, p_k is pure imaginary ($\overline{p}_k$ is still real-valued). Thus we have introduced the complex variables only into the momenta (into neither time nor positions) through the parities. Therefore $\dot{q}_k$ remains real even for the negative parity. The complex phase space (q,p) thus has a one-to-one correspondence with the real-valued phase space $(q,\overline{p})$, in which the dynamics is monitored in practice.

In fact, new equations of motion for the non-classical motion in $(q,\overline{p})$-space are derived in terms of the Euler-Lagrange variational principle that is applied to the Lagrangian of Eq.(2-3) such that

$$\delta\int L(q,\dot{q}_k,t)=0, \tag{2-5}$$

which is followed by the equation of motion

$$\frac{d}{dt}\left|\frac{\partial L}{\partial \dot{q}_k}\right|-\frac{\partial L}{\partial q_k}=0. \tag{2-6}$$

On the other hand, the total derivative of the Lagrangian is given as usual as

$$d\left[L-\sum_k\sigma_k\overline{p}_k\dot{q}_k\right]=\sum_k\sigma_k\left(\dot{\overline{p}}_k dq_k-\dot{q}_k d\overline{p}_k\right)\equiv -dH(\{\sigma\}), \tag{2-7}$$

where the last equality defines a modified Hamiltonian $H(\{\sigma\})$ that in turn brings about canonical equations of motion

$$\begin{cases} \sigma_k \dot{q}_k = \dfrac{\partial H(\{\sigma\})}{\partial \bar{p}_k} \\ \sigma_k \dot{\bar{p}}_k = -\dfrac{\partial H(\{\sigma\})}{\partial q_k} \end{cases} \tag{2-8}$$

The explicit form of the Hamiltonian is readily obtained as

$$H(\{\sigma\}) = \sum_k \frac{\sigma_k}{2} \bar{p}_k^{\,2} + V(q). \tag{2-9}$$

It is easy to show that the energy is conserved along the path. The paths generated by Eq.(2-8) with negative parities embody the non-Newtonian motions. For example, a motion in a direction with a negative parity proceeds against the force field applied. Thus, it is clear that this path can be regarded as a tunneling path if treated in the context of quantum mechanics. An important fact is that the directions even with the different parities can exchange the energy in the course of dynamics, whereby the multidimensional effects in tunneling are ensured.

The phase space $(q,\bar{p})$ thus obtained forms a sheet structure that is classified in terms of the set of parities. For instance, if all the parities are positive unity, the present phase space is nothing but the ordinary Newtonian phase space. On the other hand, if they are all negative, the corresponding sheet is filled with the so-called instanton paths (see Eqs.(2-8) and (2-9)). (For a one-dimensional problem, therefore, our theory reproduces the ordinary tunneling theory based on the instanton paths.) In between these extreme cases, there can be many intermediate phase spaces of mixed parity sets. Further distinction can be made in these intermediate spaces according to which directions the negative parities are assigned. In our view, tunneling is regarded as a set of smoothly connected paths in different sheets. For example, a Newtonian trajectory is smoothly connected at a caustic point (see the next subsection) with a path of one or more negative parities in certain (rotated) coordinate(s), and then comes back to the Newtonian sheet in the similar procedure. There can be many, practically, infinitely many variants of the tunneling paths depending on the number and

frequency of changing the parity set. However, as a matter of fact, most of these tunneling paths bear a very small tunneling probability and paths of significantly large tunneling probabilities are quite limited (see discussion in Sect.II(B)).

The mechanics described above is associated with a natural definition of an action integral [6] such as

$$S_{cl} = \int \sum_k \sigma_k \bar{p}_k dq_k - H(\{\sigma\})dt. \tag{2-10}$$

This real-valued action integral, which we call the path action, satisfies the principle of least action. It is therefore responsible for generating both classical and tunneling paths on each sheet in the real-valued phase space $(q,\bar{p})$. However, S_{cl} does not satisfy HJ equation unless the path happens to be on the Newtonian sheet where all the parities are positive unity. The local and complex-valued solution of HJ equation can be constructed as

$$S_{HJ} = \int \sum_k \sqrt{\sigma_k}\, \bar{p}\, dq_k - H(\{\sigma\})dt = \int \sum_k p_k dq_k - Hdt. \tag{2-11}$$

This action integral, which we call the HJ action, is complex-valued in the phase space (q,p), except on the Newtonian sheet. It is this HJ action that should be incorporated in the semiclassical mechanics. This is the time-dependent version of the multidimensional tunneling theory which has been proposed in Ref.[6].

It is natural to incorporate the above non-classical paths into the path integral, since it is designed to take into account all the non-classical paths in a democratic manner. To do so, we introduce the following convenient set of coordinates

$$\begin{aligned} Q_k &= \sqrt{\sigma_k}\, q_k \\ P_k &= \sqrt{\sigma_k}\, \bar{p}_k = p_k, \end{aligned} \tag{2-12}$$

in which the coordinates in configuration space are also pure imaginary if their parities are negative. Then the equations of motion of Eq.(2-8) are transformed to

$$\begin{cases} \dot{Q}_k = \dfrac{\partial H(\{\sigma\})}{\partial P_k} \\ \dot{P}_k = -\dfrac{\partial H(\{\sigma\})}{\partial Q_k}, \end{cases} \tag{2-13}$$

which looks exactly like the ordinary Hamilton canonical equations of motion. This expression is particularly useful for the semiclassical implementation of the non-classical solutions.

Due to Poincaré-Cartan theorem [5], a flow in phase space induced by the Hamiltonian $H(\{\sigma\})$ should conserve the two form

$$\omega^2 = \sum_k dP_k \wedge dQ_k \tag{2-14}$$

The Stokes theorem brings the above equation back to the path-action S_{cl}, that is,

$$S_{cl} = \int \sum_k P_k dQ_k - Hdt\,. \tag{2-15}$$

The generating functions $F_1(Q_f, Q_i)$, $F_2(Q_f, P_i)$, $F_3(P_f, Q_i)$, and $F_4(P_f, P_i)$ can be constructed as in the ordinary classical mechanics [5a, 14]. All the mathematical relations like

$$\frac{\partial F_1(Q_f, Q_i)}{\partial Q_f} = P_f \tag{2-16}$$

and

$$F_2(Q_f, P_i) = F_1(Q_f, Q_i) + Q_i P_i \tag{2-17}$$

hold as well (see Miller [14]). Furthermore, the HJ action is also given formally by the

coordinate rotation

$$(Q, P) \to (q, P) \tag{2-18}$$

as

$$S_{cl}(Q,P) \to S_{HJ}(q,P) = \int \sum_k P dq_k - Hdt\,. \tag{2-19}$$

In these expressions, all the coordinates and the associated momenta are treated as independent variables. Thus, the dynamics in (Q, P) space and the concomitant rotation to (q, P) give the essential route to the semiclassical theory.

B. Semiclassical kernel including tunneling paths

We now incorporate the tunneling paths and their associated action integrals into the time-dependent kernel [8,14]. As stated above, we evaluate the kernel locally along the paths in (Q, P) space making use of the canonical property, Eq.(2-13), together with the unitary condition for the semiclassical kernel to satisfy [14]. A nice thing to employ (Q, P) representation is that it enables a direct application of the stationary phase approximation working on S_{cl} just as in the classical case. In the final step, the semiclassical kernel with the complex action integral, namely S_{HJ}, is to be obtained with the coordinate rotation of Eq.(2-18), whereby the coordinates in configuration space come back to the real-valued space.

a) Phase space path integral

Since we would like to treat both Q_k and P_k $(k = 1,2,\cdots,M)$ as independent variables, the phase-space representation of the kernel [15, 9] is most appropriate to take account of our sheet structure for non-classical dynamics. The kernel is written as

$$K(q_f,t;q_i,0)=\lim_{N\to\infty}\int\cdots\int dp_1dq_1\cdots dq_{N-1}dp_N\left(\frac{1}{2\pi\hbar}\right)^M\exp\left[\frac{i}{\hbar}S(q_f,q_i,t)\right], \tag{2-20}$$

where q_i and q_f are the end points for the wave propagation. M is the number of dimensions, and the action function in the exponential function is

$$S(q_f,q_i,t)=\int\sum_k p_k dq_k - Hdt\,. \tag{2-21}$$

Here are two different interpretations for Eq.(2-20) [9]. One is that the trajectory goes from q_j to q_{j+1} in the time interval $jt/N\le t\le(j+1)t/N$, during which the momentum p_{j+1} is kept constant. Thus the quantity q is always continuous, while the momentum p jumps at the end points of each interval. The other is that the time period [0,t] is broken into $2N$ equivalent intervals $(\Delta t=t/(2N))$ and each end point is associated with either new p or new q alternately, i.e., $q_i=q_0=q(0)$ at time 0, $p_1(\Delta t)$ at time Δt, $q_1(2\Delta t)$ at time $2\Delta t$, $\cdots$, $p_N(t-\Delta t)$ at time $t-\Delta t$, and $q(t)=q_N=q_f$ at time t. We take this latter point of view. The quantum representation of $\langle q_f\mid q_i\rangle$ can be then written as

$$\begin{aligned}\langle q_f\mid q_i\rangle=&\int\cdots\int dp_1dq_1\cdots dq_{N-1}dp_N\\&\langle q_N(t)\mid p_N(t-\Delta t)\rangle\langle p_N(t-\Delta t)\mid q_{N-1}(t-2\Delta t)\rangle\cdots\langle q_1(2\Delta t)\mid p_1(\Delta t)\rangle\langle p_1(\Delta t)\mid q_0(0)\rangle\end{aligned} \tag{2-22}$$

by the insertion of the identity operator represented in terms of q and p, alternately. In view of this partition of the infinitesimal time interval, the semiclassical expression to this representation must have the following form

$$\begin{aligned}&K(q_f,t;q_i,0)=K(q_N,t;q_0,0)\\&=\lim_{N\to\infty}\int\cdots\int dp_1dq_1\cdots dq_{N-1}dp_N\prod_{j=1}^{N}A_2(q_j,p_j)\exp[\frac{i}{\hbar}S(q_j,p_j)]A_3(p_j,q_{j-1})\exp[\frac{i}{\hbar}S(p_j,q_{j-1})]\end{aligned} \tag{2-23}$$

where we have inserted

$$\langle q_j\mid p_j\rangle=A_2(q_j,p_j)\exp[\frac{i}{\hbar}S(q_j,p_j)] \tag{2-24}$$

and

$$\langle p_j\mid q_{j-1}\rangle=A_3(p_j,q_{j-1})\exp[\frac{i}{\hbar}S(p_j,q_{j-1})]. \tag{2-25}$$

The coefficients $A_2(q_j,p_j)$, $A_3(p_j,q_{j-1})$, and the action integrals are given explicitly in the large limit of N, which can be picked up from the systematic table due to the general semiclassical theory given by Miller [14].

b) To the tunneling phase space

As described above, the tunneling phase space in (Q,P) representation has almost the complete parallelism with the Newtonian (q,p) phase space. Thus, the algebra for the manipulations of the semiclassical theory can be generalized in a straightforward manner in (Q,P) space, even though some of the pairs (Q_k,P_k) are both pure imaginary. Besides, the action integral $S_{cl}(Q,P)$ is always real. In short, with use of the canonical property of the equation of motion in (Q,P) space and the unitary condition of the kernel given by Miller [14], one can directly extend the form of Eq.(2-23) in (Q,P) space.

The coefficients $A_2(q_j,p_j)$, $A_3(p_j,q_{j-1})$, and the action integrals are determined as follows. First of all, the action integrals have four different expressions which depend on the boundary conditions. Following Goldstein's notation of the generating functions for the canonical transformation [5a], we denote $F_2(Q_j,P_j)=S(Q_j,P_j)$ and $F_3(P_j,Q_{j-1})=S(P_j,Q_{j-1})$. Then it follows that

$$\begin{aligned}\langle Q_j\mid P_j\rangle&=A_2(Q_j,P_j)\exp\left[\frac{i}{\hbar}F_2(Q_j,P_j)\right]\\&=\left(\frac{1}{2\pi i\hbar}\right)^{\frac{M}{2}}\left[\frac{\partial^2F_2(Q_j,P_j)}{\partial Q_j\partial P_j}\right]^{\frac{1}{2}}\exp\left[\frac{i}{\hbar}F_2(Q_j,P_j)\right],\end{aligned} \tag{2-26a}$$

and

$$\langle P_j \mid Q_{j-1}\rangle = A_3(P_j,Q_{j-1})\exp\left[\frac{i}{\hbar}F_3(P_j,Q_{j-1})\right]$$
$$= (\frac{1}{2\pi i\hbar})^{\frac{M}{2}}\left[\frac{\partial^2 F_3(P_j,Q_{j-1})}{\partial P_j \partial Q_{j-1}}\right]^{\frac{1}{2}}\exp\left[\frac{i}{\hbar}F_3(P_j,Q_{j-1})\right] \qquad (2\text{-}26b)$$

(Neither $\langle Q_j \mid Q_{j-1}\rangle$ nor $\langle P_j \mid P_{j-1}\rangle$ is necessary here.)

c) The kernel of the finite time interval

The kernel in the finite time interval $[0,t]$ is obtained by connecting the above piecewise transformation functions at $P_1,Q_1,\cdots,Q_{N-1},P_N$. A new feature is that one should sum up with respect to the sheets associated with the different set of parities. Figure 1 exemplifies paths in phase space which are connected at $P_1,Q_1,\cdots,Q_{N-1},P_N$. The thick lines represent paths on the same sheet, while the thin line paths change the parities at the connecting points. In evaluating the (Q,P)-space as in Eq.(2-23), we begin with the integral over P_1 which connects $\langle P_j \mid Q_{j-1}\rangle$ and $\langle Q_j \mid P_j\rangle$ type piecewise kernels and get the kernel which connects Q_i and Q_1, that is

$$\int dP_1\langle Q_1 \mid P_1\rangle\langle P_1 \mid Q_0\rangle = \int dP_1 A_2(Q_1,P_1)A_3(P_1,Q_0)\exp\left[\frac{i}{\hbar}\left(F_2(Q_1,P_1)+F_3(P_1,Q_0)\right)\right] \qquad (2\text{-}27)$$

As noted above in Sec.II(A), a complete parallelism holds between the classical case [14] and our non-classical mechanics. Thus the systematic algebra worked out by Miller [14] can be applied in our case, too, which results in

$$\langle Q_1 \mid Q_0\rangle = \int dP_1\langle Q_1 \mid P_1\rangle\langle P_1 \mid Q_0\rangle = (\frac{1}{-2\pi i\hbar})^{\frac{M}{2}}\left[\frac{\partial^2 F_1(Q_1,Q_0)}{\partial Q_1 \partial Q_0}\right]^{\frac{1}{2}}\exp\left[\frac{i}{\hbar}F_1(Q_1,Q_0)\right] \qquad (2\text{-}28)$$

Similarly, we have

$$\langle P_2 \mid Q_0\rangle = \int dQ_1\langle P_2 \mid Q_1\rangle\langle Q_1 \mid Q_0\rangle = (\frac{1}{-2\pi i\hbar})^{\frac{M}{2}}\left[\frac{\partial^2 F_3(P_2,Q_0)}{\partial P_2 \partial Q_0}\right]^{\frac{1}{2}}\exp\left[\frac{i}{\hbar}F_3(P_2,Q_0)\right]. \qquad (2\text{-}29)$$

The successive applications of $2N$-1 times of the above propagation will give rise to the finite time form of the kernel as

$$K(Q_f,t;Q_i,0) = (\frac{1}{-2\pi i\hbar})^{\frac{M}{2}}\left[\frac{\partial^2 F_1(Q_f,Q_i)}{\partial Q_f \partial Q_i}\right]^{\frac{1}{2}}\exp\left[\frac{i}{\hbar}F_1(Q_f,Q_i)\right]$$
$$= (\frac{1}{-2\pi i\hbar})^{\frac{M}{2}}\left[\frac{\partial Q_f}{\partial P_i}\right]^{-\frac{1}{2}}\exp\left[\frac{i}{\hbar}S_{cl}(Q_f,Q_i)\right] \qquad (2\text{-}30)$$

which looks exactly the same as the ordinary semiclassical kernel.

Let us confirm that our dynamics, namely, Eq.(2-13) arises again by applying the variational principle to Eq.(2-30), that is

$$\delta S = \int\{PdQ - Hdt\} = \int\delta P(dQ - \frac{\partial H}{\partial P}dt) - \int\delta Q(dP + \frac{\partial H}{\partial Q}dt) + P\delta Q\Big|_0^t \qquad (2\text{-}31)$$

The fixed boundary condition gives immediately the canonical equations, Eq.(2-13), or equivalently Eq.(2-8)) in $(q,\bar{p})$ space.

d) Coordinate rotation for the complex action

The tunneling paths have been incorporated into the path integrations as above. However, the phase factor S_{cl} in the kernel Eq.(2-30) is real-valued and hence no damping factor due to the tunneling arises. This is because S_{cl} has been employed just in order to make a natural extension of the path integrals to the (Q,P)-space making use of the canonical properties. Thus, unlike the ordinary path-integrals, the resultant kernel, Eq.(2-30), is formulated in

Q-space rather than in q-space. However, S_{cl} is not a solution to the HJ equation, but S_{HJ} is. The solution of the HJ equation is directly related to the quantum wavefunction [11]. Moreover, the imaginary part of S_{HJ} can describe the tunnel damping. It is therefore S_{HJ} that should appear in the kernel for the tunneling domain.

A simple way to put the tunneling kernel in q-space is to rotate the coordinates as $(Q,P)\rightarrow(q,P)$, in which the imaginary momenta remain as they are. Furthermore, as briefly described in Eq.(2-19), S_{cl} is directly transformed into S_{HJ} by this coordinate rotation. Thus we have

$$K(q_f,t;q_i,0:\{\sigma\})=(\frac{1}{-2\pi i\hbar})^{\frac{M}{2}}\left[\frac{\partial q_f}{\partial P_i}\right]^{\frac{1}{2}}\exp\left[\frac{i}{\hbar}S_{HJ}(q_f,q_i,t)\right]. \tag{2-32}$$

Since P_f in the tunneling region has the pure-imaginary components in the directions of negative parities, Eq.(2-32) can be written in terms of $\overline{p}_f$ in place of P_f as

$$K(q_f,t;q_i,0:\{\sigma\})=(\frac{1}{-2\pi i\hbar})^{\frac{M}{2}}\left[\frac{\partial q_f}{\partial \overline{p}_i}\right]^{\frac{1}{2}}\exp\left[\frac{i}{\hbar}S_{HJ}(q_f,q_i,t)+i\frac{\pi}{4}N_p\right], \tag{2-33}$$

where N_p is the number of the negative parities. In addition, we have an additional phase when a path passes through a caustic point, that is, a point of $\partial q_f/\partial\overline{p}_i=0$ (see below). Thus one can write systematically as

$$K(q_t,t;q_s,s:\{\sigma\})=\sum_{\alpha}(\frac{1}{-2\pi i\hbar})^{\frac{M}{2}}\sqrt{\left|\frac{\partial q_t}{\partial\overline{p}_s}\right|}\exp[\frac{i}{\hbar}S_{HJ}+i\phi] \tag{2-34}$$

where the additional phase ϕ is given by

$$\phi=\begin{cases}-\dfrac{\pi}{2}\times N_f+\dfrac{\pi}{4}\times N_p & \text{(at an entrance of a tunneling sheet)}\\[2ex] -\dfrac{\pi}{2}\times N_f-\dfrac{\pi}{4}\times N_p & \text{(at an exit of a tunneling sheet)}\end{cases} \tag{2-35}$$

N_f is the sum of the multiplicities of the zeros of $\partial q_f/\partial\overline{p}_i=0$ along the trajectory, which is called the Maslov index [9, 11]. Equation (2-34) is our major result in the present chapter and is applied to the chemical reaction through tunneling in Chapter II of Part II.

It is quite worthwhile to note that the damping factor due to tunneling arises only from the HJ action S_{HJ}, but does not from the pre-exponential (or amplitude) factor $\left|\partial q_t/\partial\overline{p}_s\right|^{\frac{1}{2}}$. The WKB approach based on the analytic continuation of the Hamilton-Jacobi equation into the complex q-space would lead to a damping amplitude. On the other hand, it is generally assumed that the tunneling probability could reasonably estimated from the imaginary component of the action integral. Our result thus has shown that the latter assumption is valid in this level of semiclassical theory.

C. Calculational details

Let us rewrite the total kernel of Eq.(2-32) to emphasize that the tunneling effects are taken into account explicitly as

$$\begin{aligned}K_{total}(q_f,t;q_i,0:\{\sigma\})&=\sum_{\alpha}K(q_f,t;q_i,0:\{+1\})\\&+\sum_{\gamma}\int dq_s\int dq_r K(q_f,t;q_s,t_s:\{+1\})K_{\gamma}(q_s,t_s;q_r,t_r:\{\sigma_{\text{tunnel}}\})K(q_r,t_r;q_i,0:\{+1\})\\&+\cdots\cdots\end{aligned} \tag{2-36}$$

In this expression, $\{+1\}$ indicates a Newtonian path having only the positive parities, and $\{\sigma_{tunnel}\}$ denotes a set involving negative parities. Thus, the first term in r.h.s. of Eq.(2-36) represents the entirely Newtonian kernel (without the tunneling effects) which is a sum over all the classical paths connecting q_i and q_f at time t. The second one represents all the possible kernels for paths classical → tunneling → classical, the sheet being labeled by γ. The terms after the second one imply all the other tunneling modes like classical → tunneling → classical → tunneling → classical, and so on.

The imaginary part of the HJ action S_{HJ} reduces the norm of the kernel. Therefore, among the various types of the tunneling, only paths associated with a small damping can

contribute to the total kernel. Since it is obvious that the damping tends to become significant as the number of negative parities increases. (Therefore the instanton paths that are commonly used in the conventional tunneling treatments should significantly underestimate the tunneling probability in general.) In what follows, therefore, we consider only the sheet to which only one negative parity is assigned and paths of a single tunneling passage.

The next practical problem is the smooth connection of the tunneling and non-tunneling paths. The argument based on the stationary phase at the connecting points q_r or q_s in Eq.(2-36) brings about a condition that $\frac{\partial S_{HJ}}{\partial q_k}$ in a classical region should be equal to $-\frac{\partial S_{HJ}}{\partial q_k}$ in a tunnel region. That is

$$\overline{p}_k = \sqrt{-1}\,\overline{p}_k \quad \text{at caustic points.} \tag{2-37}$$

Hence, $\overline{p}_i$ has to be zero for the direction in which some of parities change their sign. For a one dimensional problem, this condition is realized at the so-called turning point. But, in multidimensional systems, the situation is not as simple, since any directions normal to the path have zero momenta. To be honest, we have no general theory that specifies unique points of connection. Nonetheless, we change one of the parities at the so-called caustic points, in which (1) the amplitude of the kernel becomes very large, actually infinitely large for the primitive semiclassical approximation, and (2) the effects of $\hbar$ is generally expected to be large. A caustic point is defined as

$$\frac{\partial \vec{q}_f}{\partial \vec{\overline{p}}_i} = 0, \tag{2-38}$$

where $\vec{q}_f$ and $\vec{\overline{p}}_i$ is final position and initial momentum vectors, respectively, on each sheet. (Note that caustics exist in the tunneling space, too.) We thus change a set of parities at a caustic point for the direction normal to the caustic line (surface) with zero momentum. Concomitantly, the orthogonal transformation of the coordinates $(q, \overline{p})$ is required to identify the direction of changing the parity. More details follows in the chapter II of Part II, where

the practical applications are reported.

III. Concluding Remarks

We have constructed a time-dependent semiclassical kernel which includes the tunneling effects. The kernel is based on the complex-valued solutions to the time-dependent Hamilton-Jacobi equation, which are generated along the non-Newtonian paths. It turns out that the mathematical form of the tunneling kernel is essentially the same as that for the well-known classical case, except that the paths are not Newtonian and the action integral is not real-valued. Another finding is that the damping factor due to the tunneling comes only from the imaginary part of the action integral, but does not arise from the amplitude factor.

In our theory, time have been kept always real-valued. One of major problems in tunneling is the so-called transversal (tunneling) time [16]. We hope to report this aspect in near future.

References

[1] As for recent progress in the tunneling in chemical reactions, see

a) A special issue on "Tunneling in Chemical Reactions," edited by V. A. Benderskii, V. I. Goldanskii and J. Jortner, Chem. Phys. **170** (1993).

b) V. A. Benerskii, D. Makarov, and C.A. Wight, the hole volume of Adv. Chem. Phys. Vol. LXXXVIII (1994).

[2] L. D. Landau and E. M. Lifshitz, *Quantum Mechanics*, (Pergamon, New York, 1958).

[3] Recently, Nakamura and Zhu have solved analytically a one-dimensional tunneling problem the barrier of which is caused by the non-adiabatic coupling, which was one of the ultimate problems in semiclassical theory for tunneling and non-adiabatic transitions,

C. Zhu and H. Nakamura, J. Chem. Phys. **102**, 7448 (1995).

See for a review,

H. Nakamura and C. Zhu, Comments At. Mol. Phys. **32**, 249 (1996).

[4] J. K. Gregory and D.C. Clary, J. Chem. Phys. **102**, 7817 (1995).

[5] (a) H. Goldstein, *Classical Mechanics*, (Addison-Wesly, Reading, 1980);

(b)V. I. Arnold, *Mathematical Methods of Classical Mechanics*, (Springer, Berlin, 1978);

(c) A. Abraham and J. E. Marsden, *Foundation of Mechanics 2nd. ed.*, (Addison-Wesley, Reading, 1985).

[6] K. Takatsuka and H. Ushiyama, Phys. Rev. **A51**, 4353 (1995).

[7] H. Ushiyama and K. Takatsuka, Phys. Rev. **E53**, 115 (1996).

[8] R. P. Feynman and A. R. Hibbs, *Quantum Mechanics and Path Integrals* (McGraw-Hill, New York, 1965).

[9] L. S. Schulman, *Techniques and Applications of Path Integration*, (Wiley , New York, 1981)

[10] K. Takatsuka, unpublished.

For the Bohm-Maslov type semiclassical theory, see

K. Takatsuka and A. Inoue, submitted for publication, and ref.[17]

[11] a) M. V. Berry and K. E. Mount, Rep. Prog. Phys. **35**, 315 (1972).

b) V. P. Maslov and M. V. Fedoriuk, *Semiclassical Approximation in Quantum Mechanics*, (Reidel, Dordrecht, 1981).

c) M. S. Child, *Semiclassical Mechanics with Molecular Applications*, oxford, 1991).

[12] Z. H. Huang, T. E. Feuchtwang, P. H. Culter and E. Kaze, Phys. Rev. **A41**, 32(1990) and references cited therein.

[13] S. Takada and H. Nakamura, J. Chem. Phys. **100**, 98(1994).

[14] W. H. Miller, Advan. Chem. Phys **25**, 69 (1974).

[15] a) H. Davies, Proc. Camb. Phil. Soc. **59**, 147 (1963).

b) C. Garrod, Rev. Mod. Phys. **38**, 483 (1966).

[16] R. Landauer and Th. Martin, Rev. Mod. Phys. **66**, 217 (1994)

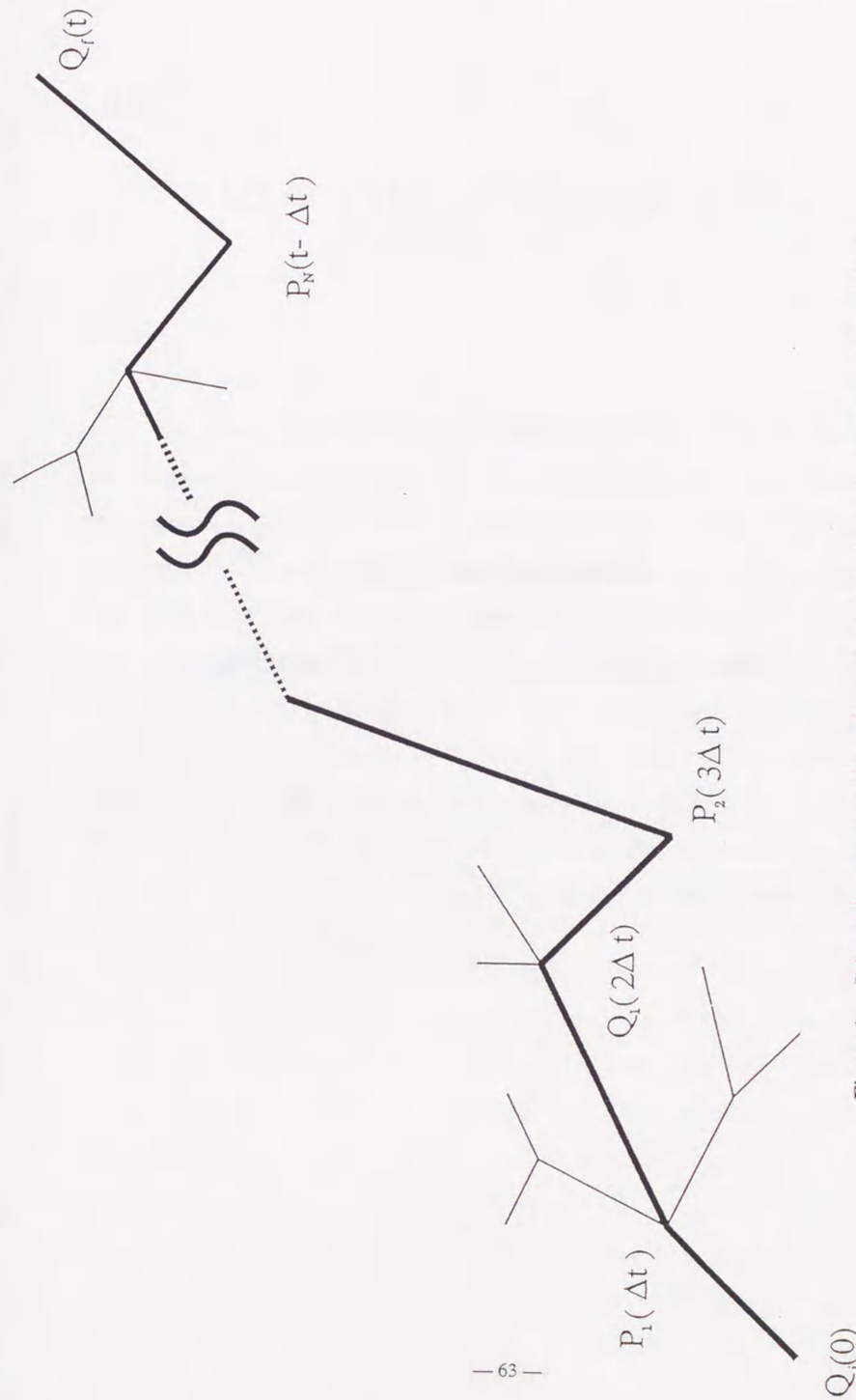

Figure 1. Schematic representation of nonclassical paths which connect Q_i and Q_f in phase space. The thick line indicates a path of the same parity set, while the thin line paths emanate from it with different parity sets.

Part II.

Semiclassical Study on Chemical Reactions through Tunneling

Chapter I.

Effects of Chaos on Dynamical Tunneling

abstracts

The effect of chaos in dynamical tunneling that induces transitions among tori in a near integrable system is investigated. Even though a system energy is moderately low for a quasiseparatrix to be sufficiently thin, in other words, even if most of phase space is filled with invariant tori, tunneling paths that connect the tori can be strongly chaotic. A direct consequence of the chaos is manifested as the mixing property of the tunneling paths, which in turn brings about a statistical redistribution of classical trajectories after the tunneling. That is, the probability for a trajectory to be found on a given torus after the tunneling is nearly proportional to the corresponding area on the Poincaré surface of section. This is highly analogous to the principle of equi-partition in statistical mechanics. However, the tunneling probability associated with each tunneling path leads to a biased distribution of the destinations of the paths. The destinations are localized in the specific regions in phase space, when the tunneling probability is considered.

I. Introduction

The tunneling effect is one of the most important quantum effects in many fields of science and technology and, has, been, explored, in various aspects [1,2]. However, for multidimensional heavy particle systems in which the straightforward application of quantum mechanics is quite difficult, with the reactive and vibrational dynamics of molecules being the typical examples, the study of tunneling should be even more difficult. There are two types of tunnelings in multidimensional systems. One is potential tunneling which is energetically forbidden motion and the other is dynamical tunneling [3] that is energetically allowed but mechanically forbidden. In chemical reaction dynamics [4], for instance, the potential tunneling has been considered in low temperature regime where the reaction can occur only through the tunnel effect. A typical example of the dynamical tunneling is found in a weakly chaotic system, in which several stable regions composed of invariant tori are surrounded by the quasiseparatrix in phase space [5]. Each stable region represents an individual mode of motion such as vibrational mode [6]. A path of the dynamical tunneling can connect two or more tori and induces the mixing of the modes.

The quantum mechanical wave functions tend to be oscillatory for heavy masses, and hence bear more classical nature. Thus multidimensional semiclassical mechanics is highly demanded [7-10]. Another important consequence of the semiclassical limit is that the density of states becomes enormous in general, which in turn brings about statistical or chaotic nature to dynamics. The tunnel effect must often be considered in the context of chaotic semiclassical dynamics. The interplay between tunneling and chaos is therefore a quite important subject, and in the present chapter we show chaotic dynamical-tunneling can give rise to a statistical redistribution of classical trajectories among invariant tori.

A general importance of the interplay between tunneling and chaos can be inferred

through the following consideration. Suppose that we are calculating a partition function using the path integrals in which the imaginary time or the inverse of the temperature, is adopted in the trace operation of the quantum mechanical evolution operator [7]. On applying the stationary approximation, a set of canonical equations of motion can be obtained, in which the ordinary Hamiltonian is replaced by the classical Lagrangian. That is, the original potential function should be inverted, on which "classical trajectories" are to be run. But, this process is essentially the same as that for generating the so-called instanton path [7,11], which is quite well known as a typical tunneling path. On the other hand, chaos is conceived as a dynamical origin of statistical mechanics. Then the partition function should depend both qualitatively and quantitatively on whether the instanton paths are chaotic or not. An interesting case is that even if the ordinary classical trajectories are non-chaotic, the corresponding tunneling paths of the same energy can be chaotic. It is this kind of problem that we address in the present chapter.

Tunneling in semiclassical mechanics has been investigated before in conjunction with chaos by the several authors. Shudo and Ikeda have shown using the complex trajectory method [12] that chaos induces a tree-structured sequence of bifurcation in the tunneling paths. Tomsovic and Ullmo [13] have shown that chaos can cause a new mechanism of tunneling between two quasimodes that are located on quantized tori. When chaotic wave functions, which can be formed along a quasiseparatrix, interact with these quasimodes, a tunneling between the quasimodes is induced and thereby leads to erratic energy levels. These observations are of fundamental importance in the theories of both chaos and tunneling.

As for the semiclassical theory for multidimensional tunneling, only a few have been proposed [1,2]. A beautiful example is the path-decomposition method in the path integral approach, in which the instanton paths arise naturally [11]. In the present chapter, we consider the dynamical tunneling within the framework of the Hamilton-Jacobi (HJ) equation. The usual tactic in semiclassical theory to cope with tunneling is to make analytic continuation of the HJ equation into complex-valued configuration space, whereby to generate imaginary solutions. This is an extremely difficult procedure except in a one-dimensional case [14]. It is

Huang, Feuchtwang, Culter, and Kaze[1] who have shown for the first time using the method of the Huygens principle that the complex WKB solutions can be propagated globally in real-valued configuration space. Takada and Nakamura [2] have numerically materialized this idea with a theoretical progress in the connection problem of the WKB solutions. Very recently, on the other hand, the present authors have shown that the time-independent HJ equation, as well as the time-dependent HJ equation [15], can have a novel class of non-classical local solutions, that is, complex-valued (not necessarily pure imaginary) local solutions along real-valued non-Newtonian paths [16], which will be briefly reviewed in the next section. These non-classical solutions can be significant only in the context of quantum (and semiclassical) mechanics. Both the Newtonian (classical) trajectories and instanton paths are regarded as special cases of such general solutions. Tunneling is viewed as a transition from one of Newtonian trajectories to a non-classical path, and coming back after some short stay in the non-classical phase space.

The purpose of Chapter I is to investigate the effects of chaos on tunneling in a weakly chaotic system. In particular, we concentrate ourselves on the consequence of chaos to the dynamical-tunneling paths. More specifically, transitions among tori through tunneling will be extensively investigated using the Hénon-Heiles system, which has six distinctive stable regions separated by two quasi-separatrices in phase space. We have observed a statistical redistribution of the trajectories from a torus to tori through chaotic dynamical-tunneling. However, the destinations of dynamical tunneling paths are localized in the specific stable regions in phase space, when the tunneling probability is considered.

The present Chapter is organized as follows. Section II is devoted to a brief review of our tunneling theory. In section III, we show how the paths of the dynamical tunneling look and verify how chaotic they are in terms of the Liapunov exponent. Then, a mixing property due to tunneling is presented. In section IV, we consider the tunneling probability and examine the distribution of tunneling paths. Concluding remarks are given in section V.

II. Theory of Tunneling

The first order approximation in any semiclassical theories begins with the Hamilton-Jacobi equation [4,7-10]. For instance, the WKB theory [7-9,14] describes a wave function in the following form

$$\phi(q) = C\exp\left[\frac{i}{\hbar}W\right] , \tag{2-1}$$

where W is an action integral as a solution of the HJ equation and C is a normalization factor. We systematically construct complex-valued action integrals in real-valued configuration space by introducing a quantity called "parity of motion" into the HJ equation such that

$$\frac{1}{2}\sum_k\left[\frac{\partial W}{\partial q_k}\right]^2 + V(q) = \frac{1}{2}\sum_k\left[\frac{1}{\sigma_k}\frac{\partial W}{\partial q_k}\right]^2 + V(q) = E , \tag{2-2}$$

where

$$\sigma_k = \begin{cases} +1 & \text{if the motion is classically allowed in the direction } k \\ -1 & \text{if the motion is classically forbidden in the direction } k. \end{cases}$$

It is obvious why σ_k is called parity. We use the so-called mass-weighted coordinate throughout the present chapter, and hence the masses do not appear explicitly in the formalism. In analogy to the standard relation between the classical Lagrangian L_{cl} and W [17],

$$\frac{\partial L_{cl}}{\partial \dot{q}_k} = \frac{\partial W}{\partial q_k} = \dot{q}_k , \tag{2-3}$$

we define a Lagrangian L as

$$\dot{q}_k = \frac{dq_k}{d\theta} = \frac{1}{\sigma_k}\frac{\partial L}{\partial \dot{q}_k} , \tag{2-4}$$

where a real-valued parameter θ mimics the role of the local time.

One should distinguish L from L_{cl} when the Newtonian mechanics is extended, since the non-classical motions can arise in terms of L rather than L_{cl}. Each coordinate has its own chronological parameter in such a way that

$$\tau_k = \frac{\theta}{\sqrt{\sigma_k}} . \tag{2-5}$$

The corresponding momentum is accordingly defined by

$$p_k = \frac{dq_k}{d\tau_k} = \sqrt{\sigma_k}\,\bar{p}_k \left(= \sqrt{\sigma_k}\,\dot{q}_k\right), \tag{2-6}$$

where the quasi-momentum $\bar{p}_k$ is kept real even in the non-classical region, while p_k is pure imaginary for the negative parity.

Applying the Euler-Lagrange variational principle, one obtains the following equation analogous to that of Lagrange

$$\frac{d}{d\theta}\left[\frac{\partial L}{\partial \dot{q}_k}\right] - \frac{\partial L}{\partial q_k} = 0 . \tag{2-7}$$

With the help of the above equations, one can take the total derivative of the Lagrangian as

$$\begin{aligned} d\left[L - \sum_k \sigma_k \bar{p}_k \dot{q}_k\right] &= \sum_k \sigma_k \left(\bar{p}_k dq_k - \dot{q}_k d\bar{p}_k\right) \\ &= -dH(\{\sigma_k\}) \quad , \end{aligned} \tag{2-8}$$

from which a new Hamiltonian $H(\{\sigma\})$ can be extracted in the usual manner as

$$H(\{\sigma_k\}) = \sum_k \frac{\sigma_k}{2}\bar{p}_k + V(q) . \tag{2-9}$$

Equation (2-8) leads to the modified canonical equations of motion

$$\begin{cases} \sigma_k \dot{q}_k = \dfrac{\partial H(\{\sigma\})}{\partial \bar{p}_k} \\ \sigma_k \dot{\bar{p}}_k = \dfrac{\partial H(\{\sigma\})}{\partial q_k} \end{cases} . \tag{2-10}$$

The law of energy conservation still holds for the non-classical paths, since we have

$$\frac{dH(\{\sigma\})}{d\theta} = 0 \quad . \tag{2-11}$$

The above equalities hold for any given set of parities $\{\sigma_1, \sigma_2, \cdots\}$. The entire solutions generated in a given set of parities constitute a sheet. Thus the whole space of all the possible solutions is classified in terms of these sheets. For example, if the parities are all positive, the modified canonical equations of motion (2-10) turns back to the Newtonian mechanics. On all the other sheets are generated non-classical solutions. For instance, when all the parities are negative unity, a sheet consisting of the instanton paths [7,11] is produced. In this way, the local solutions of the HJ equation are generated on each sheet, while the global solutions of the HJ equation are to be constructed by connecting these local solutions smoothly. We thus identify a non-classical solution of the HJ equation having some negative parities as a tunneling path .

A direct analogy from the Newtonian mechanics suggests that it is natural to define an action integral as

$$W_{cl} = \sum_k \int \sigma_k \bar{p}_k dq_k \quad , \tag{2-12}$$

which we call the path action. W_{cl} satisfies the principle of least action just as in the Newtonian mechanics, and thereby is responsible for generating both classical and non-classical paths. However, the path-action does not satisfy the HJ equation, unless all the parities happen to be positive as in the Newtonian mechanics.

Fortunately, the solution of the HJ equation can be readily constructed as

$$W_{HJ} = \sum_k \int \sqrt{\sigma_k}\, \bar{p}_k dq_k \quad , \tag{2-13}$$

which is called the HJ action. That this action is indeed a solution can be easily proved by rewriting the HJ equation as

$$\sum_k \frac{\sigma_k}{2} \bar{p}_k^{\,2} + V(q) = E \quad . \tag{2-14}$$

Thus a systematic class of solutions of the WKB theory have been constructed in real-valued configuration space with a given set of parities. W_{HJ} on the different sheets are to be connected smoothly to form a global solution to the HJ equation. Note that W_{HJ} is complex-valued for the tunneling paths, and accordingly we write W_{HJ} as

$$W_{HJ} = W_R + iW_I \quad . \tag{2-15}$$

Insertion of this expression into Eq.(2-1) leads to

$$\phi(q) = C \exp\left[\frac{-1}{\hbar} W_I\right] \exp\left[\frac{i}{\hbar} W_R\right] \quad . \tag{2-16}$$

The first exponential term represents the diminishing norm of the wave function during the tunneling. Accordingly the survival probability of a wave function becomes smaller as the number of negative parities increases. It is therefore expected in multidimensional systems that tunneling paths having only one negative parity will dominate the tunnel effect in general. We consider only such a case in what follows. For the same reason, the non-classical solutions or the tunnel effect is never physically recognized in the classical limit $\hbar \to 0$, since the norm of any wave function of this kind is reduced to zero.

The property with respect to the parity of motion holds also for the time-dependent HJ equation [15], and hence the results in what follows are not confined to the stationary state problem.

To connect the local-solutions thus obtained on the different sheets smoothly with conserving the energy, we change the sign of one of the parities at a caustic in the direction normal to the caustic line. The caustics, at which the density of the paths becomes very high (actually infinite in the primitive semiclassical approximation), are defined with the so-called Jacobi field [7] in such a way that

$$\det \left| \frac{\partial \vec{q}_f}{\partial \vec{p}_i} \right| = 0 \quad , \tag{2-17}$$

where $\vec{p}_i$ is a real-valued (quasi-)momentum vector for a given parity set $\{\sigma_k = \pm 1\}$ [cf. Eq.(2-7)] at the initial point on each sheet and $\vec{q}_f$ is the final points of a trajectory on the same sheet. The tunneling path can get back to the Newtonian sheet with the similar procedure when it encounters a caustic point on the tunneling sheet.

III. Statistical Redistribution of Tunneling Paths

We now apply the theory described above to the Hénon-Heiles system [18] to see the effect of chaos on the dynamical tunneling. The Hamiltonian is

$$H = \frac{1}{2m_x} p_x^{\,2} + \frac{1}{2m_y} p_y^{\,2} + \frac{1}{2}(x^2 + y^2) + x^2 y - \frac{1}{3} y^3 \quad , \tag{3-1}$$

where the masses are chosen as $m_x = 1.0087$ and $m_y = 1.0$ so as to break the symmetry of C_3 [6,16]. Those trajectories with the energy less than $\frac{1}{6}$ are bound in the basin area around the origin x=y=0. As seen in the contour plot of the potential of Fig.1, it has no potential barrier in the angular direction around the origin. Nonetheless there present basically 6 patterns of trajectories in the configuration space as shown in Fig.2, which seem to be classified in terms of the angular velocity around the origin. All these trajectories have the same energy E=0.09 but different initial conditions. Although the rotational mode, the pattern II in Fig.2, has two

directions, namely, clockwise (labeled as II_A) and counterclockwise (II_B), we do not distinguish them in the following consideration of the dynamics. The trajectories of the pattern III have arisen due to the aforementioned introduction of the asymmetrical mass balance. This pattern is supposed to be merged with the patterns IV and V as the mass balance approaches $m_x = m_y$. The Poincaré surface of section corresponding to Fig.2 is shown in Fig.3. The common labels have been assigned to Figs.2 and 3 to identify the modes. The section has been made at $x=0$ and $p_x \geq 0$. As seen in Fig.3, there are two quasi-separatrices surrounding the 6 stable regions. A trajectory in these thin separatrices wanders around the edges of the tori in an unpredictable manner [6]. These chaotic trajectories are labeled as VI. We are going to study the tunneling among these stable regions and quasi-separatrices for the energy $E=0.09$.

A. Dynamical tunneling of a single trajectory

We first describe how the tunneling of a single trajectory looks before the ensemble of the paths are studied. Any classical trajectory in Fig.2 has very many caustics along it, from each point of which the tunneling can be initiated. For instance, a trajectory of the type II (rotation) has about 42 caustics during a single period of this large scale rotational motion. This is in a marked contrast to a collision event such as chemical reaction, in which one expects only a few caustics that can be relevant to tunneling during a single encounter. An example of the spatial distribution of the caustics in the Hénon-Heiles system has been presented in ref.[16]. Thus it turns out that one can sample many caustics using a single classical trajectory.

Once a caustic point is encountered by monitoring the condition Eq.(2-17), the direction normal to the caustic line is identified. Then the Cartesian coordinates are orthogonally rotated so that one of the new directions coincides with the caustic line. The parity in the direction normal to the caustic line is changed to -1. The equations of motion Eq.(2-10) begin to be integrated on this sheet with the initial momentum being taken to be the same as

that of the connection point. It is obvious that the momentum normal to the caustic line is zero and thus the tunneling path is smoothly connected with the classical path at the transition point.

Reflecting the functional form of the Hénon-Heiles potential, there are two kinds of tunneling paths. One is that escaping out of the basin area far away. The other remains in the basin until it encounters the first caustic in the tunneling phase space, which thereby gives rise to a dynamical tunneling. Obviously, the former is not relevant to the present study, and only the second type is considered. This type of caustics is observed a little more than 10 % out of all the caustics, depending weakly on an individual classical trajectory. As a tunneling path stays on its sheet longer, the survival probability becomes exponentially smaller, and therefore we basically pick only the first encountered caustic in the tunneling phase space. Again, the coordinates are rotated so that one of them becomes parallel to the caustic line and the negative parity is brought back to the positive unity, whereby a new classical (Newtonian) path commences at this point.

In Fig.4 is depicted a typical example of the dynamical tunneling paths. The panel (A) shows a trajectory of the pattern IV (cf. Fig.2), which encounters a caustic at a point denoted by **I** in the panel (B). One of the parities is changed according to the above prescription, whereby a new tunneling path is born out. It runs on the tunneling sheet until the first caustic point **F** is found, where the parity is changed to positive unity. It turns out that the classical path thus obtained is of the pattern II, which is seen in the panel (C). Note that the final pattern observed after the tunneling is not determined by the position in configuration space but by that in phase space.

In order to examine whether the tunneling paths are chaotic or unstable, we calculate the maximum Liapunov exponents λ, which is defined as

$$\lambda = \frac{1}{n}\sum \frac{\ln|u_{\max}|}{\Delta t} \quad (\theta = n\Delta t) \quad , \tag{3-2}$$

with u_{max} being the maximum eigenvalue of the stability matrix [17]

$$\frac{\partial(q_f, \bar{p}_f)}{\partial(q_i, \bar{p}_i)} \quad , \tag{3-3}$$

where q_f and q_i are the final and initial position vectors, and $\bar{p}_f$ and $\bar{p}_i$ are the real-valued final and initial quasi-momentum vectors, respectively. n is the number of steps and Δt is a time step suitably chosen for integrating the equations of motion Eq.(2-10). The present definition of the Liapunov exponent has been applied both to non-classical and classical paths. Some examples for the behavior of u_{max} along tunneling paths have been presented in our preceding paper [16].

Figure 5 shows the Liapunov exponents averaged over the many classical trajectories λ_{cl} (full squares) and those for the tunneling paths λ_{tunnel} (open squares) versus the total energy. λ_{cl} have been calculated using about 10 classical trajectories that have been sampled randomly from the entire energetically-accessible region in the Poincaré surface of section Fig.3. About 200 dynamical-tunneling paths have been generated in total from these 10 classical trajectories to compute λ_{tunnel}. Naturally λ_{cl} becomes larger as the energy increases. On the other hand, λ_{tunnel} tends to be smaller in the higher energy. This is not surprising, since a tunneling path sees an effective potential that is dominated by $\frac{1}{2}(x_1^2 - y_1^2)$ around the origin, where y_1 is the direction to which the negative parity is assigned after the coordinate rotation to (x_1, y_1). It is noticed that λ_{tunnel} is much larger than λ_{cl} everywhere we have examined. One thus can anticipate that the tunneling paths can induce mixing in the tunneling phase space, which will be investigated in a greater detail in what follows.

B. Quasi-mixing property of the tunneling paths

We next study the statistical distribution of the destinations of the tunneling paths. Remember that the tunneling path shown in Fig.4 has moved from a stable region IV to II. The correspondence of the initial and final tori is given in a deterministic way by an individual tunneling path. However, since a single torus can generate infinitely many tunneling paths,

and since the tunneling paths are highly chaotic, it is expected that they will destine for many different tori and quasi-separatrices. This is indeed the case, and we now show the ratio of the transition from a stable region i to another one j $R_{i\to j}$, where the suffixes label stable regions and quasi-separatrices as given in Fig.3. $R_{i\to j}$ is defined as

$$R_{i\to j} = \frac{D(i,j)}{\sum_j D(i,j)} \quad , \tag{3-4}$$

where $D(i,j)$ is a number of the tunneling paths from a region i to j. Judgment at which stable region or quasiseparatrix a tunneling path arrives has been made on a graphical basis by dividing the Poincaré surface of section in Fig.3 into 100 by 100 segments. Although this procedure is not the best in assigning a point to the quasi-separatrices for the obvious reason, it is practically sufficient for the desired level of accuracy. We have carried out these calculations with the following two different ways of sampling.

(1) Uniform sampling

Choose 250 points uniformly with no biased weighting factor from the accessible Poincaré surface of section Fig.3, which naturally defines 250 classical trajectories. Each trajectory is run about 3.5 times as long as the period of the large-scale rotational motion of the pattern II in Fig.2, during which about 150 caustics are encountered. About 19 caustics out of these 150 generate the dynamical tunneling, and thus we have about 4800 tunneling paths in all.

Table I shows $R_{i\to j}$ with the uniform sampling. It is noticed that extensive transitions among the stable regions and quasiseparatrix have taken place as expected. If most of the tunneling paths are strongly chaotic as seen in Fig.5, one could expect that the population of the final trajectories (post-tunneling trajectories) to be found in a stable region would be roughly proportional to its corresponding area in the Poincaré section. To see this, we define

$$A_j = \frac{\sum_i D(i,j)}{\sum_{i,j} D(i,j)} \quad , \tag{3-5}$$

which is the ratio of the tunneling paths that arrive at a region j. In Table II are listed A_j, together with S_j that are the relative ratios of the areas of the regions in the accessible Poincaré surface of section. Apparently, the coincidence of these two quantities is fairy good. In other words, we have a statistical redistribution of the post-tunneling trajectories, which is a manifestation of the principle of equi-partition through tunneling. However, an objection to this conclusion could be made; since the initial sampling has been made uniformly, the final distributions can be proportional to the areas. However, a closer look at Table I clearly rejects this possibility. That is, the diagonal elements that means the probability for a trajectory to remain in the same pattern after the tunneling are quite small except for the pattern II. Thus, due to the chaotic tunneling, the post-tunneling trajectories have lost the memory of which tori they came from.

Nonetheless, Table II shows some deviation from the completely statistical distribution. In particular, the deviations in the transition from the patterns IV and V to I is considerably large. Besides, despite the symmetrical arrangement of IV and V with respect to I, $R_{4\to1}$ and $R_{5\to1}$ are not the same. (The deviation from the symmetry is more clearly observed in the pair of $R_{1\to4}$ and $R_{1\to5}$.) These results suggest that the number of the sampling points would not be sufficient. However, we ascribe the deviation from the statistical distribution mainly to the short-life nature of the tunneling paths. As described above, a path on the tunneling sheet is brought back to the Newtonian sheet by resetting the negative parity as soon as the first caustic is encountered. The life-time of a tunneling path is therefore as short as about 2π that is nearly the period for a path to oscillate once in the small scale motion. Even if a tunneling path is strongly chaotic, the complete mixing could not be achieved in such a short run. [Note that the concept of mixing is defined mathematically as a property that is to be observed in the limit of the infinitely remote future (or past).]

One of the usual practices to check the mixing is to choose small region(s) randomly

in the entire space, from which somewhat many sampling points are picked up and the destinations of the paths are monitored. We continue to check the property of the mixing based on this sampling.

(2) Localized sampling

Choose a tiny area on each stable region or quasiseparatrix (see the black rectangular areas depicted in Fig.3), the coordinates of which are shown precisely in Table III. Pick up 10 points in each area and run classical trajectories about 5.25 times as long as the period of the large-scale rotational motion, which accumulates about 225 caustics along each trajectory, from which about 30 caustics give rise to the dynamical tunneling. Thus we have prepared about 300 tunneling paths in each of the five entrance stable-regions and one quasiseparatrix.

Tables IV and V display the similar quantities as those in Tables I and II, respectively. To distinguish them, we denote the newer quantities as $\overline{R}_{i\to j}$ and $\overline{A}_j$. Although the difference between Tables IV and II is rather noticeable, they can be viewed essentially the same in a qualitative sense. The similarity between Tables II and V is even more striking. Since the initial sampling zones for $\overline{A}_j$ are highly localized in phase space, and since the number of the sampling points are virtually the same for the every initial regions, the mixing property is now more firmly concluded.

We present a graphical evidence of the equal distribution of the destined (post-tunneling) classical trajectories. Let us go back to the tiny rectangular sampling prepared in the stable region V (cf. the column for V in Table IV, and Fig.3) as an example. As explained above, there are about 300 post-tunneling classical trajectories. We have let each of these trajectories run for a while so that they make about 60 trace points on the Poincaré section. All these points are superposed on the same section, which is Fig.6. Although one can notice a slight hint of the presence of the tori, it is clearly observed that the dotted points cover the accessible area uniformly.

We further add another evidence of the mixing property. In the above calculations,

the life time of each tunneling path is short, since it is forced to finish as soon as the first caustic point is encountered. Here we intentionally let them run on the tunneling sheet until the second caustics are encountered and see what happens, although these paths cannot make a dominant contribution to the tunneling probability. It has turned out that almost half of the tunneling paths have gone out of the basin area. Using the uniform sampling we have computed the distributions analogous to $R_{i\to j}$ and A_j, which are denoted as $\hat{R}_{i\to j}$ (Table VI) and $\hat{A}_j$ (Table VII), respectively. These tables should be compared with Tables I and II, respectively. The Table VI has been particularly improved toward the completely statistical distribution.

Finally, it is noticed from Tables I, IV, and VI that the values in the column for VI (namely the separatrix as a starting region) are fairly close to the ratio of the areas S_j. Since any trajectories in the separatrix wander around the edges of the stable regions, the tunneling paths emanating from them are distributed in the wide range of the phase space from the beginning.

IV. Localization of the destination of tunneling paths

In this section, we examine the effect of the tunneling probability on the distribution of the destinations of dynamical tunneling paths. In the last section, we have found the statistical redistribution of trajectories after the dynamical tunneling caused by chaos in the tunnel region. In section III, the probability that a tunneling path arrives at its destination was always taken to be unity, in other words, the tunneling probability was not considered. In this section, we consider its effect: Is the statistical distribution of the destinations of the dynamical tunneling paths altered when the tunneling probability is considered?

According to Eq.(2-16), first we define the tunneling probability along a tunneling path such that

$$P_{i,j} = \exp\left[\frac{-2}{\hbar} W_I(i,j)\right], \tag{4-1}$$

where $W_I(i,j)$ is the imaginary part of an action integral W_{HJ} along a tunneling path which starts from the ith region and arrives at the jth one. We choose three different values for $\hbar$, namely, 0.01, 0.005 and 0.001. Next, we define the averaged tunneling probability from the ith region to jth one such that

$$\overline{P}_{i,j} = \frac{\sum_{\text{tunnel paths}} P_{i,j}}{D(i,j)}, \tag{4-2}$$

where $D(i,j)$ is the number of tunneling paths which start from the ith region and arrive at the jth one. The summation is carried out over all the tunneling paths from the ith region to the jth one with one negative parity. Tunneling paths are sampled with the procedure of *uniform sampling* which has been defined in the subsection (III-B-1). The averaged tunneling probabilities $\overline{P}_{i,j}$ corresponding to the three different values of $\hbar$ are shown in Tables VIII ($\hbar = 0.01$), IX ($\hbar = 0.005$) and X ($\hbar = 0.001$), respectively. For example, $\overline{P}_{I,II}$ is 0.0990 ($\hbar = 0.01$) in Table VIII. As the value of $\hbar$ gets smaller, the averaged tunneling probabilities become smaller. In all these Tables (Tables VIII, IX and X), the averaged tunneling probabilities are not uniform, especially $\overline{P}_{I,j}$, $\overline{P}_{IV,j}$ and $\overline{P}_{V,j}$ ($j = I,\cdots,VI$) are very large. The difference of the order between the largest tunneling probability and the smallest one is about 2 in Table VIII and it becomes large, as $\hbar$ gets smaller.

To study the distribution of trajectories after the dynamical tunneling, we next modify $R_{i\to j}$ of Eq. (3-4) as

$$\tilde{R}_{i\to j} = \frac{\overline{P}_{i,j} D(i,j)}{\sum_j \overline{P}_{i,j} D(i,j)}, \tag{4-3}$$

in which the tunneling probability has been taken into account. Only when all the averaged tunneling probabilities happen to be equal to 1, Eq.(4-3) turns out to be $R_{i\to j}$. $\tilde{R}_{i\to j}$

corresponding to three different values of $\hbar$ are also shown in the parentheses of Tables VIII ($\hbar = 0.01$), IX ($\hbar = 0.005$) and X ($\hbar = 0.001$), respectively. Compared Table VIII with Table I, $\tilde{R}_{i\to j}$ is much the same as $R_{i\to j}$, but there are large differences between $R_{i\to j}$ and $\tilde{R}_{i\to j}$ in Table X. We also modify A_j of Eq.(3-5) as

$$\tilde{A}_j = \frac{\sum_i \overline{P}_{i,j} D(i,j)}{\sum_{ij} \overline{P}_{i,j} D(i,j)} \quad . \tag{4-4}$$

$\tilde{A}_j$ represents the ratio of the destinations of the tunneling paths which arrive at the jth region without respect to the entrance regions. When all the tunneling paths have the same tunneling probability, Eq.(4-4) turns out to be A_j of Eq.(3-5) and the statistical distribution of trajectories after the dynamical tunneling is found. Table XI shows $\tilde{A}_j$ in case of the three different $\hbar$ and their related area of the Poincaré section S_j. The ratios of the regions I, IV and V are large, particularly at $\hbar = 0.001$. As the value of $\hbar$ becomes smaller, Table XI shows large deviation from the statistical distribution.

Suppose that there are only two tunneling paths, one is the *tunneling path (1)* which arrives at the region I with the imaginary part of the action integral being 0.2 and the other is *tunneling path (2)* which arrives at the region II with the imaginary part being 0.25. The tunneling probability, $\exp\left(-\frac{2}{\hbar}W_I\right)$ (where W_I is the imaginary part of the action integral), along *the tunneling path (1)* is about 0.67 and one along *the tunneling path (2)* is about 0.61 at $\hbar = 1$. Then the ratio of the destinations of the tunneling paths which arrive at region I, $\tilde{A}_I$ of Eq.(4-4), is about 0.53. At $\hbar = 0.1$, the tunneling probability along *the tunneling path (1)* is about 0.018 and one along *the tunneling path (2)* is about 0.007. Because the tunneling probability along *the tunneling path (1)* is about three times larger than one along *the tunneling path (2)*, $\tilde{A}_I$ turns out to be 0.73. As the value of $\hbar$ becomes smaller, $\tilde{A}_I$ tends to be 1.0. The *tunneling path (1)* makes relatively larger contribution to the ratio of the destinations of tunneling paths at small $\hbar$. The small difference in the imaginary parts of the action integrals generates the large difference in the ratio of the tunneling probabilities along individual tunneling paths especially at small $\hbar$. Then the contribution of tunneling paths with large

tunneling probabilities to the distribution of trajectories after the dynamical tunneling becomes large. Therefore the destinations of the dynamical tunneling paths are localized in the specific regions in phase space, when the tunnel probability is considered.

IV. Concluding Remarks

We have shown an important effect of chaos that is manifested through the dynamical tunneling. That is, even if a system under study is not chaotic at all in its classical region, the tunneling phase space may be fully chaotic, which in turn results in the mixing property and statistical redistribution of the trajectories after the tunneling is over. However, the small difference in the imaginary parts of the action integrals along individual tunneling paths generates the large difference in the ratio of the tunneling probabilities along the paths, particularly at small $\hbar$. The difference in the tunneling probabilities along individual tunneling paths makes a large contribution to the distribution of trajectories after the dynamical tunneling. The destinations of dynamical tunneling paths are thus localized in the specific regions in phase space, when the tunneling probability is taken into account. When all the tunneling paths have the same tunneling probability, the equi-partitioned redistribution of the trajectories after the dynamical tunneling is found. Chaos competes with tunneling probabilities to determine the distribution of the tunneling paths. This effect is theoretically interesting and could be important in a practical application of any semiclassical theory.

The localization or statistical distribution of the destinations of chaotic tunneling paths could be important also in the quasi-classical treatment of the quantum effects. It is well-known in chemical reaction dynamics that the so-called quasi-classical method is one of the practical methods [19], in which classical trajectories are sampled so as to be classified according to the quantized action integrals that correspond to the quantum numbers. In particular, when the full quantum theory or even a semiclassical method is hardly applicable, the quasi-classical methods should be an inevitable alternative. The present phenomena and

method can be vitally important in such a case.

References

[1] Z. H. Huang, T. E. Feuchtwang, P. H. Culter and E. Kaze,Phys. Rev. **A41**, 32(1990) and references cited therein.

[2] S. Takada and H. Nakamura, J. Chem. Phys. **100**, 98(1994).

[3] M. J. Davis and E. J. Heller, J. Chem. Phys. **75**, 246(1981).

[4] For example, M. S. Child, *Semiclassical Mechanics with Molecular Applications*, (oxford, 1991).

[5] A. J. Lichtenberg and M. A. Lieberman, *Regular and Stochastic Motion*, (Springer, Berlin, 1983).

[6] K. Takatsuka, Chem. Phys. Lett. **204**, 419 (1993); K. Takatsuka, Bull. Chem. Soc. **66**, 3189 (1993).

[7] L. S. Schulman, *Techniques and Applications of Path Integration*, (Wiley , New York, 1981).

[8] M. V. Berry and K. E. Mount, Rep. Prog. Phys. **35**, 315 (1972).

[9] V. P. Maslov and M. V. Fedoriuk, *Semiclassical Approximation in Quantum Mechanics*, (Reidel, Dordrecht, 1981).

[10] K. Takatsuka, Phys. Rev. Lett. **61**, 503(1988); Phys. Rev. **A61**, 5961(1989).

[11] A. Auerbach, S. Kivelson and D. Nicole, Phys. Rev. Lett. **53**, 411(1984); A. Auerbach and S. Kivelson, Nucl. Phys. **B257** [FS14], 799(1985).

[12] A. Shudo and K. Ikeda, Prog. Theor. Phys. Suppl. **116**, 283(1994).

[13] S. Tomsovic and D. Ullmo, Phys. Rev. **E50**, 145(1994).

[14] L. D. Landau and E. M. Lifshitz, *Quantum Mechanics*, (Pergamon, New York, 1958).

[15] Kazuo Takatsuka and Hiroshi Ushiyama, in preparation.

[16] K. Takatsuka and H. Ushiyama, Phys. Rev. **A51**, 4353(1995).

[17] (a) H. Goldstein, *Classical Mechanics*, (Addison-Wesly, Reading, 1980) ;

(b) V. I. Arnold, *Mathematical Methods of Classical Mechanics*, (Springer, Berlin, 1978);

(c) A. Abraham and J. E. Marsden, *Foundation of Mechanics 2nd. ed.*, (Addison-Wesley, Reading, 1985).

[18] M. Hénon and C. Heiles, Astron. J. **69**, 73(1964).

[19] See for example, D. G. Truhlar and J. T. Muckerman in *Atom-Molecule Collision Theory*, (R. B. Bernstein Ed., Plenum, New York, 1979, page 505).

Table I. The ratio (in %) of the tunneling paths starting from the ith region to the jth one ($R_{i\to j}$) using the method of uniform sampling.

j	Starting region i					
	I	II	III	IV	V	VI
I	28.27	8.38	4.88	0.26	0.82	6.87
II	58.64	72.46	52.61	51.78	43.93	55.71
III	1.30	4.95	10.45	11.46	11.19	5.71
IV	2.91	4.32	11.15	13.18	17.92	10.57
V	4.36	5.73	14.29	14.62	18.46	15.43
VI	4.52	4.16	6.62	8.70	7.68	5.71

Table II. The ratio (in %) for the tunneling paths to arrive at the jth region (A_j) and its relative area (S_j) on the Poincaré section with the uniform sampling.

j	A_j	S_j
I	8.25	10.10
II	60.58	64.29
III	6.79	5.41
IV	8.48	7.38
V	10.19	7.38
VI	5.71	5.44

Table III. The sampling region used to generate the tunneling paths in the local sampling. In the last column $0.31 \leftrightarrow 0.35$, for example, indicates that $p_y = 0.31,0.32,0.33,0.34,0.35$ are chosen with the same interval 0.01.

	y	p_y
I	0.26,0.27	$0.31 \leftrightarrow 0.35$
II	-0.23,-0.24	$0.01 \leftrightarrow 0.05$
	0.06,0.07	$0.01 \leftrightarrow 0.05$
III	-0.16	$-0.05 \leftrightarrow 0.04$
IV	-0.04	$0.11 \leftrightarrow 0.15$
V	-0.04,-0.03	$-0.11 \leftrightarrow -0.15$
VI	0.21,0.22	$0.26 \leftrightarrow 0.30$

Table IV. The ratio (in %) of the tunneling paths starting from the ith region to the jth one ($\overline{R}_{i \to j}$) using the method of localized sampling.

j	Starting region i					
	I	II	III	IV	V	VI
I	16.90	2.22	3.98	2.07	2.85	14.66
II	71.19	83.70	57.52	59.47	55.16	56.55
III	1.66	5.94	11.08	9.47	8.90	4.71
IV	2.49	1.48	7.96	12.13	11.74	6.28
V	2.49	3.70	11.50	9.46	13.52	13.09
VI	5.27	2.96	7.96	7.40	7.83	4.71

Table V. The ratio (in %) for the tunneling paths to arrive at the jth region ($\bar{A}_j$) and its relative area (S_j) on the Poincaré section with the localized sampling.

j	$\bar{A}_j$	S_j
I	7.21	10.10
II	64.39	64.29
III	6.65	5.41
IV	7.27	7.38
V	8.38	7.38
VI	6.10	5.44

Table VI. The ratio (in %) of the tunneling paths starting from the ith region to the jth one ($\hat{R}_{i\to j}$) after the second caustic point is encountered in the tunnel phase space using the uniform sampling.

j	Starting region i					
	I	II	III	IV	V	VI
I	9.79	11.49	5.99	9.26	8.25	10.53
II	65.11	51.91	75.58	67.59	69.91	60.90
III	7.23	7.45	6.91	3.25	3.13	4.89
IV	9.79	1.92	3.23	8.33	10.16	13.53
V	0.85	21.91	2.30	6.48	5.08	1.50
VI	7.23	5.32	5.99	5.09	3.52	8.65

Table VII. The ratio (in %) for the tunneling paths to arrive at the jth region ($\hat{A}_j$) after the second caustic is encountered, and its relative area (S_j) on the Poincaré section with the uniform sampling.

j	$\hat{A}_j$	S_j
I	9.56	10.10
II	63.13	64.29
III	5.72	5.41
IV	7.17	7.38
V	8.49	7.38
VI	5.90	5.44

Table VIII. The averaged tunneling probabilities $\overline{P}_{i,j}$ and the ratio of the transition with tunneling probabilities along the paths which start from the ith region and arrive at the jth one $\tilde{R}_{i\to j}$ (in %) in parentheses are shown. $\hbar$ is chosen as 0.01.

j	Starting region i					
	I	II	III	IV	V	VI
I	0.2877 (29.57)	0.0356 (21.40)	0.0597 (7.79)	0.0829 (1.48)	0.0587 (0.93)	0.0596 (6.51)
II	0.0990 (55.79)	0.0057 (59.94)	0.0503 (64.13)	0.1139 (44.20)	0.1017 (39.79)	0.0590 (56.00)
III	0.1400 (4.70)	0.0115 (5.27)	0.0509 (4.30)	0.2114 (8.04)	0.2437 (10.69)	0.1312 (10.31)
IV	0.0573 (1.35)	0.0080 (3.85)	0.0897 (9.31)	0.5003 (38.17)	0.0750 (0.80)	0.1155 (9.65)
V	0.0234 (0.65)	0.0039 (1.72)	0.0790 (9.08)	0.0441 (0.51)	0.5123 (40.96)	0.0672 (6.07)
VI	0.1804 (7.94)	0.0160 (7.82)	0.0617 (5.39)	0.2115 (7.60)	0.2052 (6.83)	0.1440 (11.46)

Table IX. The averaged tunneling probabilities $\overline{P}_{i,j}$ and the ratio of the transition with tunneling probabilities along the paths which start from the ith region and arrive at the jth one $\tilde{R}_{i\to j}$ (in %) in parentheses are shown. $\hbar$ is chosen as 0.005.

j	Starting region i					
	I	II	III	IV	V	VI
I	0.2144 (40.36)	0.0237 (34.65)	0.0203 (7.04)	0.0395 (1.16)	0.0172 (0.44)	0.0186 (4.98)
II	0.0454 (46.87)	0.0019 (47.93)	0.0189 (64.30)	0.0513 (32.84)	0.0476 (29.93)	0.0256 (59.65)
III	0.0678 (4.17)	0.0051 (5.63)	0.0177 (3.98)	0.1192 (7.49)	0.1514 (10.68)	0.0548 (10.60)
IV	0.0191 (0.83)	0.0022 (2.58)	0.0363 (10.05)	0.4073 (51.28)	0.0224 (0.38)	0.0414 (8.52)
V	0.0055 (0.28)	0.0009 (0.95)	0.0305 (9.35)	0.0152 (0.30)	0.4061 (52.20)	0.0186 (4.14)
VI	0.0929 (7.49)	0.0070 (8.26)	0.0227 (5.28)	0.1170 (6.93)	0.1190 (6.37)	0.0618 (12.11)

Table X. The averaged tunneling probabilities $\overline{P}_{i,j}$ and the ratio of the transition with tunneling probabilities along the paths which start from the ith region and arrive at the jth one $\tilde{R}_{i\to j}$ (in %) in parentheses are shown. $\hbar$ is chosen as 0.001.

j	Starting region i					
	I	II	III	IV	V	VI
I	0.0589 (80.51)	0.0060 (83.83)	0.0000 (1.39)	0.0021 (0.24)	0.0003 (0.03)	0.0001 (2.98)
II	0.0020 (14.89)	0.0000 (10.98)	0.0001 (65.85)	0.0019 (4.72)	0.0024 (6.73)	0.0002 (76.99)
III	0.0031 (1.40)	0.0002 (2.32)	0.0000 (1.79)	0.0124 (3.03)	0.0181 (5.60)	0.0002 (56.51)
IV	0.0003 (0.08)	0.0000 (0.01)	0.0003 (16.45)	0.1830 (89.52)	0.0007 (0.05)	0.0001 (4.74)
V	0.0000 (0.00)	0.0000 (0.00)	0.0002 (12.57)	0.0003 (0.02)	0.1506 (84.74)	0.0000 (0.90)
VI	0.0053 (3.12)	0.0002 (2.86)	0.0000 (1.95)	0.0108 (2.47)	0.0122 (2.85)	0.0002 (7.88)

Table XI. The ratio (in %) of the destinations of tunneling paths with tunnel probabilities which arrive at the jth region ($\tilde{A}_j$) corresponding to three different $\hbar$, and its relative area (S_j) on the Poincaré surface of section are shown.

	$\tilde{A}_j$			
	$\hbar$=0.01	$\hbar$=0.005	$\hbar$=0.001	S_j
I	9.15	10.90	14.00	10.10
II	48.40	38.16	7.28	64.29
III	7.94	7.87	3.78	5.41
IV	13.27	17.70	38.43	7.38
V	13.60	18.18	33.90	7.38
VI	7.64	7.19	2.70	5.44

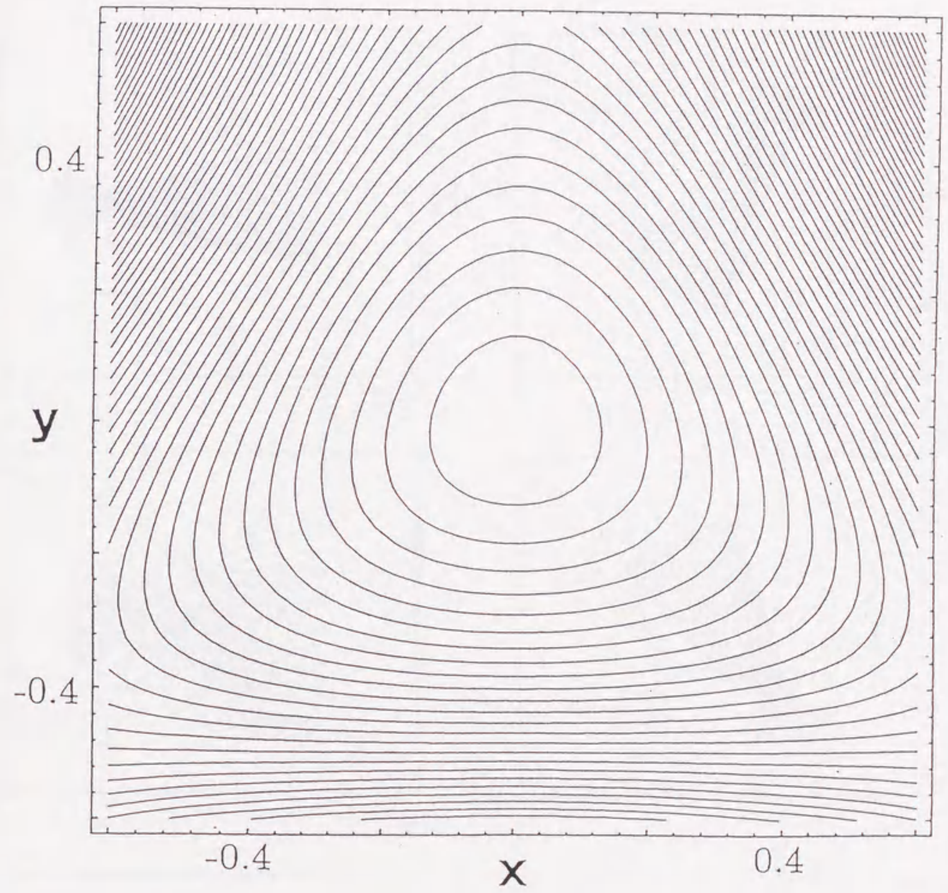

Figure 1. Contour plot of the Hénon-Heiles potential function. There is no potential barrier in the angular direction.

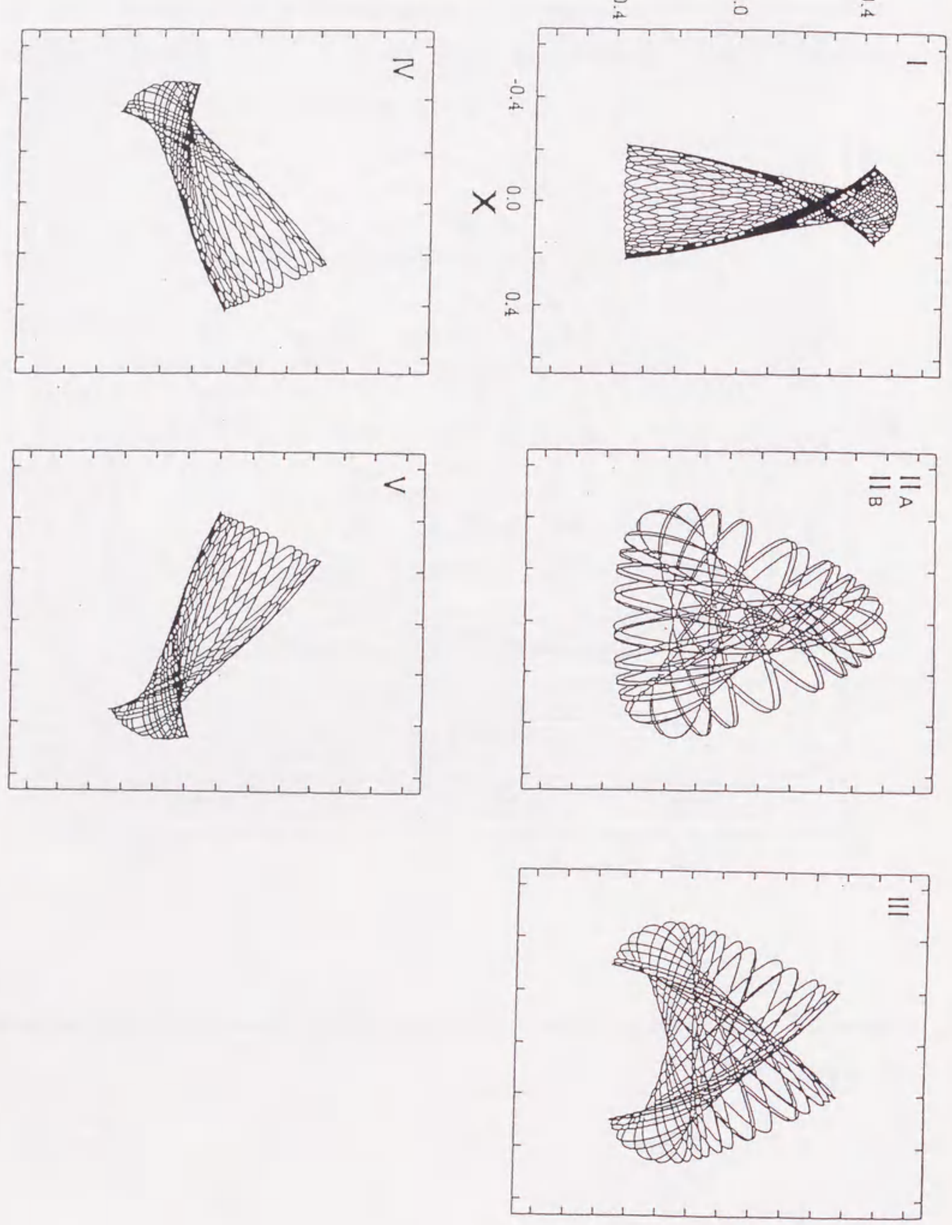

Figure 2. Six distinctive patterns of traiectories. All the traiectories have the same energy

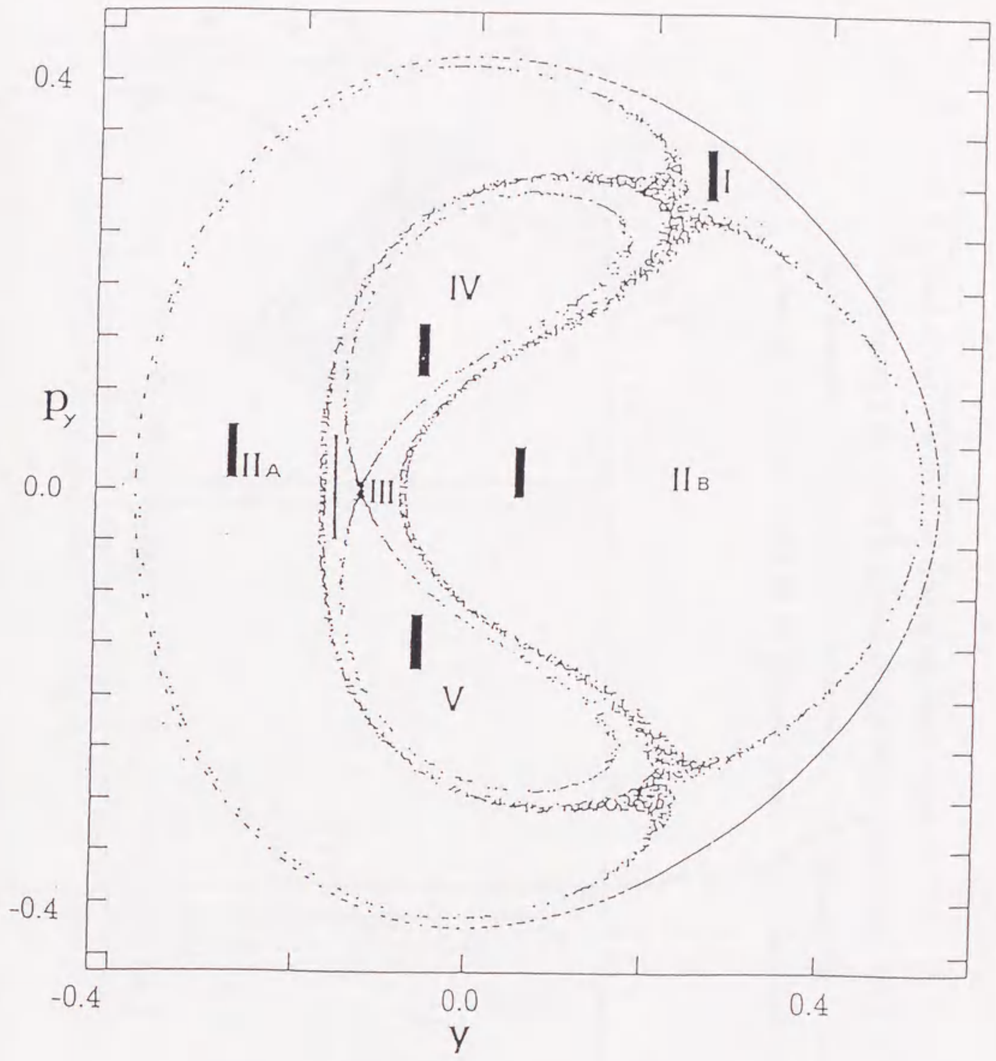

Figure 3. The quasi-separatrix on the Poincaré surface of section at x=0 and p_x>0. The stable regions are separated by the thin quasi-separatrices. The stable regions are labeled according to the pattern in the configuration space of Fig.2. The black rectangular boxes located in the regions are the area from which the sampling trajectories are picked up to check the mixing property. See Sec.III and Table III.

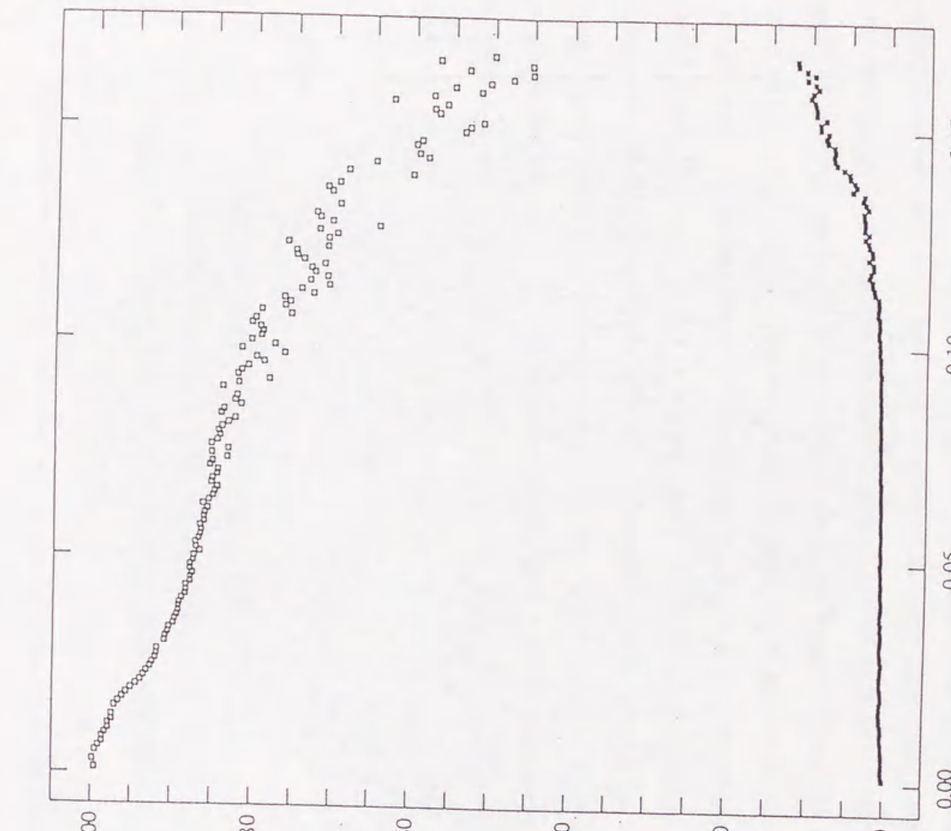

Figure 5. The averaged maximum Liapunov exponents of classical trajectories λ_{cl} (full squares) and those for the tunneling paths λ_{tunnel} (open squares) as functions of the energy. λ_{tunnel} are much larger than λ_{cl} at all the energies.

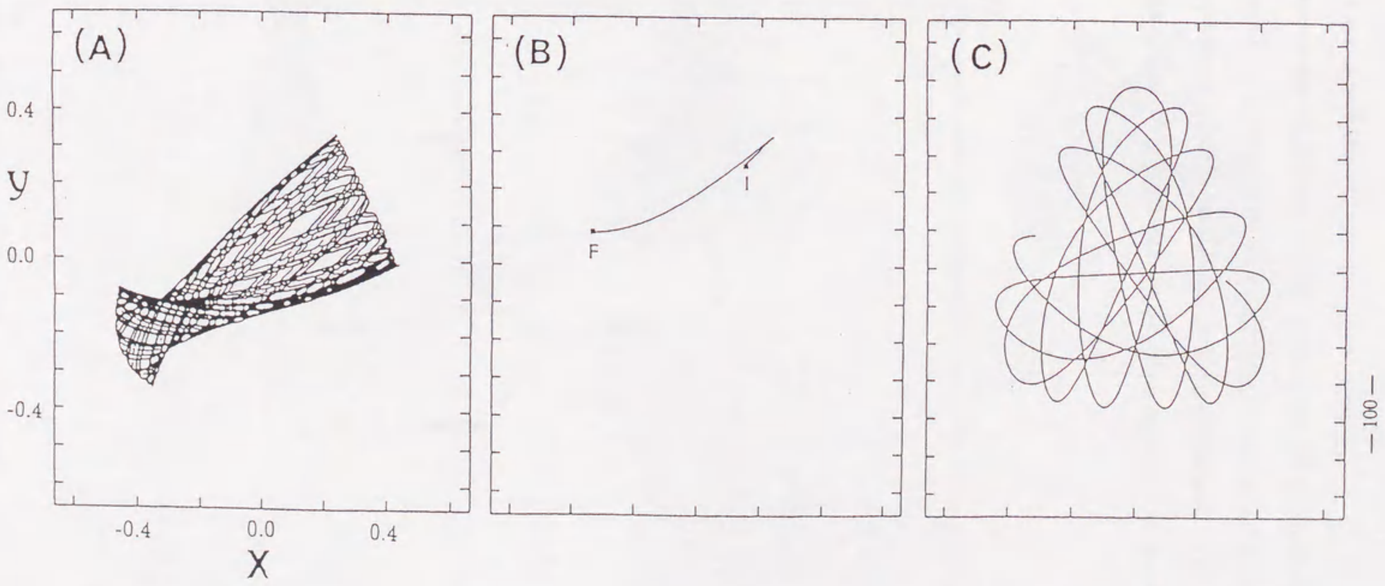

Figure 4. A typical example of the tunneling path. (A) An initial classical trajectory corresponding to pattern IV that has a caustic at a point denoted **I**. (B) A tunneling path starting from **I** and ending at **F** where the first caustic is encountered in the tunneling phase space. (C) At the point **F**, the classical trajectory resumes.

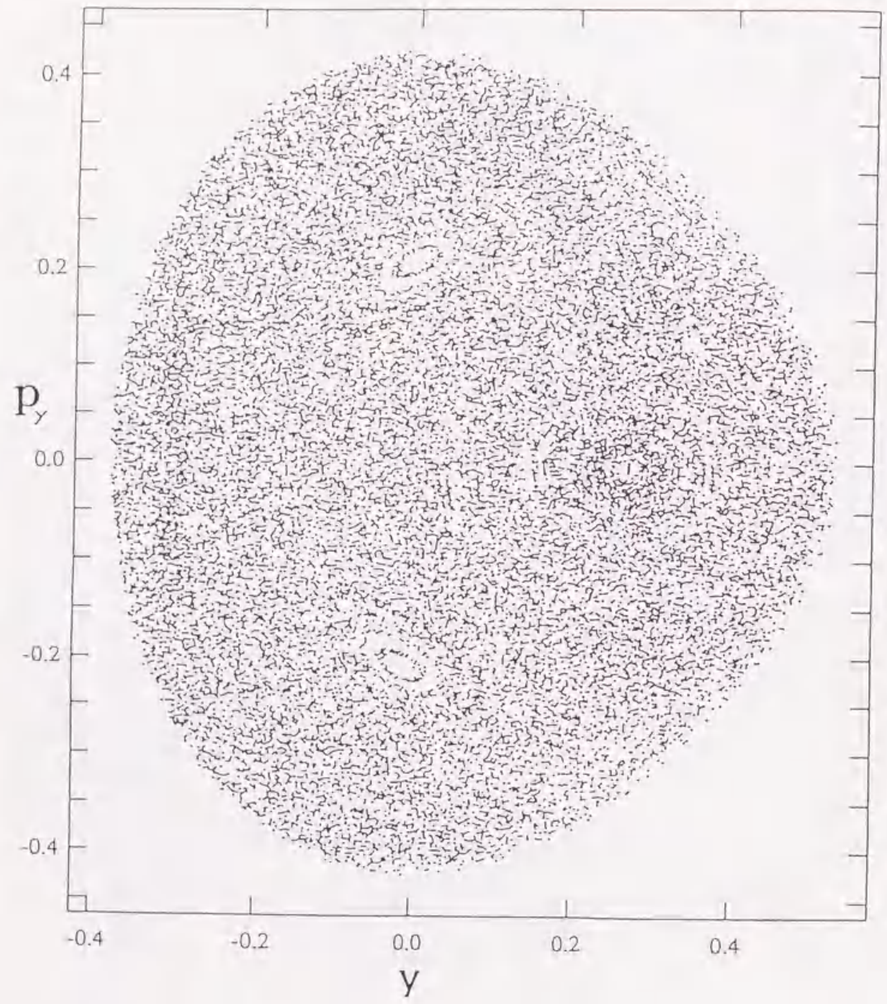

Figure 6. The Poincaré section generated by the post-tunneling classical trajectories, the initial sampling trajectories before the tunneling of which have been taken from the black squared tiny area on the region V of Fig. 3. A uniform distribution is apparent.

Chapter II.

Semiclassical Study on Multidimensional Effects in Tunneling Chemical Reactions - Tunneling Paths and Tunneling Tubes

abstracts

The effects of multidimensionality in the quantum mechanical tunneling of chemical reactions are investigated. To study the mechanism of tunneling reaction, a quasi-classical treatment of the semiclassical mechanics is developed to characterize the real-valued tunneling paths. In the present chapter, some typical tunneling reactions in collinear three atomic systems on the LEPS potential surface are investigated in terms of our semiclassical theory constructed in Chapter II of Part I. The initial energy distribution among the vibrational and translational modes is investigated asking which is preferable for tunneling and what is the resultant distribution of the energy in the product molecules. And the effects of the initial translational energy on the property of tunneling paths are also studied. Mainly the following two factors to control the tunneling reactions are examined as our first case study: (a) the mass effects featuring heavy-light-heavy and light-heavy-light patterns and (b) the anisotropy of the potential surface, namely, the early or late barrier. Tunneling paths of the types of Marcus-Coltrin and Miller-George are both generated spontaneously. A path of Marcus-Coltrin type takes a major role when the translational energy dominates in tunneling, while that of Miller-George type does in a case where the vibrational excitation is important. As a distinguished feature of the multidimensionality in tunneling, we have identified the existence of what we call a tunneling tube which is a bunch of tunneling paths with large tunneling probabilities.

I. Introduction

The study of the quantum mechanical tunneling has its long standing history. Nevertheless, tunneling is getting more prominent as its universality in various branches of science and technology is recognized. Among others, our concern in the present chapter is about the tunneling in chemical reactions [1]. In particular, we study the effects of multidimensionality and/or many-body effects on tunneling in chemical reactions. A gap lying between one- and two-dimensional tunneling theories is quite deep and wide, just as in other general subjects in science. One dimensional tunneling has been clearly understood and nothing much is left for further study [2,3]. Two dimensional tunneling can generally undergo energy transfer between the available modes. Cooperative or resonant tunneling in which two or more protons transfer simultaneously can happen only in systems with even higher dimensions as in water clusters, DNA chains, and so on. Recently, Clary et al. [4] have developed an extensive study of tunneling splitting in water dimer and trimer by means of the quantum Monte Carlo method. However, theoretical study on high-dimensional tunneling in *reaction dynamics* is still a very tough problem.

Our aim in the present chapter is directed towards conceptual understanding of multidimensional tunneling-reactions rather than numerically accurate estimate of tunneling probability. To accomplish our aim, we have first formulated a new semiclassical theory for tunneling in Chapter II of Part I, with which the tunneling paths and associated tunneling probabilities are generated. Then, in the present chapter, on the basis of this theory, we ask the following questions: How does the distribution of the initial energy affect the tunneling probability? In other words, which chemical modes should be excited to accelerate tunnel reactions, vibrational or translational mode? What will be the energy distributions after tunneling? Can we describe the effects of mass balance (heavy-light-heavy and light-heavy-light) and the anisotropy of the location of the potential barrier (early and late potential surfaces) in terms of the nature of our tunneling paths? Is the property of our tunneling paths

with the high translational energy different from one of the tunneling paths with the low translational energy?

An idea of attempting to seek for "paths" even in a tunneling system is natural, in view of the great success of classical mechanics. There are basically two kinds of treatment of tunneling paths. One is a path that is rather artificial, at most intuitive, that is regarded as a kind of reaction coordinate. They can be curvilinear or simply linear. For instance, Garrett and Truhlar tried to find a curvilinear path that supports the optimal tunneling probability [5]. Sewell etc. [6] and Guo etc. [7] treat multidimensional tunneling within the framework of the so-called quasi-classical method with tunneling paths which was proposed by B. A. Waite and W. H. Miller [8] and by N. Makri and W. H. Miller [9]. Their tunneling paths are the minimum energy path or the straight-line path connecting the desired points. These methods are applied to estimate reaction rates and the tunneling-splitting of bound states. The multidimensional effect could have been taken into account by treating the coordinates orthogonal to the tunneling path as bath modes. The other attitude to tunneling path is more lyric. A tunneling path is regarded as a generalization of classical trajectory, through which not only the tunneling probability but also the multidimensional *mechanisms* of tunneling are extracted. The instanton paths [10] are the typical example. We here take the latter approach.

The present chapter is concerned about the application of our semiclassical theory described in Chapter II of Part I to tunneling chemical reactions. We begin with the very basic investigation using a typical reaction $A+BC \rightarrow AB+C$ in the collinear arrangement. We take a general and conceptual approach rather than analyzing a realistic system. For this reason, the potential surface we use is merely the so-called LEPS surface [11,12]. In practical applications of our semiclassical theory, the semiclassical kernel proposed in Chapter II of Part I is partly treated in such a manner as the so-called quasi-classical method [13]. We examine which kind of tunneling paths dominate as functions of both the initial distribution of energy and the initial translational energy. The final energy distribution in the product molecules is also presented. The effects of the following two major factors, namely, mass balance and the anisotropy of the potential surface that can control the tunneling reactions are

also studied. We have found the existence of "tunneling tube" in which a continuous bunch of tunneling paths emanate from the so-called caustic lines. This is a peculiar characteristic to the multidimensional tunneling.

II. Multidimensional Effects in Tunneling Chemical Reactions

In this section, we investigate the multidimensional effects in the tunneling chemical reactions. As a first step of the application of our semiclassical theory described in Chapter II of Part I, we choose some typical tunneling reactions for collinear three atomic system on the LEPS potential surface [11,12]. In the present chapter we do not intend to attempt to analyze any particular experimental result. Rather, we would like to seek universal and conceptually characteristic phenomena that could be step stones for analyses of more complicated tunneling reactions. Mainly the following five factors are examined as our preliminary case study: (a) the initial distribution of the energy among the vibrational and translational modes to identify a preferable mode for tunneling, (b) the resultant energy distribution in the product vibrational states, (c) the mass effect featuring heavy-light-heavy and light-heavy-light patterns, (d) the anisotropy of the potential surface, namely, the early or late barrier, and (e) the effects of the initial translational energy on the property of tunneling paths.

Although we have developed a semiclassical theory based on the Feynman kernel in Chapter II of Part I, we rather do not apply the theory in a full semiclassical way in the present chapter. By semiclassical way, we mean an approach in which an initial wavepacket (or eigenfunction), which is prepared beforehand, is propagated in terms of the kernel [14,15]. However, this is considerably tedious. Besides, we are not interested here in the quantitative study of the tunneling probabilities for the individual wavepackets. We thus simplify the semiclassical method by partially borrowing the idea of the so-called quasi-classical method [13]: The initial conditions for running trajectories are sampled as follows. In the subsections (A-1-a), (A-2-a) and (B), only the paths of the same total energy, which is lower than the

height of energy barriers, are compared, and the effects of the initial energy distribution between translational and vibrational modes are examined. In the subsections (A-1-b) and (A-2-b), only the paths of the same initial vibrational energy, whose total energies are chosen to be lower than the height of the energy barrier, are compared and the effects of the initial translational energy on the property of tunneling paths are studied. In the quasi-classical method, the initial vibrational energies are sampled from bins that sandwich the eigenvalues in phase space. However, in our method, the initial vibrational energies are sampled only from the manifolds in phase space having the energies of the eigenvalues. Each classical trajectory encounters several caustics, from each of which a tunneling path emanates with only one negative parity. They come back to the Newtonian space when they hit the first caustic point in the tunneling space. Then we calculated the tunneling probability on the basis of our semiclassical expression (see Eq.(2-34) in Chapter II of Part I) in which not only the dumping due to the complex-valued action integral but also the variance due to the amplitude (pre-exponential) factor are evaluated. (The quasi-classical approach does not take account of the amplitude factor.) Thus the evaluation of the tunneling probability is not made to quantify the reaction probability but to identify which paths dominate the tunneling.

The LEPS potential for a reaction $A+BC \rightarrow AB+C$ is given by

$$V(r_{AB},r_{BC},r_{AC}) = \frac{Q_{AB}}{1+S_{AB}} + \frac{Q_{BC}}{1+S_{BC}} + \frac{Q_{AC}}{1+S_{AC}} - \{\frac{1}{2}[(\frac{J_{AB}}{1+S_{AB}} - \frac{J_{BC}}{1+S_{BC}})^2 + (\frac{J_{BC}}{1+S_{BC}} - \frac{J_{AC}}{1+S_{AC}})^2 + (\frac{J_{AC}}{1+S_{AC}} - \frac{J_{AB}}{1+S_{AB}})^2]\}^{\frac{1}{2}} \quad (2\text{-}1)$$

where, for instance,

$$\frac{Q_{AB}+J_{AB}}{1+S_{AB}} = D_{AB}\{\exp[-2\beta_{AB}(r_{AB}-r_{AB}^0)] - 2\exp[-\beta_{AB}(r_{AB}-r_{AB}^0)]\} \quad (2\text{-}2a)$$

$$\frac{Q_{AB}-J_{AB}}{1-S_{AB}} = \frac{1}{2}D_{AB}\{\exp[-2\beta_{AB}(r_{AB}-r_{AB}^0)] + 2\exp[-\beta_{AB}(r_{AB}-r_{AB}^0)]\} . \quad (2\text{-}2b)$$

We take a collinear system, i.e. $r_{AC}=r_{AB}+r_{BC}$, where, for example, r_{AB} is the distance

between the atoms A and B, and so on. On the other hand, the orthogonal coordinates (x, y) that removes the mass polarization term (i.e. the crossing term $\frac{\partial}{\partial x}\frac{\partial}{\partial y}$) and makes all the effective masses be unity can be generated such that

$$x = a\, r_{AB} + b\, r_{BC}\cos\varphi \qquad \text{and} \qquad y = b\, r_{BC}\sin\varphi, \tag{2-3}$$

where

$$a = \left(\frac{m_A(m_B + m_C)}{M}\right)^{\frac{1}{2}} \quad \text{and} \quad b = \left(\frac{m_C(m_B + m_A)}{M}\right)^{\frac{1}{2}} \tag{2-4}$$

with $M = m_A + m_B + m_C$. φ in Eq.(2-3) is the well-known skew angle. In comparing Eq.(2-2) and (2-3), it is noticed that a pair of the parameters (β_{AB}, a) are mutually dependent in determining the dynamics. So is (β_{BC}, b). Although the physical origins of β_{AB} and a are completely different, one can make use of this redundancy to deduce the independent parameters as far as the LEPS potential is concerned. Thus we set $(a,b) = (1,1)$ and instead, β_{AB} and β_{BC} are reread as

$$\frac{\beta_{AB}}{a} \to \beta_{AB} \qquad \text{and} \qquad \frac{\beta_{BC}}{b} \to \beta_{BC}. \tag{2-5}$$

The implication of this parameter setting is that the effect of the mass balance, namely, m_A/m_B is taken into account only through the skew angle. By mass effect, we mean this way in what follows. The overlap parameters, S_{AB} and so on, are all set to zero. The other parameters are given below depending on the aspects we want to study. Throughout this chapter , the Planck constant is taken as $\hbar = 0.1$, and the mass weighted coordinates are used.

A. Mass effects

We first study the mass effects in a symmetric case of $A = C$. The LEPS parameters

are selected as $D_{AB} = D_{BC} = D_{AC} = D$, and are listed in Table I. As usual, two typical cases are picked up, that is, a Light-Heavy-Light (L-H-L) system with $\varphi = \frac{\pi}{2}$ (Fig.1) and a Heavy-Light-Heavy (H-L-H) system with $\varphi = \frac{\pi}{6}$ (Fig.5).

For the investigation of the effects of a initial energy distribution on tunneling in the subsection (A-1-a), (A-2-a) and (B), the initial vibrational energies are samples so as to have the values corresponding to the vibrational quantum numbers $v = 0, 1, \cdots$ for BC molecule in both systems. About 150 points are selected from each quantized torus in the phase space (y, p_y). We then let BC collide with A at the total energy $E_{total} = -6.0$, which is lower than the height of the saddle point $E_{saddle} = -5.5$. The translational energies are given automatically by specifying the vibrational quantum number. The reaction thus takes place only through the tunneling.

For the study of the effects of the initial translational energy on the property of tunneling paths in the subsection (A-1-b) and (A-2-b), only one of the vibrational quantum numbers corresponding to an eigenvalue about 2.0 is chosen for the initial vibrational quantum number. About 300 points are selected from a quantized torus corresponding to the initial vibrational quantum number in phase space as the initial condition of the vibrational mode. We then let BC collide with A at the various initial translational energies E_{trans} keeping the initial vibrational energy fixed. $E_{trans} = 0.2, 0.4, \cdots, 2.0$ are chosen with the same interval 0.2. Because the height of the energy barrier is about 4.5, only tunneling reactions occur.

When each classical trajectory arrives at caustics, the coordinates are rotated $(x,y) \to (\bar{x},\bar{y})$ following the prescription described above. A single path can have plural caustics along it, from which different tunneling paths can branch. However, as is easily guessed, tunneling paths emanating from caustics that are closer to the transition states tend to have a large tunneling probability. Only the case of one negative parity is considered. The tunneling paths are brought back to the Newtonian sheet when encounter the first caustic point in their phase spaces.

(A-1) Light-Heavy-Light system

(A-1-a) The effects of the initial distribution of energy

Figures 1(a)-(c) represent the tunneling paths whose initial vibrational states are $v=0-2$, respectively. The vibrational states up to $v=9$ are open for the present energy. For $v\geq 3$, however, there is no tunneling paths appreciable, because those classical paths cannot reach the vicinity of the saddle point.

In Fig.1(b) are observed two different types of path. One is the so-called Marcus-Coltrin (M-C) type [16] that goes almost parallel along with the reaction coordinate. The other is the Miller-George (M-G) type [17] which is transversal to the lines of the contour plots of the potential energy. Both types are generated automatically from our tunneling dynamics. It is well anticipated that the initial excitation in the translational mode is preferable to the M-C paths, while the vibrational excitation should be favorable to the M-G paths. The product distribution should of course depend on these types. Which type of the paths then dominates the tunneling probability in Fig.1(b), where both of the two types coexist?

To find an answer to this question, we now proceed to the semi-quantitative arguments of the tunneling probability. First we note a fact that the number of the tunneling paths is largest at $v=1$. However, this does not mean the maximum of the tunneling probability, since each path is associated with a different probability. The tunneling probability in our quasi-semiclassical treatment is defined as follows. We first evaluate

$$T=\sum_{\gamma}\left|K_{tunnel}(q_t,t;q_s,s;\{\sigma\})\right|^2, \tag{2-6}$$

where γ denotes all the possible tunneling paths. Since K_{tunnel} (Eq.(2-34) in Chapter II of Part I) diverges at both ends (caustics) of each tunneling path, the so-called uniform approximation based on the Airy function [14] has been adopted to reduce the end values to be finite. To make a meaningful comparison which does not depend on the sampling number (N_{tr}), we define an average of tunneling probability per classical trajectory as

$$T_{tr}=\frac{T}{N_{tr}}. \tag{2-7}$$

Table II lists the tunneling probabilities thus defined as a function of the vibrational quantum numbers. The initial state with $v=2$ gives the largest tunneling probability. The qualitative reason for this is that the tunneling path is short and passes through a place of high potential energy, as observed in Fig.1(c). The absolute values of the tunneling probability in an L-H-L system are very low as expected generally.

We next try to visualize the tunneling probability along the tunneling paths. Suppose we have a tunneling path for which $\left|K_{tunnel}(q_t,t;q_s,s;\{\sigma\})\right|^2$ is known. Then we assign this value uniformly along the tunneling path from the entrance q_s to the exit q_t. Superposition of all theses numbers along the tunneling paths provides a distribution of the probability density in configuration space. Figures 1(A)-(C) corresponding to the paths of Figs.1(a)-(c), respectively, show thus obtained density plots, which is referred to the tunneling density in what follows. It turns out that the M-G type paths in Fig.1(b) bear much smaller tunneling probabilities and hence has disappeared from Fig.1(B). The M-C type path looks really like a straight-line and hence happens to be able to be treated as a one-dimensional tunneling.

Let us look at the energy distribution in the product. In view of the quality of our calculation, the state-to-state cross section is not addressed. Instead, here we calculate only the ratio of the produced populations in the final vibrational states. The assignment of the product channels has been carried out using the bins of vibrational energy that are set so as to sandwich the quantized energy with equal spacing. This is exactly the same practice as used in the quasi-classical method [13]. Suppose the initial classical trajectories are started from the manifold of the quantum number $v_i=m$. Some of them can reach the exit valley through tunneling and are assigned to one of the quantum states $v_f=n$ after the interaction is effectively over. Among these paths, suppose that the j-th path has a probability of tunneling $T_j(m\rightarrow n)$ defined by

$$T_j(m \to n) = \left| K_{tunnel,j}\left(v_f = n; v_i = m; \{\sigma\}\right) \right|^2 . \tag{2-8}$$

Then the ratio in the product channel is

$$R(m \to n) = \frac{\sum_{channels} T_j(m \to n)}{\sum_k \sum_j T_j(m \to k)} \tag{2-9}$$

In Fig.2, $R(0 \to n)$, $R(1 \to n)$, and $R(2 \to n)$ for $n = 0-9$ are shown. Although the tunneling probability is very small, the general behavior in the product distribution is quite interesting in that it is highly selective. For instance, $R(0 \to 4)$, $R(1 \to 3)$, $R(2 \to 3)$, and $R(2 \to 2)$ are predominant almost exclusively. Thus the peaks are found at $v_i + v_f \approx 4$. Presumably we need to accumulate more date to make a firm conclusion about the selectivity due to tunneling in the L-H-L system.

(A-1-b) The effects of the initial translational energy

We also investigate the density plots at different initial translational energies with a fixed initial vibration energy. The initial vibrational state is fixed at $v = 4$ which corresponds to the initial vibrational energy 1.9. We change only the initial translational energy from 0 to 2.0, for which the total energies are lower than the height of the energy barrier $E_{barrier} = 4.5$. Figures 3 (A)-(C) show the tunneling density at the initial translational energies 1.6, 1.8 and 2.0, respectively. Only the M-C type paths or the minimum energy paths appear at the high translational energy range. The length of the density of tunneling paths gets shorter as the initial translational energy increases. Then we can expect tunneling paths to have large tunneling probabilities at the high translational energy range. Figure 4 shows the tunneling probability (Eq.(2-7)) as a function of the initial translational energy. The tunneling probability becomes larger as the initial translational energy is increased as expected.

(A-2) Heavy-Light-Heavy system

(A-2-a) The effects of the initial distribution of energy

We now turn to a case of the mass balance of Heavy-Light-Heavy system, which is known to be far more favorable to tunneling. Figures 5(a)-(e) show the tunneling paths for the initial vibrational states $v = 0-4$, respectively, and 5(A)-(E) depict their tunneling density plot. The highest vibrational state allowed by this energy is $v = 4$. As expected, the number of tunneling paths are much larger than the L-H-L system by the factor 10^2, which is peaked at $v = 3$. However, the tunneling probability T_{nt} has its maximum at $v = 2$ as seen in Table III.

The reason why $v = 2$ has the maximum probability can be described as follows. A classical trajectory having the initial high vibrational energy cannot come close to the saddle point, and thereby the tunneling path emanating from it should have a long path-length. This would generally reduce the tunneling probability. On the other hand, although a classical path with the high translational energy (low vibrational one) can approach deeply into the vicinity of the transition state, the resultant tunneling path is not directed towards the product channel and accordingly the high tunneling probability is not expected. One should have some intermediate state that compromises these two factors to maximize the tunneling probability. This is important to design an experiment to enhance the tunneling reaction.

There are involved several types of tunneling paths throughout Figs.5(a)-(e), which are again classified basically as M-C type and M-G type. It is observed that the M-C type dominates the lower vibrational states (Fig.5(a)), while the M-G type is virtually exclusive in the higher vibrational states (Fig.5(e)). The tunneling density plots Figs.5 (A) through (E) demonstrate this tendency clearly. Even significant number of the M-G type paths are observed in Fig.5(a), their contributions to the tunneling probability is quite low (compare with Fig.5(A)).

A very important characteristic is noticed in Fig.5(B)-(E) (and (b)-(e)) that was not

found in the L-H-L system (Fig.1). That is, the major tunneling regions have a band structure (manifold) in the configuration space. We call this manifold tunneling tube. This class of tunneling is of essentially multidimensional nature and should not be treated in terms of the conventional reaction-coordinate (one-dimensional) approach. The higher is the dimensionality, the more important should become the tunneling tube.

The final energy distribution, which is shown in Fig.6, exhibits less characteristic features than in the L-H-L system. Although the higher states tend to be produced more in general, $R(m \to n)$ for $m \geq 1$ has relatively wide distribution. A very clear exception for this is $R(0 \to n)$, which has the tunneling probability only at $v = 4$. Comparison of Fig.5(A) with Figs.5(B)-(E) makes this reason clear: The diameter of the tunneling tube for $v = 0$ (Fig.5(A)) is overwhelmingly smaller than those for $v = 1-4$. We also recall that the diameters of the tunneling tubes in the L-H-L system (Fig.1(A)-(C)) are all very narrow. Thus it is suggested that the final energy distribution would generally be governed by the size of the tunneling tube.

(A-2-b) The effects of the initial translational energy

In this subsection, we study the property of the tunneling tubes and the tunneling paths at different initial translational energies with a fixed initial vibrational state. The initial vibrational state is fixed at $v = 2$ which gives the initial vibrational energy at about 2.1 Only the initial translational energies are changed from 0 to 2.0, for which the total energies are lower than the height of the energy barrier $E_{barrier} = 4.5$.

Figures 7(A) - Fig.7(H) show the tunneling tubes for the initial translational energies 0.6, 0.8, 1.0, 1.2, 1.4, 1.6, 1.8 and 2.0, respectively. In Fig.7(B), there are three individual tunneling tubes which start from a small region in the reactant valley. As the initial translational energy increases, the length of the tunneling tubes gets shorter and the width of them becomes wider. In the low translational energy range, the shape of the tunneling tubes looks like the M-G type path. On the other hand, the M-C type tunneling tube appears in the high translational

energy range. In the study of collinear $H + H_2$ system by Altkorn and Schatz [18], the reaction probabilities estimated along the M-G path are in good agreement with the quantum mechanical values at the low translational energies. In the high translational energy range, on the other hand, the reaction probabilities along the M-C path show good agreement with the quantum mechanical values. The tunneling tubes generated by the quasi-semiclassical method thus yield the similar conclusion. In the quasi-semiclassical method, all the tunneling paths are generated only by solving the modified canonical equations of motion (Eq.(2-8) in Chapter II of Part I) in both the low and the high translational energy ranges. The tunneling tube is a bunch of these tunneling paths with large tunneling probabilities. Therefore two different types of tunneling tubes, the M-C type tubes in the high translational energy range and the M-G type tubes at the low translational energies, are born automatically in our theory.

We next calculate the tunneling probability T_{nr} (Eq.(2-7)) at the different initial translational energies. Figure 8 shows the tunneling probability as a function of the initial translational energy. The tunneling probability becomes larger as the initial translational energy increases. However, there is a dip at $E_{trans} = 1.4$, where the shape of tunneling tubes change from M-G type to M-C type which corresponds to Fig.7(E).

In order to examine whether the tunneling paths are chaotic or stable, we calculate the averaged maximum Liapunov exponents λ with use of the same procedure in Chapter I of Part I and Chapter I of Part II. In both classical and tunneling regions, the averaged maximum Liapunov exponent λ is defined as

$$\lambda = \frac{1}{n} \sum \frac{\ln |u_{\max}|}{\Delta t} \quad (t = n \times \Delta t), \tag{3-3}$$

where n is the number of a time step Δt which is suitably chosen for integrating a set of the canonical equations of motion (Eq.(2-8) in Chapter II of Part I). And $u_{\max}$ is the maximum eigenvalue of the stability matrix [19]

$$\frac{\partial(q_f, \bar{p}_f)}{\partial(q_i, \bar{p}_i)}, \tag{3-4}$$

where q_f and q_i are the final and initial position vectors, and $\bar{p}_f$ and $\bar{p}_i$ are the real-valued final and initial quasi-momentum vectors, respectively. The present definition of the averaged maximum Liapunov exponents is applied to both classical (pre-tunneling) and tunneling paths and we denote them as $\lambda_{classical}$ and λ_{tunnel}, respectively. Figure 9 shows both $\lambda_{classical}$ (full squares with line) and λ_{tunnel} (open squares with broken line) versus the initial translational energy. At each initial translational energy, $\lambda_{classical}$ has been calculated using about 300 classical trajectories and about 700 tunneling paths are used for the calculation of λ_{tunnel}. It is noticed that λ_{tunnel} is two to three times larger than $\lambda_{classical}$ everywhere we examined.

Because of the large averaged maximum Liapunov exponents in the tunnel region, we can expect that chaos in the tunnel region induces the mixing of tunneling phase space and the destinations of tunneling paths are widely distributed in the product valley. The tunneling tube is a bunch of these unstable tunneling paths with large tunneling probabilities. Then almost all the figures in Fig.7 show that the exit of the tunneling tube is wider than the entrance of the tunneling tube. Particularly in Fig.7(B) and Fig.7(G), which correspond to two peaks of λ_{tunnel} in Fig.9, chaos divides the tunneling tube which starts from a small region in the reactant valley into two or three parts and these parts of the tunneling tube spread in the product valley. The diameter of the exit of the tunneling tube is an important factor that determines the final energy distribution. In the H-L-H system, chaos in the tunneling region generally leads the relatively wider exit of the tunneling tube and can be one of the important factors that determine the final energy distribution.

B. Effect of the anisotropy of the potential (early or late barriers)

Here we investigate the effects of the location of the transition state, namely, early or late barrier [20, 21]. The anisotropy of the location of the saddle point has been adjusted by changing the parameter D_{AB} (the depth of the bonding energy of the product molecule AB). D_{AC} is also changed to make a late barrier. All the other parameters are the same as before.

In particular, the initial vibrational quantization is unaltered at all by this modification of the potential. The skew angle is fixed at $\varphi = \frac{\pi}{6}$ and the initial vibrational energies are samples so as to have the values corresponding to the vibrational quantum numbers $v = 0, 1, \cdots$. The translational energies are given automatically by specifying the vibrational quantum number to keep the given total energy for each system. It is well known that the initial vibrational excitation is favorable to the non-tunneling reaction on the late barrier. We now check what happens in the tunneling regime.

a) The early barrier

The present potential surface, Fig.10, has been made up with $D_{AB} = 20.0$. The saddle point energy is pulled down to $E_{saddle} = -8.1$. The total energy is chosen as $E_{total} = -8.4$. The entrance and exit channels are open up to $v = 1$ and $v = 10$, respectively. Figures 10(A) and (B) represent the tunneling density plot for the initial vibrational state $v = 0$ and 1, respectively. The density plot in Fig.10(A) simply looks like the minimum energy path and thus the translational energy in the initial distribution is vital in this case. On the other hand, the case of $v = 1$ is rather peculiar. There are two major tunneling tubes. In reality, however, the tunneling probability for this case is negligibly small, as shown in Table IV. Thus the tunneling takes place, as a matter of fact, only in the channel of $v = 0$, and just as in the non-tunneling case, the translational energy dominates the reaction rate.

The product distribution for $v_i = 1$ is rather uniform (Fig.11). However, the tunneling from the state $v_i = 0$ forms two peaks. Although two tunneling tubes are recognized in Fig.10(A) (for $v = 0$), we cannot conclude whether each is responsible for a single peak. It can occur by the way that a seemingly single tube happens to be composed of two superposed tubes in reality.

b) The late barrier

The bonding energies are chosen as $D_{AB}=D_{AC}=5.0$, which lift the barrier up to $E_{saddle}=-4.2$. We choose the total energy $E_{total}=-4.5$ just below that of the saddle point. Seven states are allowed, namely $v=0-6$, in the entrance channel and the exit valley can support only $v=0$ state. Figures 12(A)-(D) show the tunneling density plot for the initial vibrational states of $v=3-6$, respectively. The trajectories of $v=0-2$ have virtually no tunneling probability. Thus the vibrational excitation is essential. Nonetheless, the density plots of Fig.12 look almost like the M-C type path. In particular, Fig.12(B) is similar to the reaction coordinate.

The length of the tunneling tubes becomes shorter as the initial vibrational quantum number increases, which suggests the higher tunneling probability in the higher vibrational states. In fact, Table V supports this view. Another reason for this fact will be deduced from the position of the entrance of the tunneling tube, i.e., the caustic points of the classical trajectories. As is noticed in Fig.12, the larger the initial vibrational quantum number is, the entrance of the tunneling tube is located at the higher potential energy. Thus, again as in the non-tunneling case, the tunneling reaction is enhanced by the initial excitation in the vibrational mode.

III. Concluding Remarks

We have investigated the effects of multidimensionality in rather elementary chemical reactions. The theory in Chapter II of Part I has been applied to a series of collinear tunneling reactions on the LEPS potential surface. The major results are summarized as follows: (1) The tunneling tube has been found that highlights the multidimensional tunneling. The tunneling tube is a bunch of unstable tunneling paths with large tunneling probabilities. As the length of the tube is shorter, the gross tunneling probability tends to be larger. Moreover, the diameter of the tunneling tube can be an important factor that determines the final energy distribution. That is, the narrower the tunneling tube becomes, the higher tends to become the selectivity

in the product vibrational states. (2) The well-known types of tunneling paths, namely, of the Marcus-Coltrin in the high translational energy range and Miller-George at the low translational energies are born automatically in our theory, and more over in a single system. (3) Although the L-H-L system does not have a significant tunneling probability, the dominant paths are of the M-C type. A high selectivity in the product energy distribution has been observed, because of the narrow tunneling tubes. (4) From the study of the effects of the initial energy distribution, the H-L-H system has the maximum tunneling probability at some intermediate vibrational state like $v=2$, in which the shortest tunneling paths are associated. As the initial vibration is excited, the M-G type paths dominate the tunneling. (5) The potential surface of the early barrier can have a short-cut tunneling path parallel along the reaction coordinate that is promoted by the initial excitation in the translational mode. (6) Virtually no tunneling has occurred on the potential surface of the late barrier. As in the non-tunneling case, the vibrational excitation is vital to enhance the tunneling reaction. (7) The effect of chaos on the exit of the tunneling tube has been studied. Chaos in the tunnel region generally leads relatively wider exit of the tunneling tube in the H-L-H system and can be one of the important factors that determine the final energy distribution.

Finally, we stress that our quasi-semiclassical approach is quite promising for the analysis of the tunneling reaction of the higher dimension. In fact, the studies along this line, together with an investigation about the collective tunneling, are in progress in our laboratory, since we would like to find general and qualitative rules and concepts in multidimensional tunnelings.

References

[1] As for recent progress in the tunneling in chemical reactions, see

a) A special issue on "Tunneling in Chemical Reactions," edited by V. A. Benderskii, V. I. Goldanskii and J. Jortner, Chem. Phys. **170** (1993).

b) V. A. Benerskii, D. Makarov, and C.A. Wight, the hole volume of Adv. Chem. Phys. Vol. LXXXVIII (1994).

[2] L. D. Landau and E. M. Lifshitz, *Quantum Mechanics*, (Pergamon, New York, 1958).

[3] Recently, Nakamura and Zhu have solved analytically a one-dimensional tunneling problem the barrier of which is caused by the non-adiabatic coupling, which was one of the ultimate problems in semiclassical theory for tunneling and non-adiabatic transitions, C. Zhu and H. Nakamura, J. Chem. Phys. **102**, 7448 (1995).
See for a review,
H. Nakamura and C. Zhu, Comments At. Mol. Phys. **32**, 249 (1996).

[4] J. K. Gregory and D.C. Clary, J. Chem. Phys. **102**, 7817 (1995).

[5] B.C. Garrett and D.G. Truhlar, J. Chem. Phys. **79**, 4931 (1983).

[6] T. D. Seawall, Y. Guo and D. L. Thompson, J. Chem. Phys. **103**, 8557(1995).

[7] Y. Guo, Y. Qin, D. C. Sorescu and D. L. Thompson, J. Chem. Phys. **104**, 4041(1996); ibid. **105**, 1070(1996).

[8] B. A. Waite and W. H. Miller,J. Chem. Phys. **73**, 3713(1980).

[9] N. Makri and W. H. Miller, J. Chem. Phys. **91**, 4026(1989).

[10] A. Auerbach, S. Kivelson and D. Nicole, Phys. Rev. Lett. **53**, 411(1984); A. Auerbach and S. Kivelson, Nucl. Phys. **B257** [FS14], 799(1985).

[11] S. Sato, J. Chem. Phys. **23**, 592 (1955).

[12] J. I. Steinfeld, J. S. Francisco and W. L. Hase, *Chemical Kinetics and Dynamics*, (Prentice-Hall, 1989).

[13] See for example, D. G. Truhlar and J. T. Muckerman in *Atom-Molecule Collision Theory* (R. B. Bernstein Ed., Plenum, New York, 1979, page 505).

[14] L. S. Schulman, *Techniques and Applications of Path Integration*, (Wiley , New York, 1981)

[15] a) M. V. Berry and K. E. Mount, Rep. Prog. Phys. **35**, 315 (1972).

b) V. P. Maslov and M. V. Fedoriuk, *Semiclassical Approximation in Quantum Mechanics*, (Reidel, Dordrecht, 1981).

c) M. S. Child, *Semiclassical Mechanics with Molecular Applications*, oxford, 1991).

[16] R. A. Marcus and M. E. Coltrin, J. Chem. Phys. **67**, 2609 (1977).

[17] T. F. George and W. H. Miller, J. Chem. Phys. **56**, 5722 (1972) ; ibid. **57**, 2458 (1972).

[18] R. I. Altkorn and G. C. Schatz, J. Chem. Phys. **72**, 3337 (1980)

[19] V. I. Arnold, *Mathematical Methods of classical Mechanics*, (Springer, Berlin, 1978); A. Abraham and J. E. Marsden, *Foundation of Mechanics 2nd. ed.*, (Addison-Wesley, Reading, 1985)

[20] J. C. Polanyi, Acc. Chem. Res. 5, 161 (1972)

[21] R. D. Levine and R. B. Berstein, Molecular reaction Dynamics and Chemical Reactivity (Oxford, 1987)

Table I. The parameters for the LEPS potential.

D	10.0
β	1.0
r^0	1.0

Table II. Tunneling probability T_{nr} for L-H-L system.

vibrational numbers[a]	T_{nr}
v=0	2.76 (-7)[b]
v=1	2.36 (-6)
v=2	1.62 (-5)

a The highest state allowed is v=9.

b Number in parenthese are multiplicative of ten.

Table III. Tunneling probability T_{nr} for H-L-H system.

vibrational numbers[○]	T_{nr}
v=0	3.36 (-4)
v=1	3.65 (-3)
v=2	6.96 (-2)
v=3	2.85 (-3)
v=4	9.12 (-9)

○ The highest state is v=4.

Table IV. Tunneling probability T_{nr} for the early potential barrier.

vibrational number[○]	T_{nr}
v=0	2.46 (- 3)
v=1	1 .43 (-15)

○ The highest states allowed are v=1 and v=10 for the entrance and exit channels, respectively.

Table V. Tunneling probability T_{nr} for the late potential barrier.

vibrational numbers○	T_{nr}
v=0	5.32 (-39)
v=1	7.24 (-27)
v=2	5.65 (-18)
v=3	3.18 (-10)
v=4	2.41 (- 9)
v=5	1.30 (- 7)
v=6	7.41 (- 6)

○ The highest vibrational states allowed are v=6 and v=0 for the entrance and exit valleys, respectively.

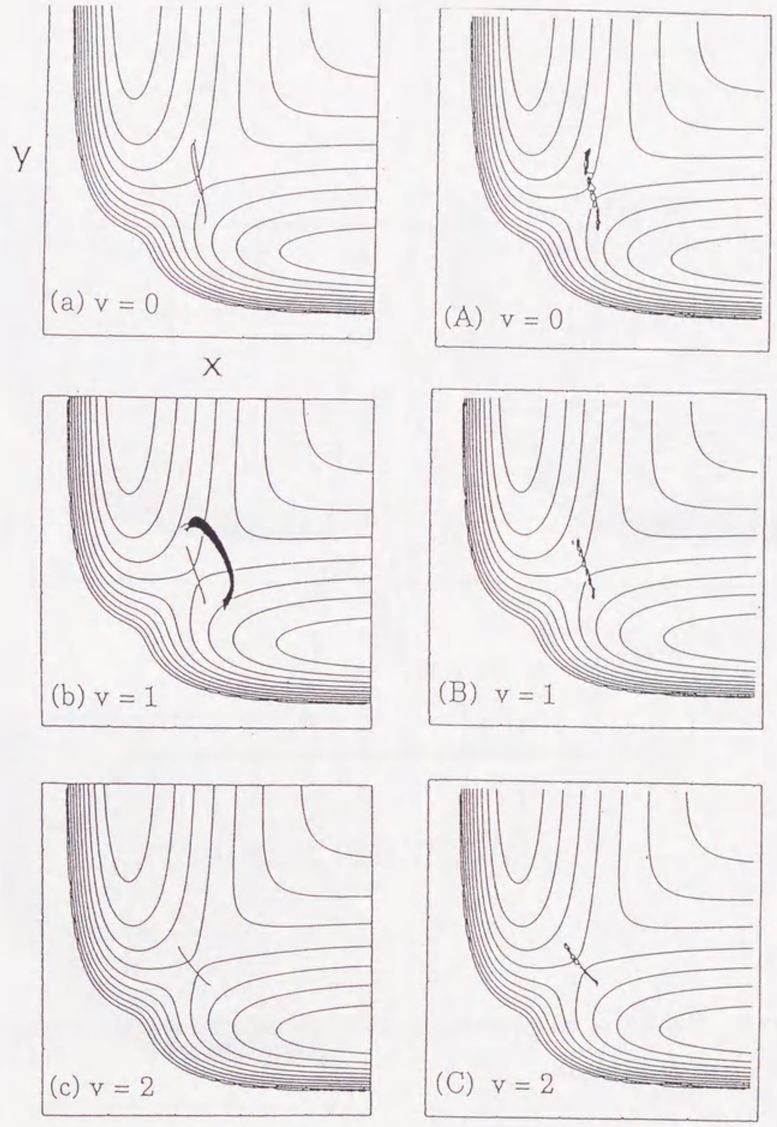

Figure 1. Panels (a)-(c); the tunneling paths on the LEPS potential for Light-Heavy-Light system having the initial vibrational quantum numbers $v = 0 - 2$, respectively. Panels (A)-(C); the density plots of kernel T corresponding to (a)-(c), respectively. There are two groups of the tunneling paths in (b), but one has disappear in (B), because of its small survival probability.

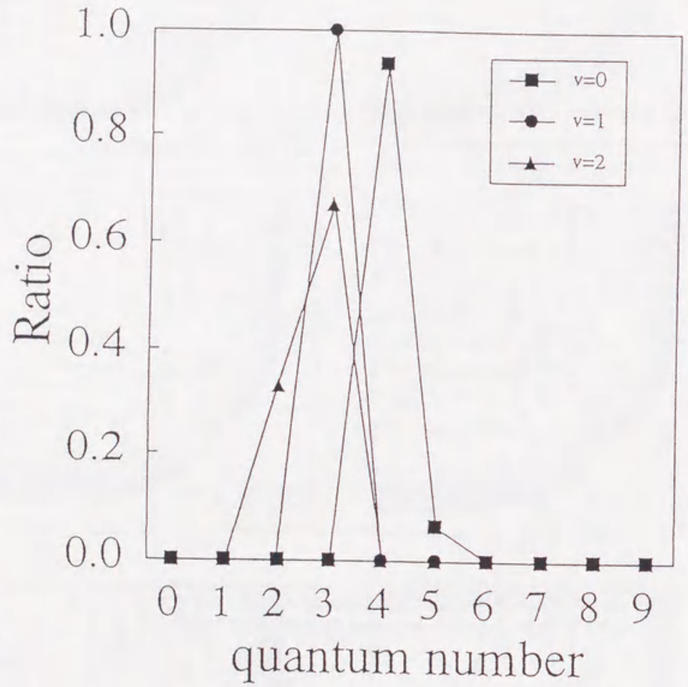

Figure 2. The ratio of the vibrational energy distributed to the product after the tunneling reaction in the L-H-L system.

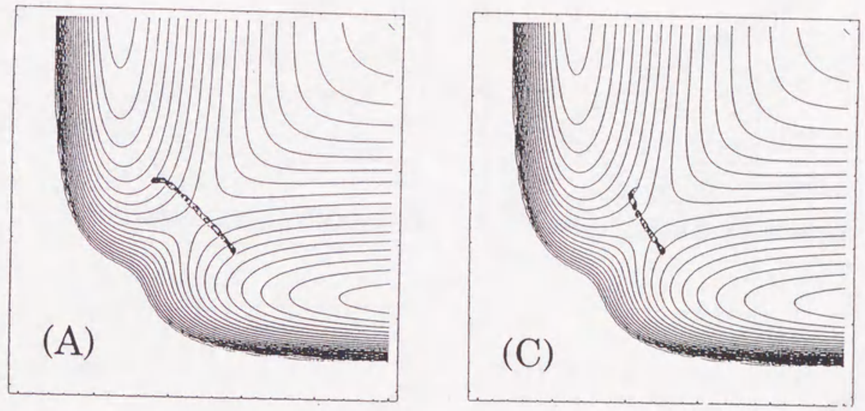

Figure 3. Panels (A)-(C) show the density plots of tunneling paths for the initial translation energies 1.6, 1.8 and 2.0 for the L-H-L system, respectively. Only the Marcus -Coltrin type path appear at high translational energy range.

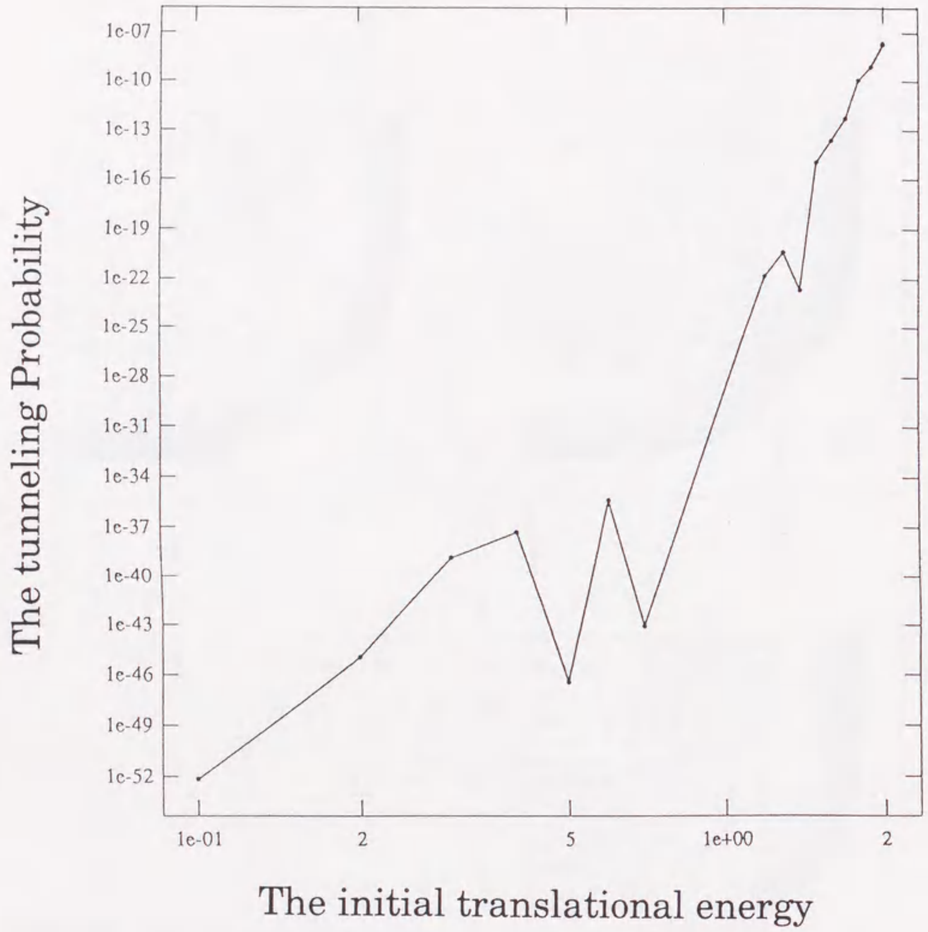

Figure 4. The tunneling probability versus the initial translational energy for the L-H-L system

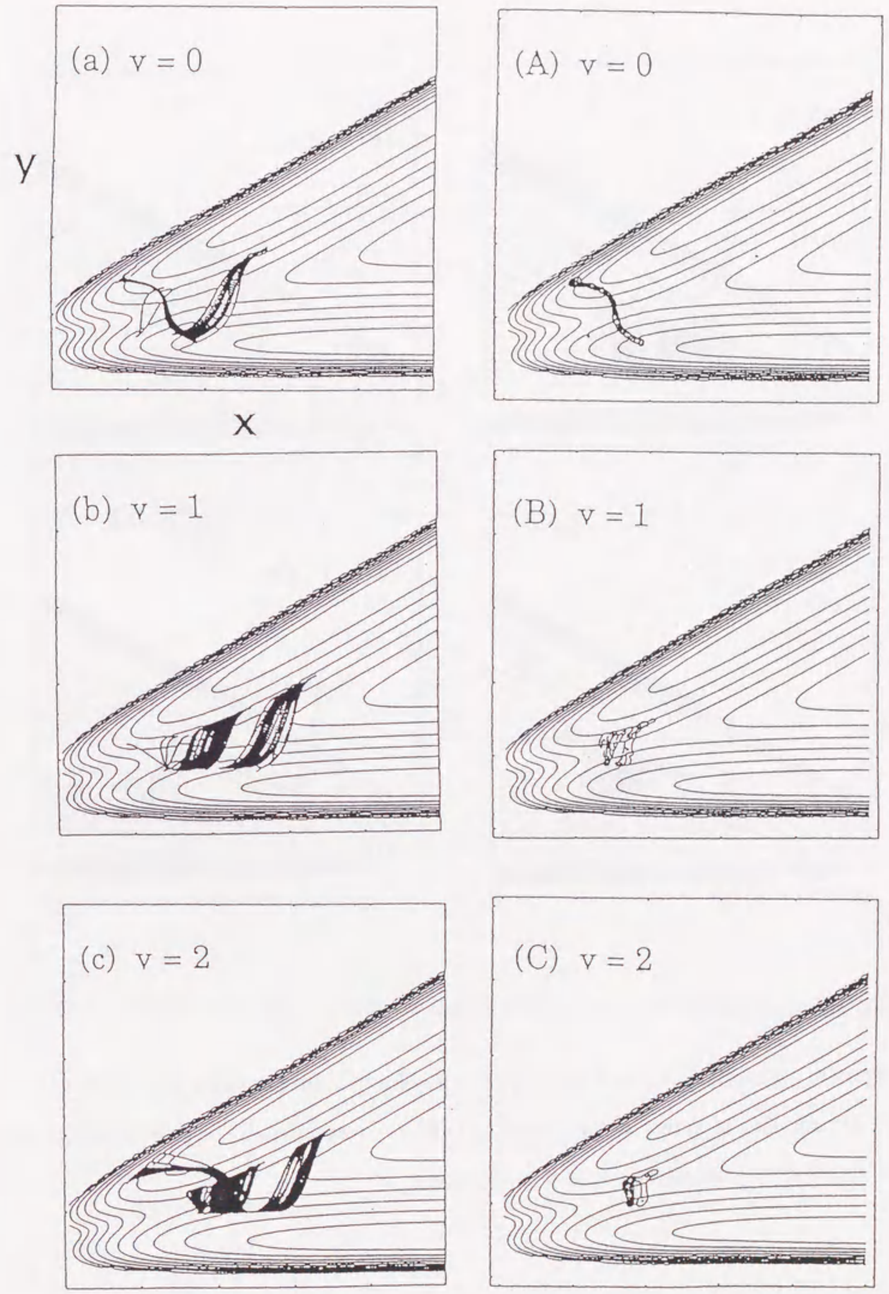

Figure 5.

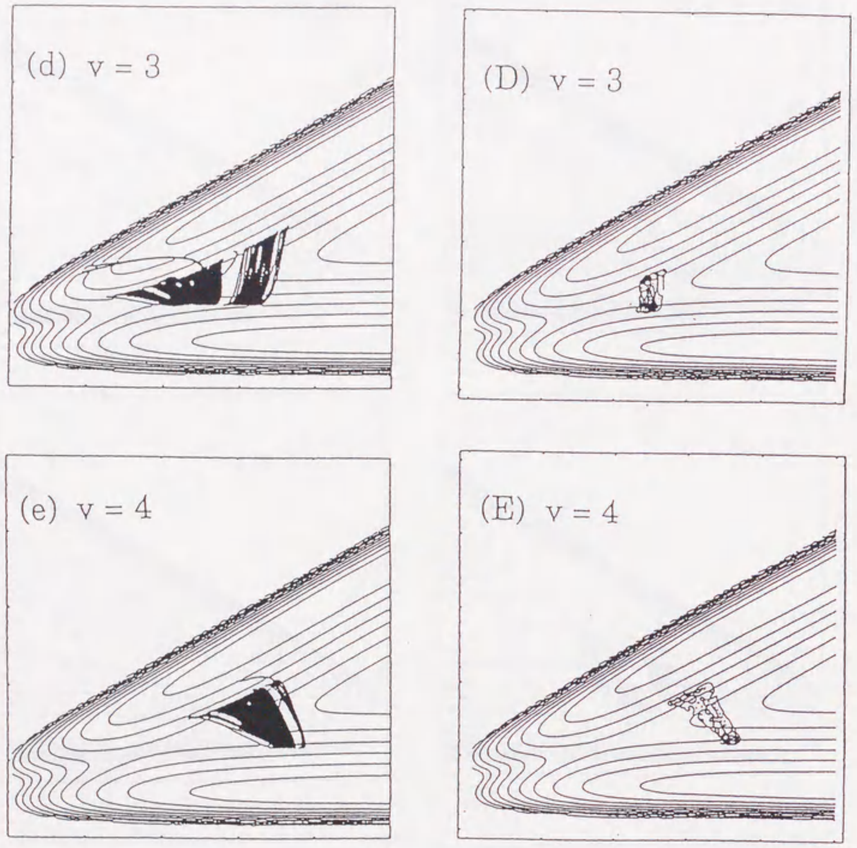

Figure 5. Panels (a)-(e); the tunneling paths for Heavy-Light-Heavy system. Panels (A)-(E); the density plots of kernel T corresponding to (a)-(e), respectively. The paths of (a)-(e) have the initial vibrational states $v = 0 - 4$, respectively.

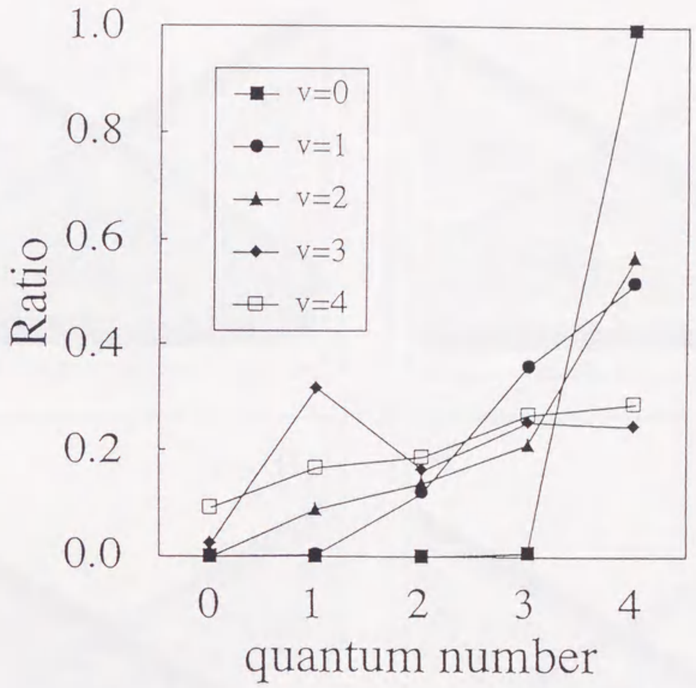

Figure 6. The same as Fig.2, except that the results of the H-L-H system are shown.

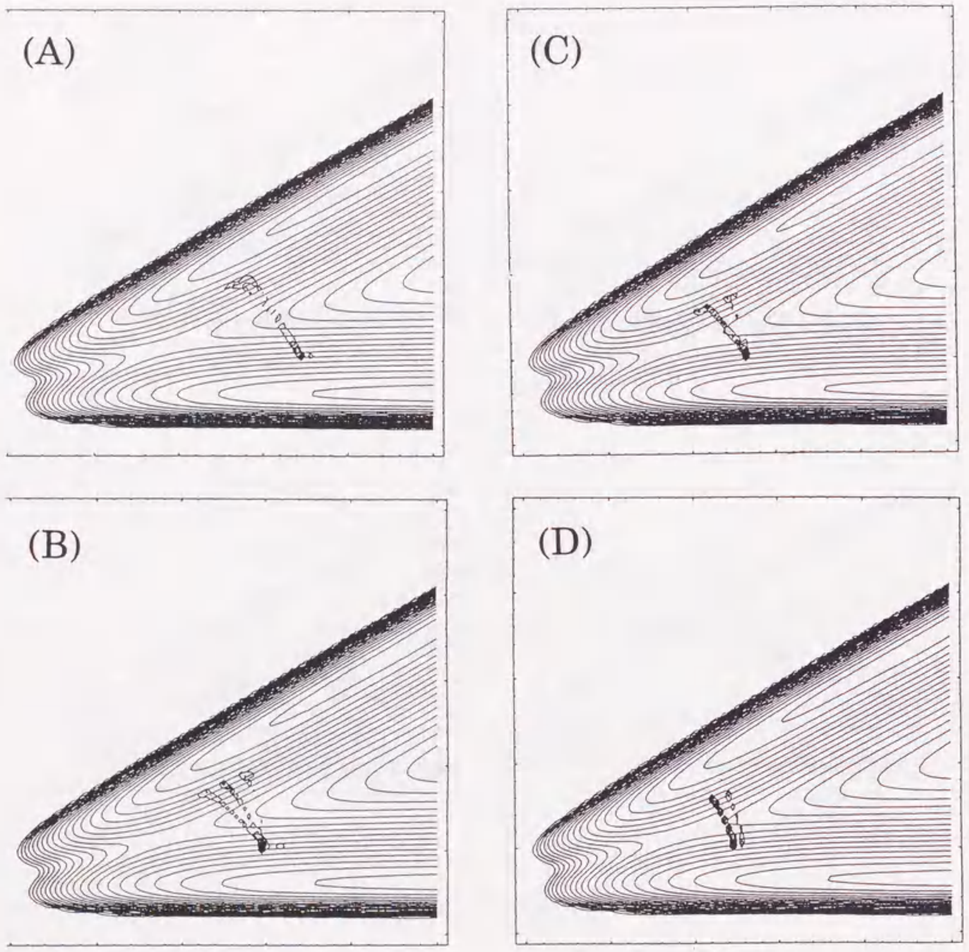

gure 7.

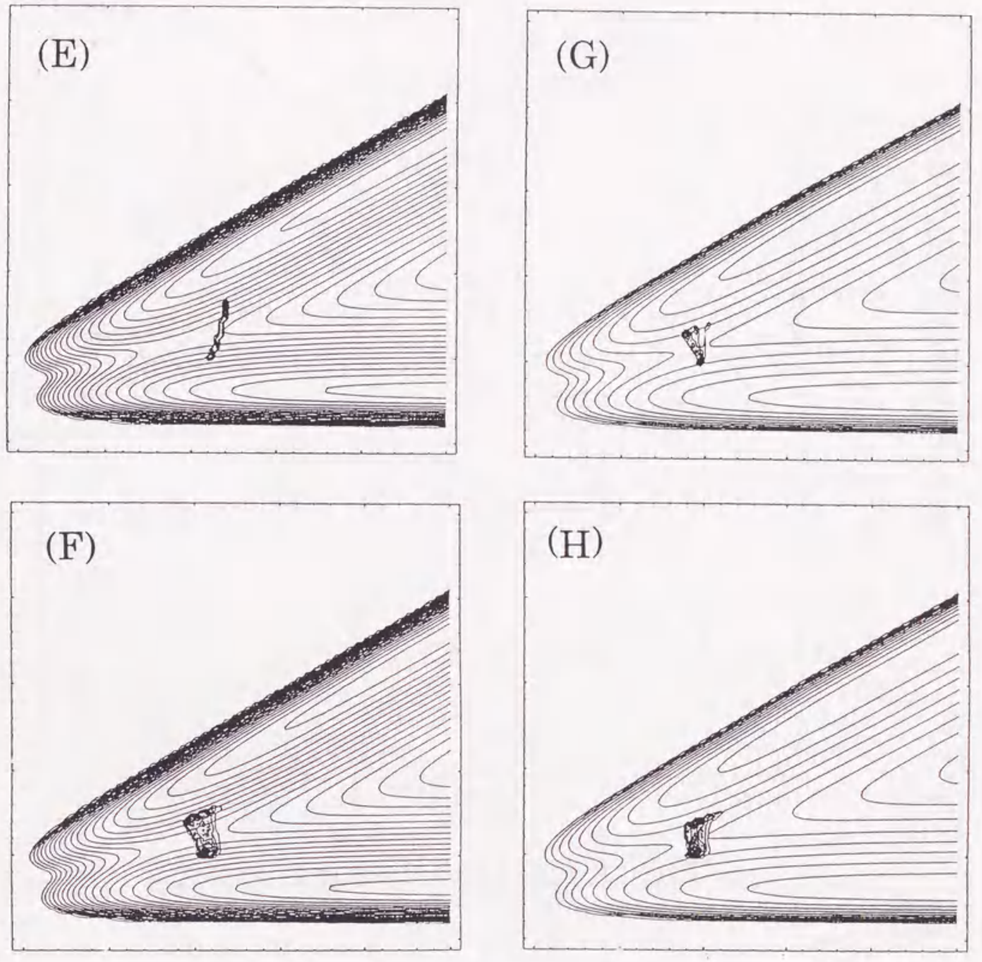

Figure 7. Panels (A)-(H) show the density plots of tunneling paths for the initial translational energies 0.6, 0.8, 1.0, 1.2, 1,4, 1.6, 1.8 and 2.0 for the H-L-H system, respectively. In the low translational energy range, the tunneling tubes look like the Miller-George path and the Marcus-Coltrin type tubes appear in the higher range.

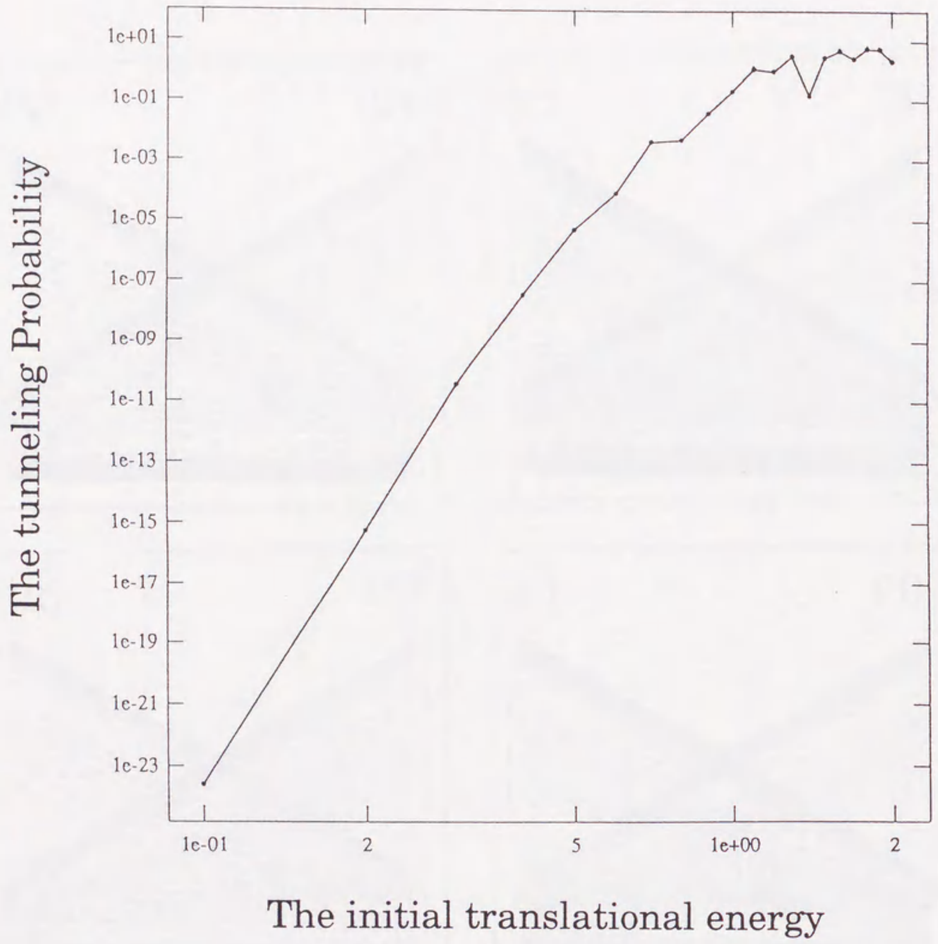

Figure 8. The tunneling probability versus the initial translational energy for the H-L-H system

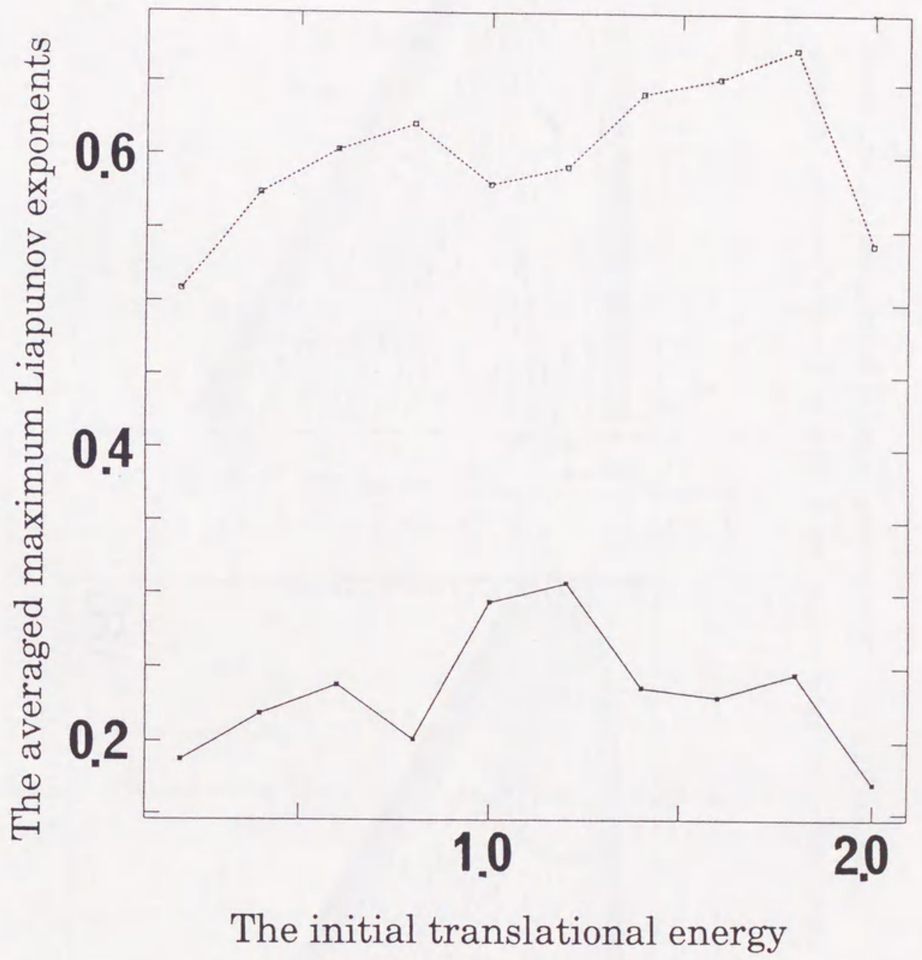

Figure 9. The averaged maximum Liapunov exponents of classical paths λ_{cl} (full squares) and those for the tunneling paths λ_{tunnel} (open squares) as a function of the initial translational energy. λ_{tunnel} are two to three times larger than λ_{cl} at all the translational energies investigated.

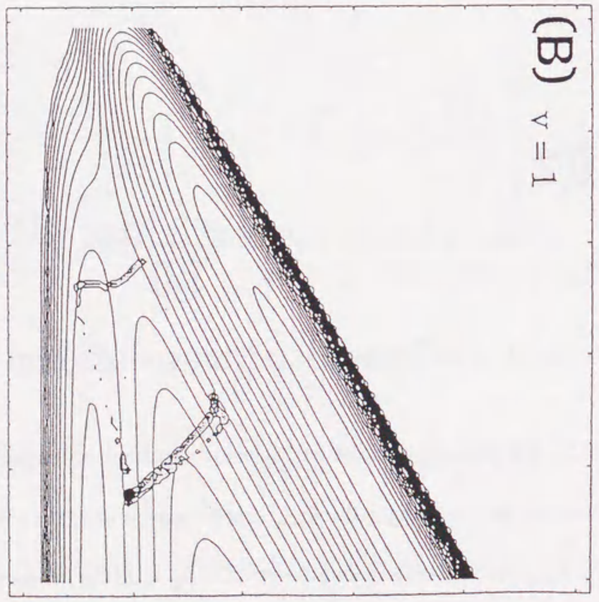

Figure 10. The density plots of the kernel in the tunneling region for the early barrier system. Panels (A) and (B) are for the initial vibrational energy $v = 0$ and 1, respectively.

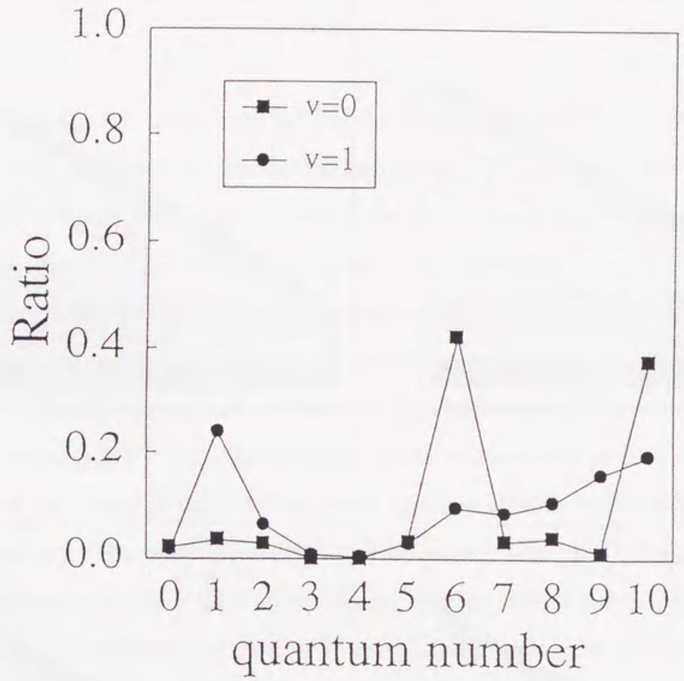

Figure 11. The same as Fig.2, except that the results of the early barrier are shown.

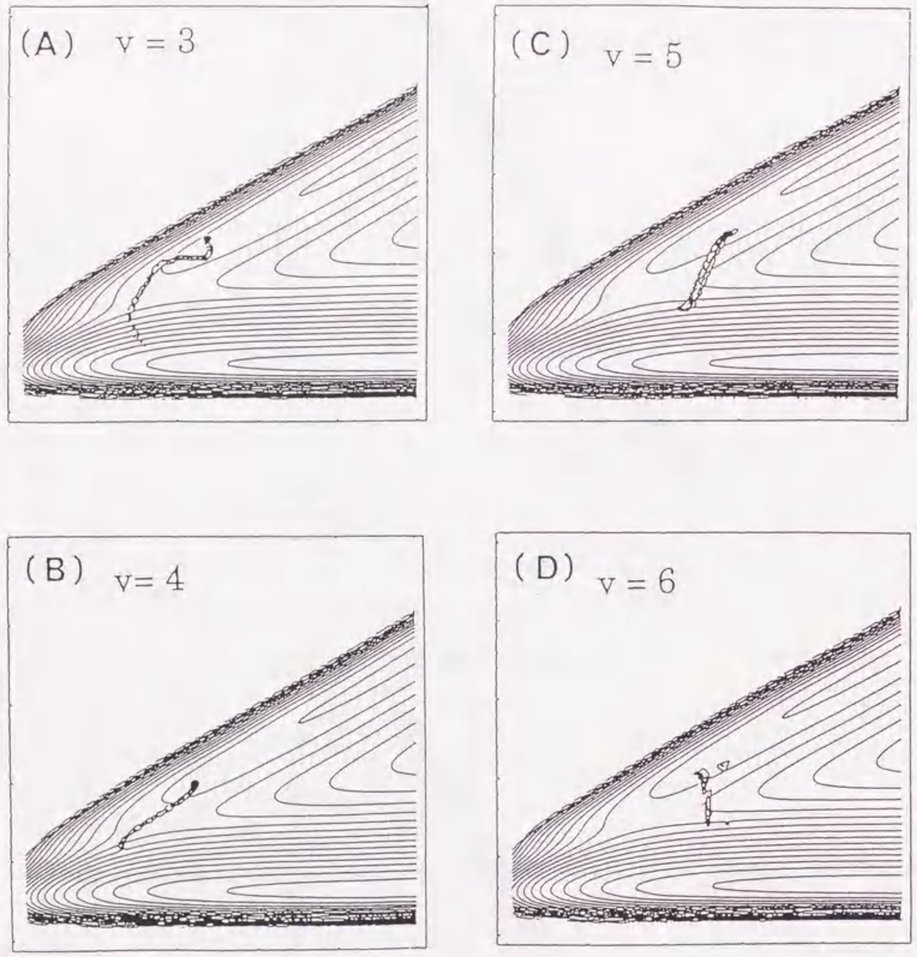

Figure 12. The density plots of the kernel in the tunneling region for the late barrier system. Panels (A) to (D) are for the initial vibrational states $v = 3 - 6$, respectively.

General Conclusions

In the present thesis, chemical reactions through tunneling have been investigated. In Part I, to study tunneling in chemical systems, a semiclassical theory for multidimensional tunneling has been constructed. In Part II, the effects of chaos on the dynamical tunneling have been discussed and the multidimensional effects on chemical reactions through tunneling have been examined on the basis of the semiclassical theory constructed in Part I. From these studies in the present thesis, the following general conclusions have been obtained.

(1) A semiclassical theory for multidimensional tunneling has been constructed. By introducing a quantity of 'parity of motion' which can take only positive or negative unity into each coordinate of the Hamilton-Jacobi equation, complex-valued action integrals are provided in real-valued configuration space. The complex-valued action integral is propagated as a tunneling solution of the Hamilton-Jacobi equation along a real-valued tunneling path. The parity of motion modifies the ordinary classical Hamiltonian and tunneling paths are generated by solving a set of the modified canonical equations of motion in real-valued phase space with negative parities. Thus the complex-valued action integrals can be constructed in a large dimensional system. The complex-valued solutions of the Hamilton-Jacobi equation have a layer structure composed of many sheets, each of which is characterized in terms of its own set of parities. The real-valued tunneling paths have been incorporated into the time-dependent semiclassical kernel with conserving real-valued time. The mathematical form of the semiclassical kernel is the same as one for the well-known classical case except that the complex-valued action integrals are taken into account. The dumping factor caused by tunneling does not arise from the amplitude factor but from the imaginary part of the action integral only. As the number of negative parities gets large, the norm of the semiclassical kernel decreases. This theory can be applied to tunneling in large dimensional chemical systems.

(2) The behavior of tunneling paths and the effects of chaos on the dynamical tunneling

have been investigated on the Hénon-Heiles potential. Even in a nearly integrable system in which six stable regions coexist with two quasi-separatricies, tunneling paths are found to be fully chaotic. Chaos in the tunnel region induces the mixing of tunneling phase space and the destinations of tunneling paths spread widely. It brings about the statistical redistribution of trajectories after the dynamical tunneling. However, the tunneling probability associated with each tunneling path leads to a biased distribution of the paths. After all the destinations of dynamical tunneling paths are localized in the specific stable regions in phase space, when the tunneling probability is considered. Thus, chaos competes with tunneling probabilities to determine the distribution of trajectories after the dynamical tunneling.

(3) To study chemical reaction through tunneling, the 'quasi-semiclassical method' has been proposed. In the quasi-semiclassical method, tunneling paths are generated by solving a set of the modified canonical equations of motion and the tunneling probability can be calculated on the basis of our semiclassical theory. In the H-L-H system, both two different types of tunneling paths, the Marcus-Coltrin path in the high translational energy range and the Miller-George path at the low translational energies, are born automatically. The present method is quite promising for the analysis of the tunneling reaction of the higher dimension.

(4) Some typical tunneling reactions in the collinear three atomic systems have been investigated by the 'quasi-semiclassical method' on the so-called LEPS potential. To examine which mode, vibrational or translational mode, should be excited to enhance the tunneling reaction, the effect of the initial energy distribution on tunneling probabilities has been examined with changing the mass balance and the anisotropy of potential surface. The high vibrational energy enhances tunneling reaction in the H-L-H system and the late barrier system. On the other hand, the high translational energy enhances the tunneling reaction in the L-H-L system and the early barrier system.

(5) A 'tunneling tube' which is a bunch of tunneling paths with large tunneling probabilities has been found. This is the most remarkable feature peculiar to the multidimensional tunneling and a distinguished feature of multidimensional tunneling from one-dimensional tunneling. As the length of the tunneling tube gets shorter, the tunneling probability becomes

large. The width of the tunneling tube determines the energy distribution among the vibrational and the translational modes in a product molecule. In the L-H-L system, a high selectivity in the product energy distribution has been observed because of the narrow tunneling tube. On the other hand, because of the wide tunneling tube, the product molecules have various vibrational states in the H-L-H system. The tunneling tube plays a key role in the investigation of the chemical reaction through tunneling and leads us to deep understanding of chemical reactions through tunneling.